A PROTON MAGNETIC RESONANCE STUDY OF SOME CYCLOPROPANE DERIVATIVES

A Thesis

Submitted to

the Faculty of Graduate Studies and Research

The University of Manitoba

In Partial Fulfillment

of the Requirements for the Degree

Doctor of Philosophy

by

Harold M. Hutton

August 1963

ACKNOWLEDGEMENTS

I would like to thank Dr. T. Schaefer for the constant encouragement and advice given during the course of this work.

I wish to express my gratitude to Canadian Industries Limited for their financial assistance in the form of a Fellowship and a grant for research.

Also, I would like to thank Dr. W. F. Ringk of Benzol Products, Co., Dr. L. L. McCoy of Columbia University, Dr. G. L. Closs of the University of Chicago, Dr. B. T. Gillis of Duquesne University, and Dr. J. W. Wilt of Loyola University for donating some of the cyclopropane derivatives used in this thesis. I thank Dr. R. Freeman for advice on the construction of the double resonance apparatus.

Finally, I would like to acknowledge my indebtedness to Mr. G. Epp for photographing and printing the diagrams used in this thesis, and to Mr. E. Erickson of the Science Technical Laboratory for the construction of the double resonance apparatus and for his assistance in maintaining the Varian spectrometer.

TO MY WIFE, NATALIE

ABSTRACT

The high-resolution proton magnetic resonance spectra of a series of cyclopropane derivatives have been studied. The vicinal proton spin coupling constants for the cyclopropane ring were found to be $J_{\underline{cis}}$ = 8.7 cps and $J_{\underline{trans}}$ = 5.4 cps, in reasonable agreement with Karplus' theoretical calculations. The geminal coupling constants were obtained for a number of cyclopropane derivatives. The results were tabulated and compared with the previous results and those from the literature. Substituent effects did not appear to follow a simple dependence on the electronegativity as in the ethanes. It was suggested, and later proven by a nuclear magnetic double resonance experiment, that the geminal couplings are of opposite sign to the vicinal couplings and therefore negative.

It was shown that bis (2,2-dichlorocyclopropyl) ether formed a complex with benzene molecules. From the temperature dependence of the shifts of the cyclopropyl protons the heat of formation and the entropy of formation of the complex was estimated to be -1700 ± 100 cal/mole and -6.3 ± 0.3 e.u., respectively. The association shifts are 52 ± 2 cps, 64 ± 5 cps, and 88 ± 5 cps at 60 Mcps for the three protons situated at different points in the molecule.

A_2B_2 spectra for 1,1-disubstituted cyclopropanes were calculated for the known range of the geminal and vicinal coupling constants. 1-Phenylcyclopropylcarboxylic acid was analyzed in three solvents to

illustrate the applicability to the analysis of an experimental A_2B_2 system. The cyclopropyl protons of 1-phenylcyclopropylcarbinol were found to be isochronous and not sufficiently coupled to any substituent to cause any fine structure. The C^{13}--H_2 sidebands of the cyclopropyl protons in 1,1-diphenylcyclopropane were analyzed as a slightly perturbed A_2X_2 system to obtain the vicinal coupling constants.

By means of the anisotropic solvent effect of benzene, the A_2B_2X system for cyclopropylamine was converted to an $A_2A'_2X$ system. A pseudo first-order spectrum with combination lines was found which allowed a fairly complete set of coupling constants to be derived. Conversely, this approach, when applicable, allows the derivation of reliable input parameters for a computer program.

TABLE OF CONTENTS

LIST OF TABLES

LIST OF FIGURES

CHAPTER I

INTRODUCTION

1. General

During recent years there has been considerable interest in the correlation of coupling constants which arise in high resolution nuclear magnetic resonance with molecular structure and substituents. When the work described in this thesis was initiated very little had been published on the nuclear magnetic resonance of cyclopropane derivatives. It was thought that a study of this nature on the three-membered cyclopropane ring would be useful.

In addition to a comparison of the theoretical and experimental values of the geminal and vicinal coupling constants for substituted cyclopropanes, an evaluation of the relative signs of these couplings has been made. The absolute signs of coupling constants are not ordinarily obtainable experimentally by NMR (see, however, reference 61), but often the relative signs between couplings can be found, and these, as well as the magnitudes are important in evaluating the agreement between theory and experiment. Initially, relative signs were found by the analysis of complex spectra where the coupling constants were of similar magnitude to the chemical shift. Recently the technique of double resonance has enabled the evaluation of the relative signs for coupling constants of systems with shifts which are large with respect to the coupling constants. Both of these methods,

the analysis of complex spectra and double resonance, were used to find the relative signs of the geminal and vicinal coupling constants in the cyclopropane ring.

The theoretical aspects of NMR will be omitted from this thesis since there are a number of excellent monographs (1 - 5), e.g. the one by Pople, Schneider, and Bernstein[1]. The theories which are used for a particular project are discussed where necessary in the individual chapters. In the following paragraphs in Chapter I no references have been made to the literature since the individual topics are discussed in detail in the remaining chapters.

2. Vicinal and Geminal Couplings of Cyclopropanes

The cis and trans coupling constants for substituted cyclopropanes were obtained from the proton resonance spectra of a mixture of the cis and trans isomers of ethyl chrysanthemumic esters and the individual cis-chrysanthemumic and trans-chrysanthemumic acids. The cyclopropyl proton spin coupling constants were found to be in reasonable agreement with Karplus' calculations of the dependence of coupling constants on the dihedral angle. Coupling constants were obtained for a series of cyclopropane derivatives and compared with both geminal and vicinal couplings previously published. It was suggested, and later proven, that the geminal coupling is of opposite sign to the vicinal couplings and therefore negative, so that the comparison by Karplus between the H-C-H angle and the coupling constant is no longer valid. There was also a comparison made between the

geminal coupling constants in cyclopropanes, ethylene sulfides, and ethylene oxides. There is a change in the sign of this coupling constant in going from carbon through sulfur to oxygen as the third atom in the ring. The vicinal coupling constants depend on the dihedral angle as predicted by theory, but the substituent effects do not appear to follow a simple dependence on the electronegativity as they do in substituted ethanes.

3. Relative Signs of the Geminal and the Vicinal Coupling Constants

Recent work on the relative signs of the coupling constants in ethane derivatives has shown that the geminal coupling is opposite in sign to the two vicinal couplings. From theoretical considerations and experimental data, the geminal coupling constant is considered to be negative and the vicinal couplings are considered to be positive. It was of interest to see if this was also true for cyclopropane derivatives. Using the double resonance technique on 1-methyl-2,2-dichlorocyclopropane the results showed that there was indeed a difference in sign between the geminal and vicinal couplings, in analogy to the ethanes.

4. Complex Formation of bis (1,1-Dichlorocyclopropyl) Ether with Benzene

Originally it had been thought that the compound bis (1,1-dichlorocyclopropyl) ether would have a simple ABX resonance spectrum which could be used for the double resonance experiment. However, two overlapping ABX spectra due to the meso and d,l isomeric forms

of this compound were obtained, making the double resonance interpretation unreliable. The stereochemical difference caused by the two asymmetric carbon atoms in this substituted cyclopropyl ether was sufficient to give a different magnetic environment for the protons in the meso form in comparison to the d,l forms. There was, however, no reliable way of assigning these isomers to a particular spectrum. In a benzene solution the spectrum of this ether changed gradually from an ABX to an A_2X system with an increase in temperature. In carbon disulfide solution over a larger range of temperature this change in chemical shift was not observed. Since it was not possible to explain this equivalence of the chemical shifts of H_A and H_B at a high temperature by any internal molecular motion, it was postulated that this substituted cyclopropyl ether formed a complex with benzene molecules. From the change of the chemical shifts with temperature, the heat of formation and the entropy of formation was estimated for the most abundant isomer.

5. A_2B_2 Analysis of 1,1-Disubstituted Cyclopropanes

With a prior knowledge of the magnitudes of the geminal and vicinal coupling constants for a number of cyclopropane derivatives, the analysis of the more complex A_2B_2 spectrum arising from unsymmetrically 1,1-disubstituted cyclopropanes was attempted. Theoretical A_2B_2 spectra were calculated for a range of probable values of the molecular parameters. The energy transitions and the molecular parameters are obtained from an experimental spectrum by a comparison with

these theoretical spectra. The A_2B_2 analysis of 1-phenylcyclopropylcarboxylic acid in three different solvents was used to illustrate the method. 1-Phenylcyclopropylcarbinol was also examined, but it was found that all the cyclopropyl ring protons were isochronous and were not sufficiently coupled to any of the substituents to cause any fine structure. The A_2X_2 analysis of the C^{13}-H sidebands of the proton resonance of 1,1-diphenylcyclopropane was used to illustrate the analysis of symmetrically 1,1-disubstituted cyclopropanes.

6. $A_2A_2'X$ Analysis of Cyclopropylamine

The five spin system of the ring protons of cyclopropylamine was examined and found to give, in general, an A_2B_2X spectrum. However, by means of the anisotropic solvent effect of benzene on the ring protons the proton spectrum is converted to an $A_2A_2'X$ system. Since the cross-coupling from the A_2 to the A_2' protons is large, the spectrum does not approximate to a pseudo first-order A_4X spectrum. Instead, it is one which may be described as pseudo first-order with combination lines. The presence of the latter allows a fairly complete set of coupling constants to be derived in a simpler way than by a computer attack on the general A_2B_2X spectrum. Conversely, the approach developed here, when applicable, allows the derivation of reliable input parameters for a computer program. From the temperature dependence of the $A_2A_2'X$ case the A_2 and A_2' protons can be distinguished and it is found that the protons <u>trans</u> to the amino group are preferentially shifted to high field by the benzene molecules.

CHAPTER II

VICINAL COUPLING CONSTANTS IN SUBSTITUTED CYCLOPROPANES: PMR OF CHRYSANTHEMUM ETHYL ESTER

1. Introduction

There had been no unequivocal measurements of the cis and trans proton coupling constants in the cyclopropane ring. It had been thought that these two coupling constants were nearly equal[6] in disagreement with the theoretical calculations of Karplus.[7] Later, Closs[8] analyzed 1-chloro-2,2-dimethylcyclopropane as an ABX system and assigned J_{cis} as the smaller of the two vicinal coupling constants with a value of 4 cps and J_{trans} as the larger with a value of 7 cps. In the present work[9] the analyses of the cis- and trans-chrysanthemum ester and the corresponding acids were used to obtain these values. The chrysanthemum ester sample was a mixture of both the cis and the trans isomers, making a complete assignment of spectral lines difficult. It was found more convenient to analyze the cis- and trans-chrysanthemumic acids separately in order to identify the resonance peaks of the ring protons and the substituents. Since the two ring protons interact only with the isobutenyl proton the analysis was that of an ABX system.

It was necessary to use solvents which preferentially shifted the proton signals in such a manner that the resonance peaks of the ring protons were not obscured by the other peaks. Carbon disulfide was used for the cis-chrysanthemumic acid and benzene for the trans acid.

2. Dependence of Vicinal Coupling Constants on Dihedral Angle

The coupling constant $J_{H_aH_b}$ (in units of cps) for a pair of protons H_a and H_b is defined by the expression:[10]

$$\Delta E_{H_aH_b} = \hbar J_{H_aH_b} \underline{I}_{H_a} \cdot \underline{I}_{H_b}$$

where $\Delta E_{H_aH_b}$ is the energy of interaction between the two protons with spins $\underline{I}_{H_a}$ and $\underline{I}_{H_b}$ (in units of $\hbar$), respectively. It has been shown[7,11,12] that the H_a - H_b coupling constant can be calculated semiquantitatively by a valence-bond method which includes nonperfect pairing structures in the ground state wave function Ψ_o, where

$$\Psi_o = \sum_j c_j \Psi_j \quad ,$$

and the Ψ_j's are the nonionic valence-bond structures and the C_j's the coefficient constants. The primary problem of calculating the coefficients is usually done by a variation method. To simplify the calculations only the possible structures which make a significant contribution to the coupling constant are included in the calculation.

For the calculation of the theoretical vicinal coupling constants in substituted ethanes Karplus[7] defined the ground-state wave function as

$$\Psi_o = c_o \Psi_o + \sum_{j=1}^{n} c_j \Psi_j + \sum_{k>n} c_k \Psi_k$$

where Ψ_o is the perfect pairing structure with valence bonds between "chemically bonded" pairs of atoms and no valence bond between H_a and H_b; the Ψ_j's are nonperfect pairing structures with an H_a-H_b valence

bond; and the Ψ_k's are the nonperfect pairing structures with no H_a-H_b valence bond. Applying this method to the proton coupling in ethane the necessary integrals and coefficients were evaluated at 30° intervals of the dihedral angle ϕ between the planes of H_a-C-C and C-C-H_b for the H_a-C-C-H_b fragment from 0° to 180°. The coupling constants calculated for these values can be fitted approximately by a $\cos^2\phi$ curve of the form (7):

$$J = 8.5 \cos^2\phi - 0.28 \text{ (cps)} \quad 0^\circ - \phi - 90^\circ$$
$$= 9.5 \cos^2\phi - 0.28 \text{ (cps)} \quad 90^\circ - \phi - 180^\circ$$

3. Experimental

The spectra were obtained on a Varian DP 60 Mcps spectrometer at room temperature. The chrysanthemum ester (Min. 95%), the cis-chrysanthemumic acid (99.9%), and the trans-chrysanthemumic acid (100%) were of known purity as supplied by Benzol Products Co., and were not purified further. Benzol Products' assignment of the cis and trans forms of the chrysanthemumic acid by infrared methods was assumed to be correct. The results obtained for the later chapters of this thesis indicate that this assumption was justified. Since the acids were of limited solubility, saturated solutions were used; the ester concentrations were approximate by volume since the solvents were only used to obtain preferential proton shifts. Internal benzene was used as the reference point in the measurement of the shifts. The cyclopropyl ring protons coupled to the isobutenyl proton were analyzed

as an ABX system. Appendix I gives the basic wave functions and the energy transitions for this three spin system.

4. Results

A. Cis-Chrysanthemumic Acid in Carbon Disulfide

The spectrum of the cis-chrysanthemumic acid is shown in Figure 2.1 together with the calculated spectrum for the ring protons corresponding to the AB part of an ABX system. The X part of the spectrum, at 114 cps with respect to internal benzene, consists of two doublets whose components are further split by the two isobutenyl methyl groups. The peaks of the latter occur at 324 cps and 328 cps. The methyl groups attached to the cyclopropane ring have the same chemical shift, 357 cps. The carboxyl proton peak is situated at -287 cps with respect to internal benzene and is not shown in Figure 2.1. The results of the ABX analysis gave $J_{AB}(\text{cis}) = 8.7$ cps, $J_{AX} = 8.1$ cps, $J_{BX} \approx 0$ cps. The coupling constant of the X proton to the isobutenyl group protons was about 1.4 cps.

Figure 2.1 Proton resonance spectrum at 60 Mcps of cis-chrysanthemumic acid in carbon disulfide; calibration is with respect to internal benzene.

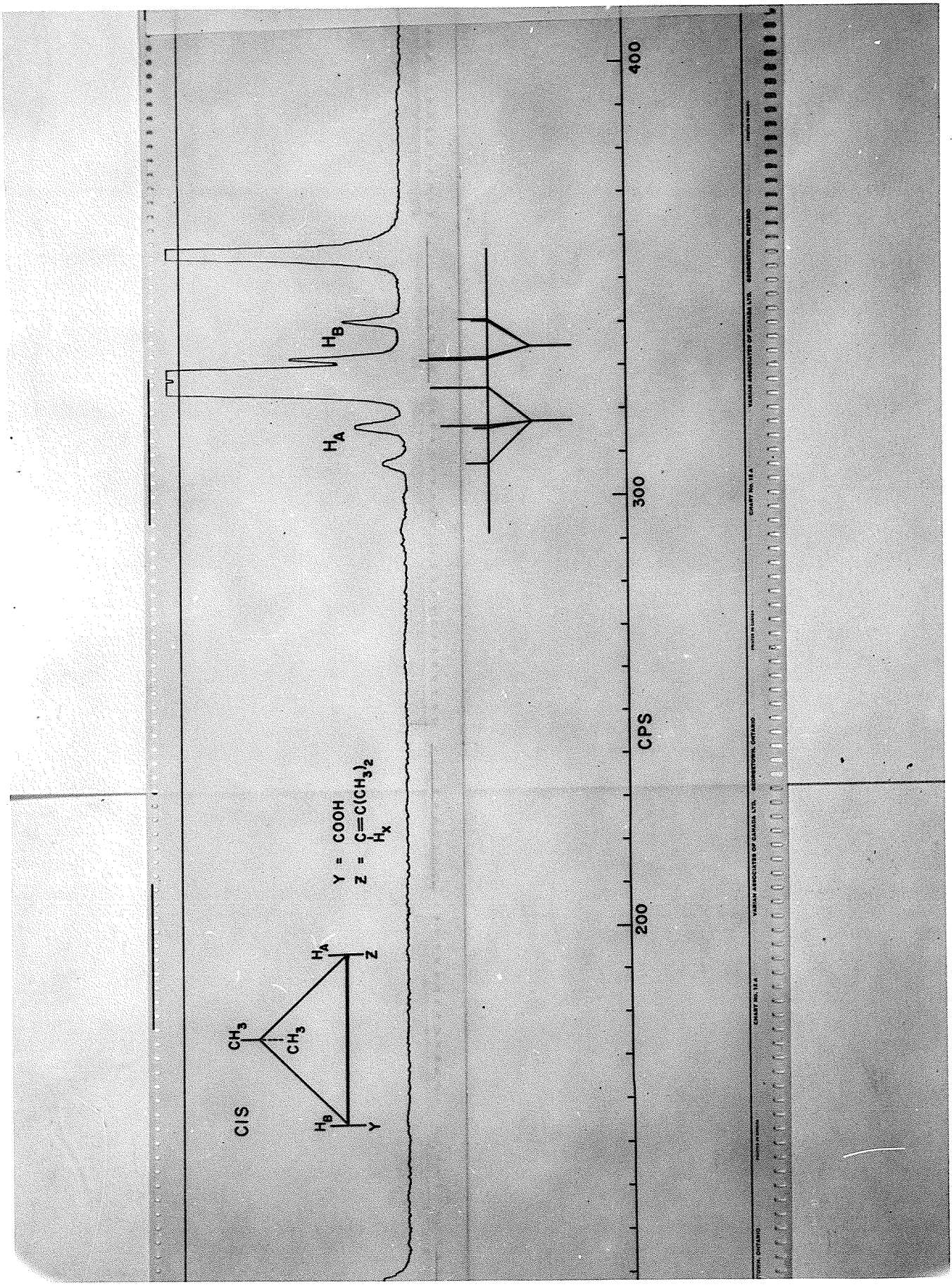
CIS
CH_3
CH_3
H_A
H_B
Z
Y
Y = COOH
Z = $C{=}C(CH_3)_2$
H_X
H_A
H_B
400
300
200
CPS

B. Trans-Chrysanthemumic Acid in Benzene

The proton spectrum is shown in Figure 2.2 together with the calculated spectrum corresponding to the AB part of an ABX system. The X part of the spectrum, at 144 cps from internal benzene, consists of two doublets whose components are further split by the isobutenyl methyl groups by about 1.4 cps. The isobutenyl methyl group peaks occur at 335 cps. The two methyl group peaks attached to the ring occur at 353 cps and 373 cps from internal benzene. The results of the ABX analysis gave J_{AB}(trans) = 5.4 cps, J_{AX} = 7.6 cps, $J_{BX} \approx 0$ cps.

C. Chrysanthemum Ester

The spectra of the chrysanthemum ester are given in Figure 2.3 with the interpretation and the assignment of peaks relative to internal benzene in Table 2.1. The coupling constants have been included in Table 2.2.

Figure 2.2. Proton resonance spectrum at 60 Mcps of trans-chrysanthemumic acid in benzene; calibration is with respect to internal benzene.

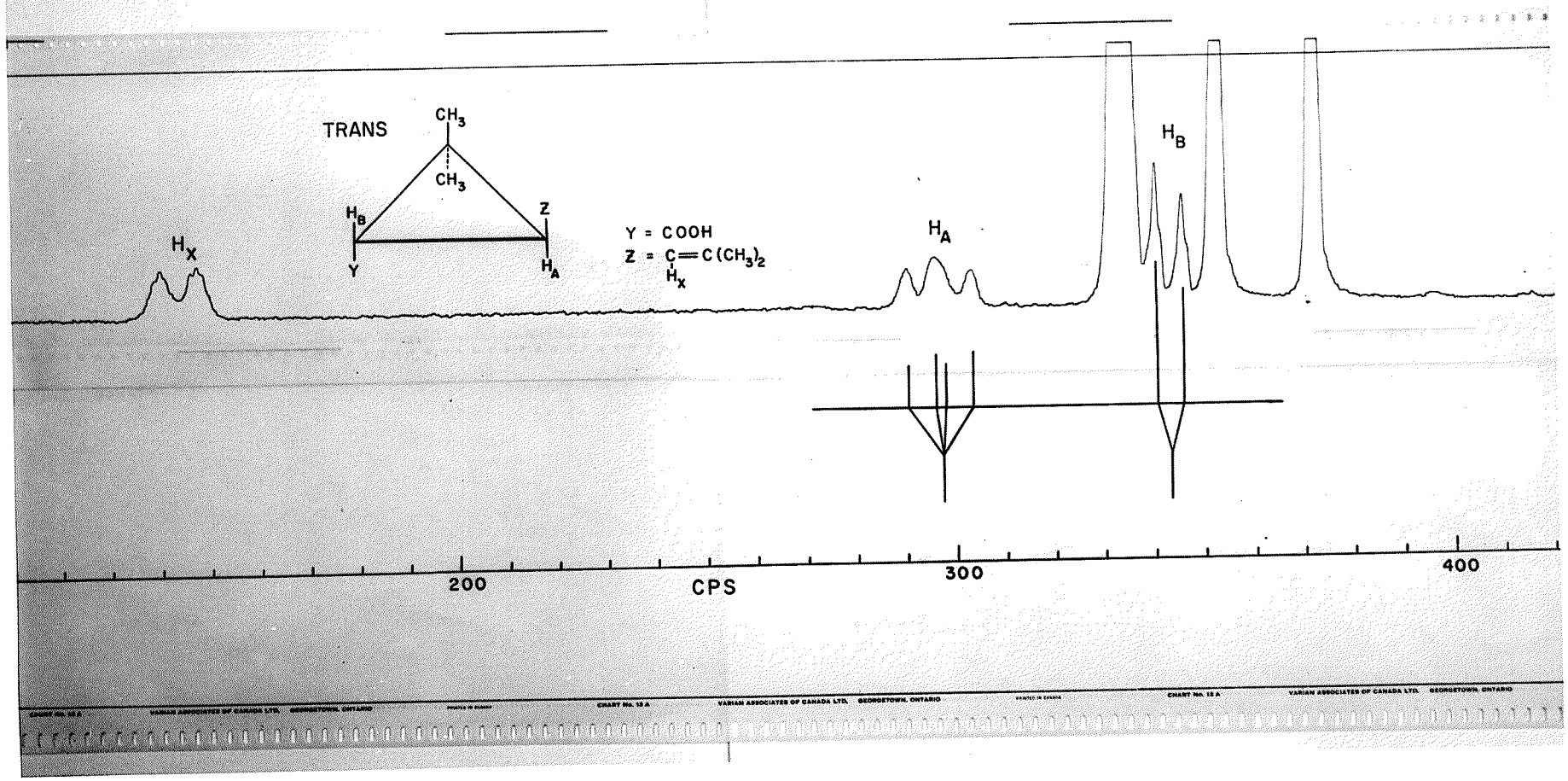
TRANS
CH3
CH3
HB
Z
Y
HA
Y = COOH
Z = C(CH3)2
HX
HX
HA
HB
200
CPS
300
400

Figure 2.3. Proton resonance spectra at 60 Mcps of chrysanthemum monocarboxylic acid ethyl ester: (a) neat; (b) 1:1 in benzene; (c) 1:6 in carbon disulfide. Calibration is with respect to internal benzene.

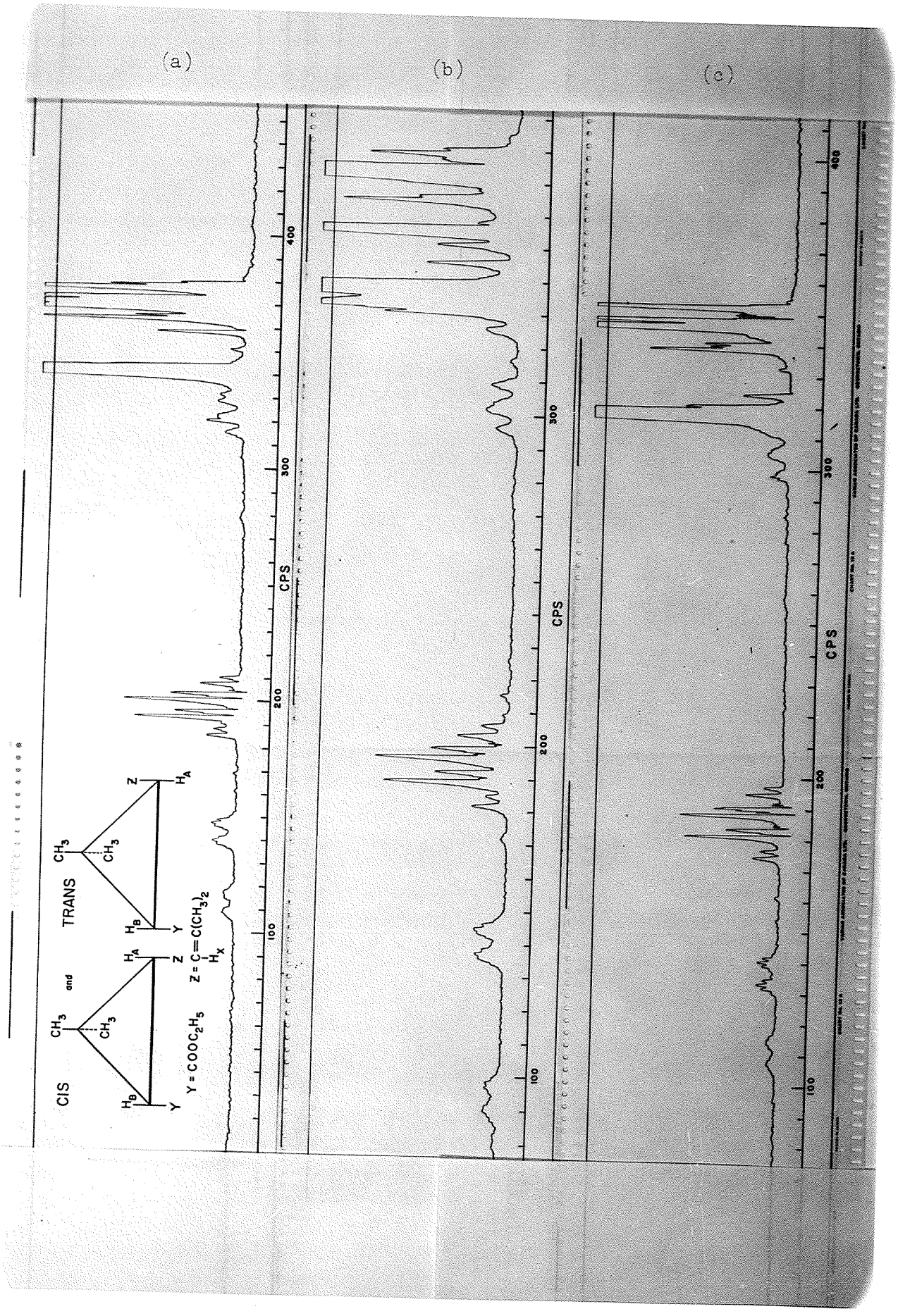
(a)
(b)
(c)
CIS and TRANS
Y = COOC2H5
Z = C(CH3)2
CPS
100
200
300
400

TABLE 2.1

Assignment of peaks of the chrysanthemum ester*

Resonance peak	Neat ester (c.p.s.)	1:1 benzene (c.p.s.)	1:6 CS_2 (c.p.s.)
H_X group (cis)	112	94	111
H_X group (trans)	142	141	136
$-CH_2$ ester (trans)	185	182	174
	192	189	181
	199	196	188
	206	203	195
CH_2 ester (cis)	187	185	176
	194	192	183
	201	199	190
	208	206	197
H_A (trans)	313	297	299
	321	302	304
	321	304	307
	329	309	—
H_A (cis)	332	316	—
	—	325	—
CH_3 isobutenyl (cis)	341	333	318
	—	337	—
CH_3 isobutenyl (trans)	341	337	318
H_B (cis)	351	—	323
	—	—	332
H_B (trans)	358	345	—
	—	351	—
CH_3 ring (trans)	372	356	347
	377	373	352
CH_3 ring (cis)	370	373	345
CH_3 ester (trans)	363	365	338
	370	372	345
	377	379	352
CH_3 ester (cis)	365	367	340
	372	374	347
	379	381	354

*Measurements are with respect to internal benzene.

TABLE 2.2

Chrysanthemum ester coupling constants in c.p.s.

	Neat	1:1 benzene	1:6 CS_2
J_{AB} (cis)	—	8.7±0.2	8.7±0.1
J_{AB} (trans)	5.7±0.2	5.5±0.1	—
J_{AX} (cis)	8.2±0.3	8.0±0.3	7.9±0.3
J_{AX} (trans)	8.1±0.1	7.7±0.1	7.9±0.1
J_{BX} (cis)	0	0	0
J_{BX} (trans)	0	0	0
$J_{X\text{-}CH_2}$ (cis)	—	1.2±0.1	1.4±0.2
$J_{X\text{-}CH_2}$ (trans)	—	1.4±0.1	1.5±0.2
$J_{CH_2\text{-}CH_3\ (ester)}$ (cis)	7.2±0.1*	7.1±0.1*	7.2±0.1*
$J_{CH_2\text{-}CH_3\ (ester)}$ (trans)	7.1±0.1*	7.1±0.1*	7.2±0.1*

*A first-order analysis value.

Since the ethyl group in the cis isomer is in a different magnetic environment than the ethyl group in the trans isomer, the cis and trans CH_3 resonance peaks from this group are slightly shifted from each other. Similarly the CH_2 peaks are displaced from each other as is shown in Figure 2.3. From spectra of the ester mixture the percentage of the trans and the cis isomers was readily calculated by taking advantage of this displacement of the CH_2 lines in the cis and trans esters. A comparison of the heights of corresponding resonance peaks gave the percentage of the trans isomer. A more accurate method would be the comparison of peak areas, but since the peak widths are no doubt very nearly the same this first method was thought to be sufficient. Within experimental error the same percentage, $62.0 \pm 1.1\%$ trans isomer, was obtained for the ester neat, in benzene, and in carbon disulfide. A previous infrared study gave 65% trans ester.[13]

5. Discussion

A. Cyclopropane

Karplus has expressed the coupling constant between protons a and b in the fragment H_a-C-C-H_b as a squared cosine function of the dihedral angle.[7] A consideration of the electron-diffraction results of Hassel and Viervoll for cyclopropane yield 0° and approximately 147° for the dihedral angle between the cis-vicinal and trans-vicinal protons, respectively.[14] Karplus then predicts 8.2 and 6.4 cps for the cis and trans coupling constants, respectively, compared to 8.7

and 5.4 found experimentally. From a more recent study of the cyclopropane geometry,[15] the dihedral angle is about 144° and the calculated J_{trans} would be 5.9 cps. It is not impossible that the large groups in these substituted cyclopropanes distort the angle somewhat. There is, however, a rough agreement between calculated and observed values.

It had been thought that Karplus' calculations did not apply to the cyclopropane ring.[6] Jackman found $J_{cis} = J_{trans} = 6.3$ cps from an analysis of trans-1,2-dibromocyclopropane.[6] The triplet observed for the proton resonances of the CHBr groups in this A_2X_2 system was taken as evidence that J_{cis} and J_{trans} are equal. However, it has since been shown that in an A_2X_2 analysis a triplet does not necessarily indicate the equality of two of the couplings in the system. Abraham and Bernstein[16] showed that the same triplet A_2X_2 spectrum could be calculated using the average value of the coupling constants. The value of 6.3 cps obtained by Jackman for the cis and trans coupling constants in cyclopropanes must therefore represent only an average value of these two vicinal coupling constants. There may also be a small effect depending on the electronegativity of the substituents. Small effects have been observed in substituted ethanes for which the H-C-C-H coupling constant is given by 8.4 - 0.4E, where E is the electronegativity of the substituent.[17] The smaller value of 6.3 cps found by Jackman as compared to our average of 7.0 cps is in the right direction. From data on over 100 substituted ethylenes a definite correlation has been established between the

electronegativity of the atom in the substituent group attached to the vinyl carbon and the values of the proton coupling constants.[18, 19] Such electronegativity effects are larger for unsaturated systems such as ethylenes than for the ethanes.

The proton coupling constants for cyclopropane itself have been measured from the C^{13} satellites of its proton spectrum.[20] The value of 7.5 ± 0.5 cps quoted for both the *cis* and the *trans* coupling constants is again, no doubt, an average value.[21]

A recent publication gives the proton spectrum of thujopsene and hinokiic acid.[22] Only the X part of an ABX spectrum is visible and only the sum of J_{cis} and J_{trans} can be obtained. This is 14.0 cps, a value in keeping with the sum of 14.1 obtained here.

B. Comparison with Other Ring Systems

In Table 2.3 there are collected the calculated and observed proton coupling constants for eight different values of the dihedral angle. They are taken from data given for three-, five-, and six-membered rings.[23-25] The six-membered rings are assumed to exist in one conformation only.[24] A certain amount of distortion from the assumed dihedral angle is possible for most of these rings but the overall agreement between theory and experiment is encouraging.

On the other hand, values of proton coupling constants in three-membered rings containing the heteroatoms oxygen, nitrogen, and sulfur do not agree very well with Karplus' predictions,[26-30] although the ratios of *cis* to *trans* coupling constants are roughly those predicted

TABLE 2.3

CALCULATED AND OBSERVED PROTON COUPLING CONSTANTS IN CPS FOR SOME RING COMPOUNDS

Angle	Coupling Constants Calculated	Observed	Reference
0°	8.2	7.7 - 9.3	9, 23, 25
ca. 44°	4.1	4.0 - 4.4	23
ca. 60°	1.7	2 - 4	24
ca. 79°	0	0	23
ca. 90°	0	0	23
ca. 120°	2.1	2.2 - 4.6	23, 25
ca. 144°	5.9	5.4	9
ca. 180°	9.2	5 - 8	24

TABLE 2.4

A COMPARISON OF THE VICINAL COUPLING CONSTANTS IN THREE-MEMBERED RINGS

Compound	J_{cis} (cps)	J_{trans} (cps)	J_{cis}/J_{trans}	Reference
Cyclopropanes	8.7	5.4	1.6	9
Ethylene Sulfides	7.15	5.65	1.27	26, 29
Ethylene Oxides	4.5	3.1	1.43	26
Ethylene Imines	6.3	3.8	1.66	26
(Theoretical)	8.2	5.9	1.4	7

by Karplus. These are given in Table 2.4. It is interesting to note that the deviation from the predicted values increases with the difference in electronegativity between the heteroatoms and carbon. The deviation is in the same direction as for the substituted ethylenes mentioned above. For sulfur, with an electronegativity similar to that of carbon, the coupling constants are close to the value found for the cyclopropanes. The geometries of these molecules show relatively small changes,[26] and it seems reasonable to assume that the couplings in these heterocyclic rings depend not only on angular factors but also on the electronegativity of the heteroatom.

6. Conclusion

Unequivocal values for the cis and trans proton coupling constants in the substituted cyclopropane ring have been observed. They fall reasonably well into the scheme devised by Karplus. A consideration of the proton coupling constants in heterocyclic propanes suggests that both angular factors and electronegativities are important in determining their magnitudes. It was also shown that the measurements of relative concentrations of geometrical isomers of substituted cyclopropanes can be measured rapidly in favorable cases by nuclear magnetic resonance methods.

CHAPTER III

PROTON COUPLING CONSTANTS IN SUBSTITUTED CYCLOPROPANES

1. Introduction

In Chapter II the cis proton coupling constant in the cyclopropane ring was shown to be larger than the trans coupling constant.[9] The magnitudes of these vicinal couplings are in reasonable agreement with the $\cos^2\phi$ relationship between the coupling constant and the dihedral angle ϕ as predicted by Karplus.[7] There had been some disagreement in the literature about the relative magnitudes of these constants.[8] The coupling constants between geminal protons have been measured for a number of cyclopropane derivatives.[31] The results are compared with the coupling constants for the cyclopropane ring which have been measured by others.[32-35] It is suggested that the geminal couplings are of opposite sign to the vicinal coupling constants and therefore negative. Thus the comparison of the geminal coupling with the H-C-H angles[36] is no longer valid. It is also suggested that the geminal couplings are zero in ethylene sulfides and positive in epoxides and that there is a change of sign in going from carbon through sulfur to oxygen as the third atom in the ring. The vicinal coupling constants depend on the dihedral angle as predicted by theory but the substituent effects do not appear to follow a simple dependence on the electronegativity as they do in substituted ethanes.

2. Experimental

The proton resonance spectra were obtained on a Varian DP 60 Mcps spectrometer at room temperature. The analyses were the averages of ten spectra run forward and reverse and were repeated on a separate occasion to verify the findings.

The compounds were a gift from Dr. Layton L. McCoy. Their physical constants are given in his paper[37] and were certainly of sufficient purity since a weak impurity peak was found in only one case. Solvents were used which preferentially shifted the ring protons so that they were not obscured by other peaks. For reasons of solubility a mixed solvent of acetone and benzene was used for the dicarboxylic acids. For these reasons chemical shift comparisons are of doubtful value. Tetramethylsilane (TMS) was the internal reference.

3. Results

Coupling between ring protons and substituents such as methyl groups was not observable and must thus be less than 0.4 cps. Therefore, the ring proton spectra were of the four-peak AB type and were analyzed as such. Figure 3.1 shows the structure and the proton resonance spectrum of a concentrated solution of trans-1-chloro-2-methyl-1,2-cyclopropanedicarboxylic acid (I) in a mixed solvent of 1:8 acetone to benzene. The spectrum of a concentrated solution of cis-1-chloro-2-methyl-1,2-cyclopropanedicarboxylic acid (II) in a mixed solvent of 1:1 acetone to benzene and in formic acid as a

Figure 3.1. Proton resonance spectrum at 60 Mcps of trans-1-chloro-2-methyl-1,2-cyclopropanedicarboxylic acid (I) in a mixed solvent of 1:8 acetone to benzene; calibration is to low field of internal TMS.

I TRANS DICARBOXYLIC ACID

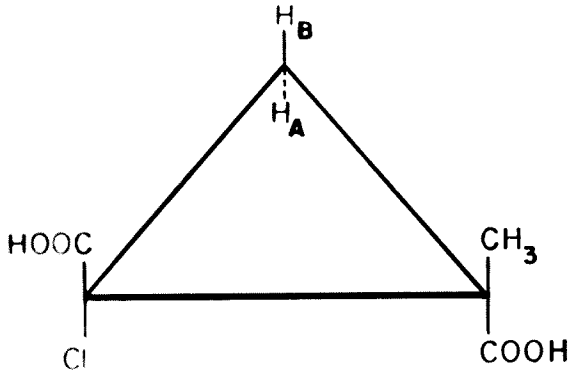

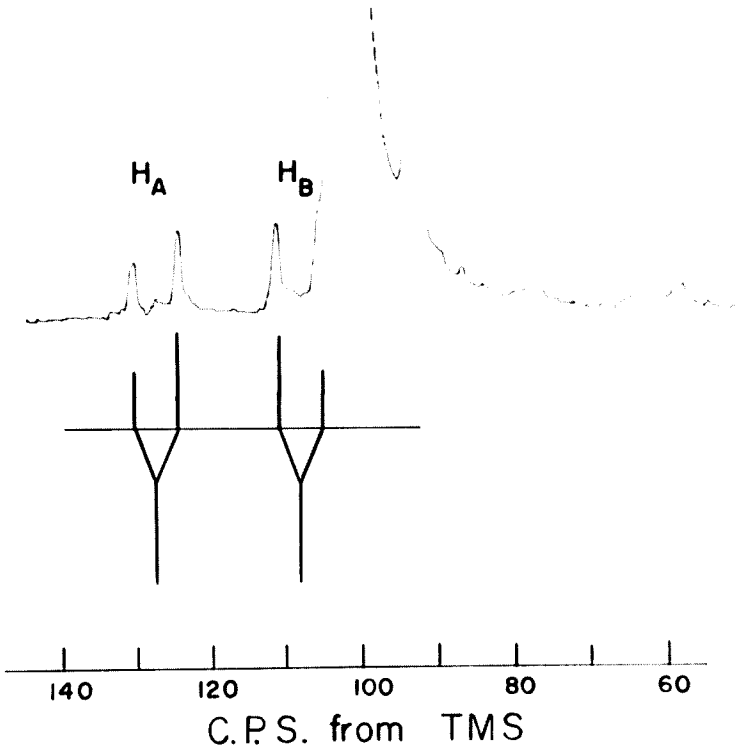

solvent is shown in Figures 3.2 and 3.3, respectively. The proton resonances of acetone in Figures 3.1 and 3.2 and of formic acid in Figure 3.3 also occur in the AB region of these spectra. Figure 3.4 shows the proton resonance spectrum of cis-dimethyl-1-chloro-2-methyl-1,2-cyclopropanedicarboxylate (III) diluted 1:3 in benzene. Figure 3.5 shows the proton resonance spectrum of a mixture of cis- (IV) and trans-1-chloro-2-methyl-2-cyanocyclopropane (V) carboxylates diluted 1:3 in benzene.

Table 3.1 gives the chemical shifts relative to internal tetramethylsilane as well as the coupling constants for the compounds I to V. The assignment of the A and B ring protons was made on the basis of that given by Graham and Rogers[32] for cyclopropane-1,1,2-tricarboxylic acid and could conceivably be interchanged. The carboxyl protons are not included in Table 3.1. They occurred at approximately 600 cps to low field of the reference and are omitted from the discussion.

Figure 3.2. Proton resonance spectrum at 60 Mcps of cis-1-chloro-2-methyl-1,2-cyclopropanedicarboxylic acid (II) in a mixed solvent of 1:1 acetone to benzene; calibration is to low field of internal TMS.

II CIS DICARBOXYLIC ACID

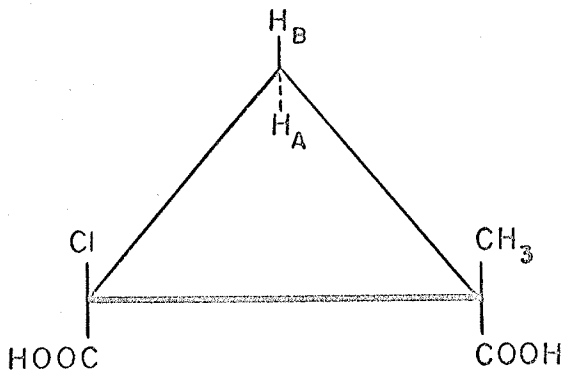

III

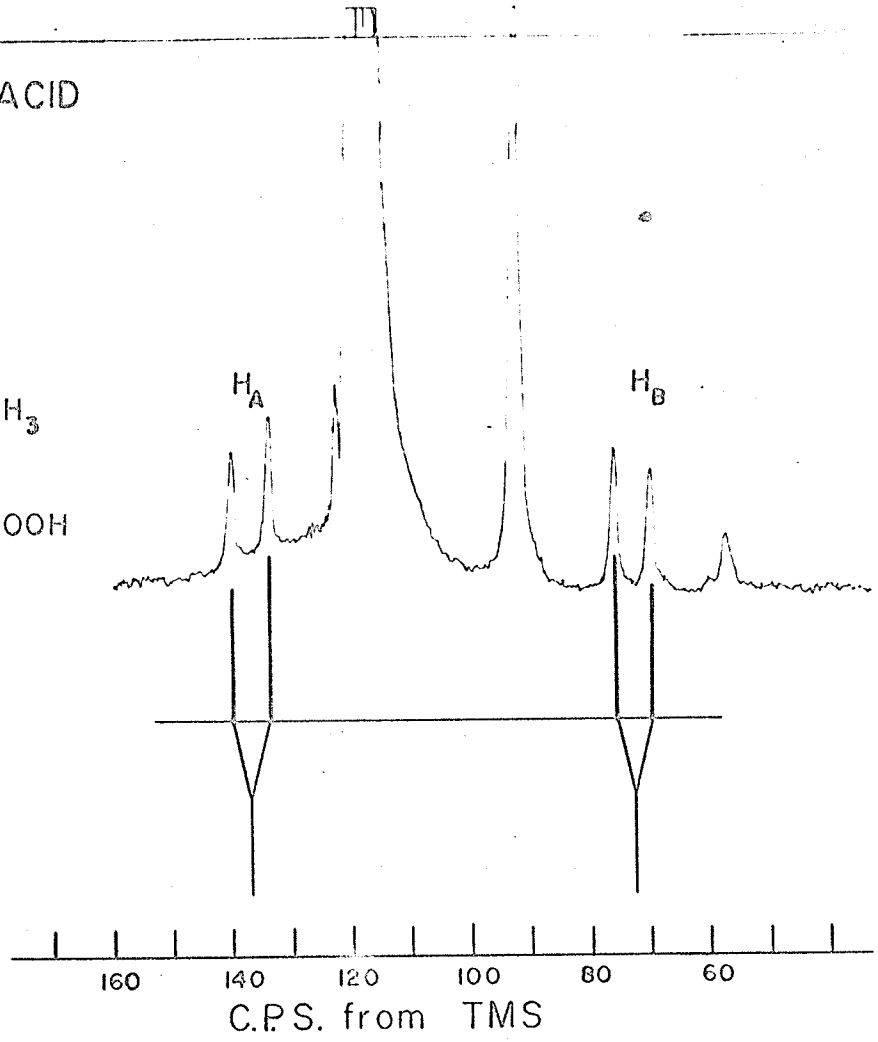

Figure 3.3. Proton resonance spectrum at 60 Mcps of cis-1-chloro-2-methyl-1,2-cyclopropanedicarboxylic acid (II) in formic acid; calibration is to low field of internal TMS.

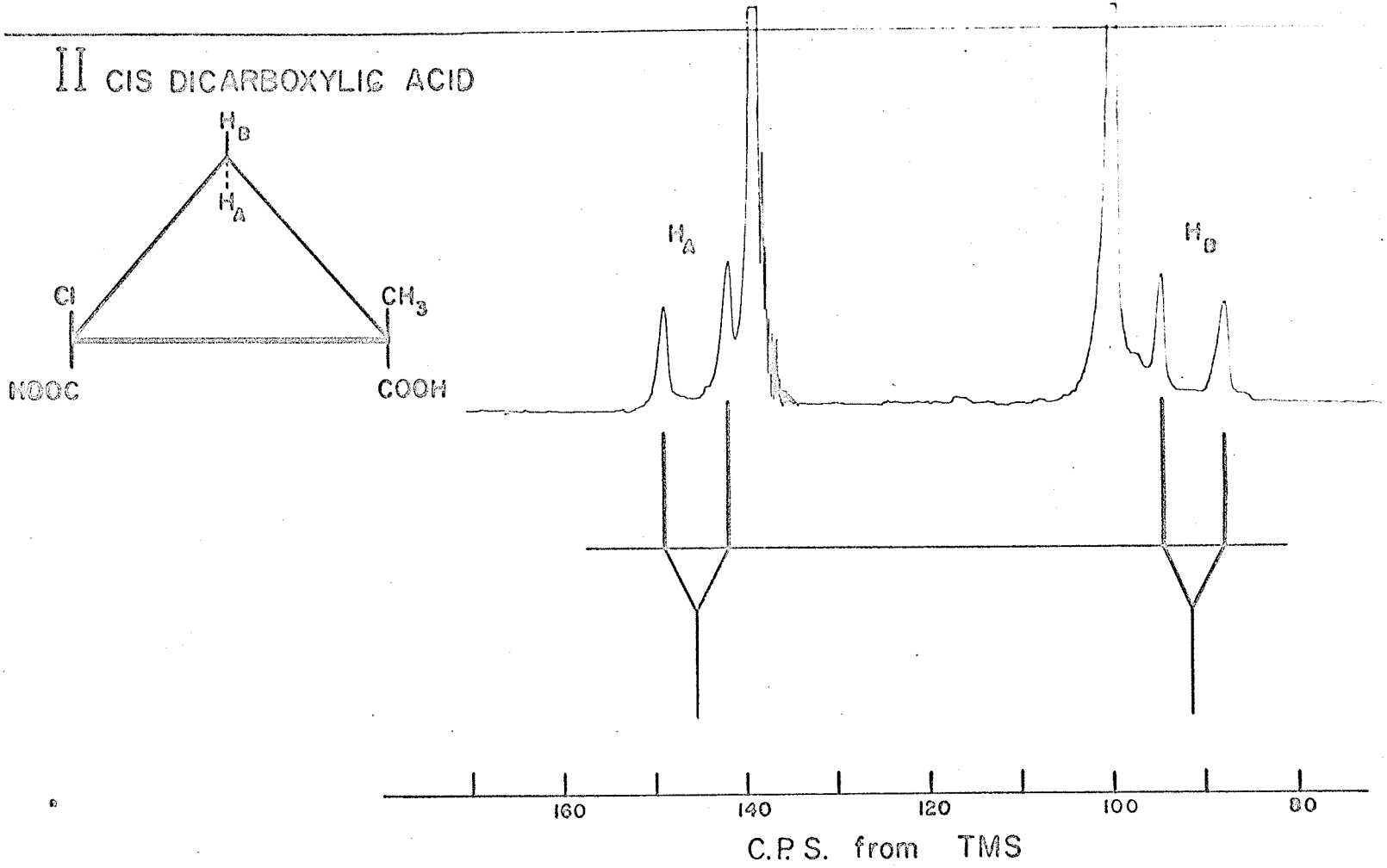
II CIS DICARBOXYLIC ACID
H_B
H_A
Cl
CH_3
NOOC
COOH
H_A
H_B
160
140
120
100
80
C.P.S. from TMS

Figure 3.4. Proton resonance spectrum at 60 Mpcs of cis-dimethyl 1-chloro-2-methyl-1,2-cyclopropanedicarboxylate (III) diluted 1:3 in benzene; calibration is to low field of internal TMS.

III CIS DICARBOXYLIC ESTER

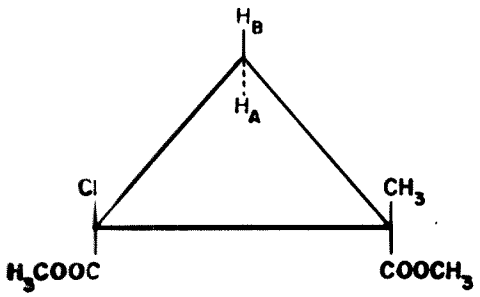

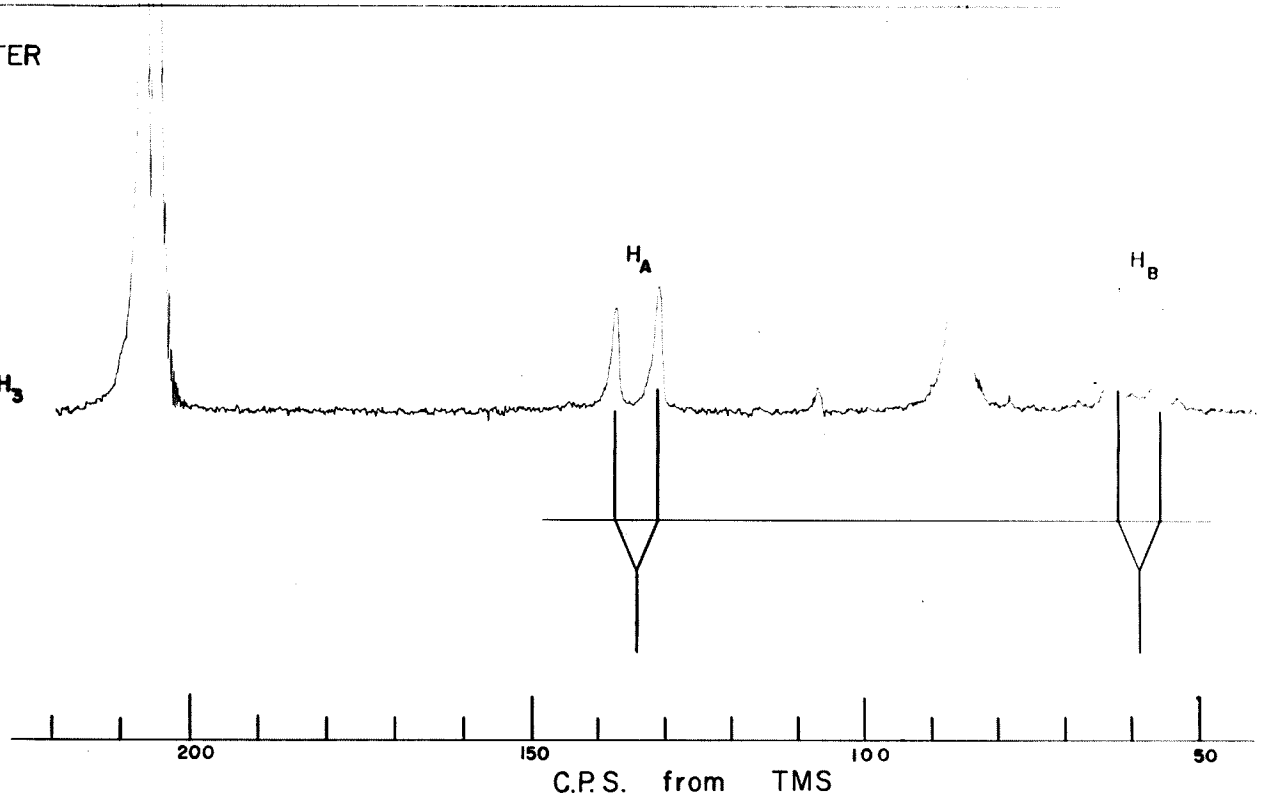

Figure 3.5. Proton resonance spectrum at 60 Mcps of a mixture of cis- (IV) and trans-1-chloro-2-methyl-2-cyanocyclopropane (V) carboxylates in benzene solution; calibration is to low field of internal TMS.

CIS CYANO CARBOXYLATE

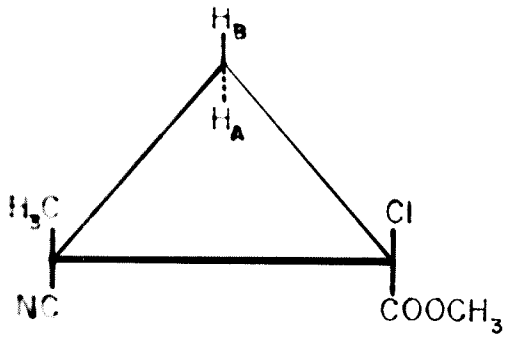

(IV)

TRANS CYANO CARBOXYLATE

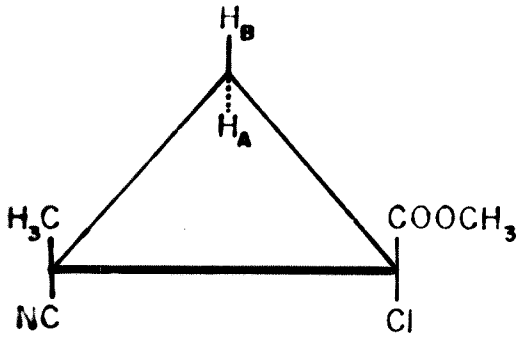

(V)

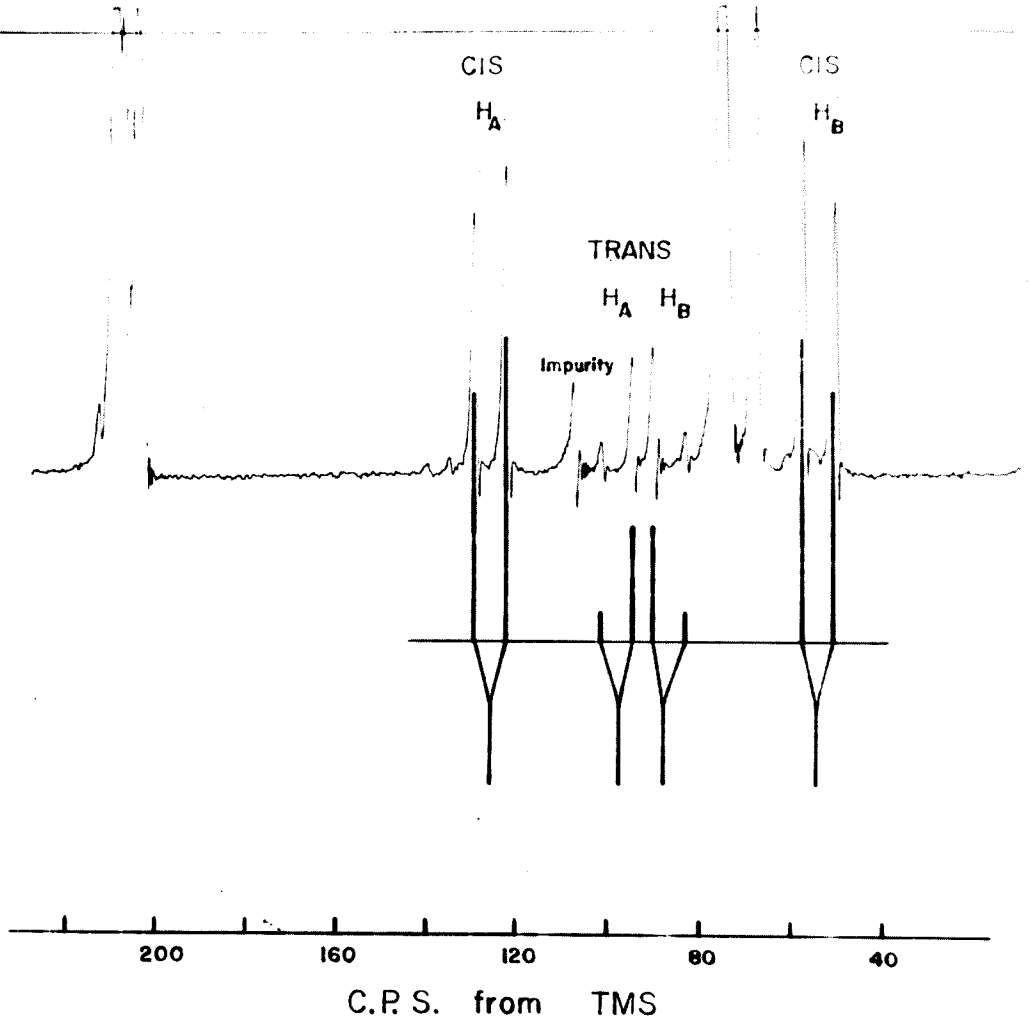

TABLE 3.1

PROTON CHEMICAL SHIFTS AND COUPLING CONSTANTS OF SOME SUBSTITUTED CYCLOPROPANES

Compound (numbered as in text)	State	Chemical Shifts*				Coupling Constant $J_{AB} = J_{gem}$ (cps)
		H_A	H_B	CH_3	$COO\ CH_3$	
I	Sat'd in 1:8 acetone/benzene	126.4	108.0	90.3	-	6.44 ± 0.12#
I	Sat'd in 1:10 acetone/benzene	128.2	108.6	91.0	-	6.37 ± 0.09
II	Sat'd in 1:1 acetone/benzene	136.4	72.7	94.1	-	6.39 ± 0.05
II	Sat'd in formic acid	145.2	91.5	100.3	-	6.97 ± 0.18
III	Diluted 1:3 in benzene	134.0	59.5	85.6	203.9, 206.0	6.52 ± 0.12
IV	Diluted 1:3 in benzene	125.7	53.5	74.5	210.3	7.02 ± 0.11
V	Diluted 1:3 in benzene	98.5	87.0	67.5	206.1	7.06 ± 0.13

*In cps at 60 Mcps from internal TMS.

#Standard deviations.

4. Discussion

A. Coupling Constants

The values of the three types of coupling constants for cyclopropane derivatives which are known fairly accurately are given in Table 3.2. The labelling in this Table corresponds to I. They are

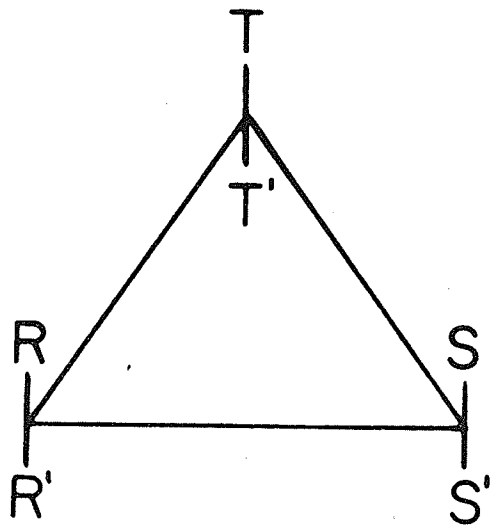

I

examined as to magnitude and sign.

i. Vicinal Couplings

The average values of $J_{\underline{cis}}$ and $J_{\underline{trans}}$ in Table 3.2 are 8.78 and 5.65 cps, respectively. The most recent determination of the cyclopropane geometry gives 113.8 ± 2° for the H-C-H angle,[15]

TABLE 3.2

COUPLING CONSTANTS IN SUBSTITUTED CYCLOPROPANES IN CPS

Compound	R	R'	S	S'	T	T'	J_{cis}	J_{trans}	J_{gem}	Reference
1	H	H	H	COOH	H	H	ST = 8.0 TR = 10.5 T'R' = 11.0	ST' = 4.6	-4.3	34
2	COOH	Cl	CH_3	COOH	H	H	-	-	6.44	This chapter
3	Cl	COOH	CH_3	COOH	H	H	-	-	6.39 (6.97)	This chapter
4	Cl	$COOCH_3$	CH_3	$COOCH_3$	H	H	-	-	6.52	This chapter
5	CH_3	CN	Cl	$COOCH_3$	H	H	-	-	7.02	This chapter
6	CH_3	CN	$COOCH_3$	Cl	H	H	-	-	7.06	This chapter
7	OCH_3	H	Cl	Cl	H	H	7.90	5.28	8.38	32
8	OC_2H_5	H	Cl	Cl	H	H	8.25	5.27	8.09	32
9	COOH	H	COOH	COOH	H	H	9.33	6.55	4.80	32
10	CH_3	C_6H_5	Cl	Cl	H	H	-	-	7.10	32
11	H	C_6H_5	Cl	Cl	H	CH_3	8.28	-	-	32
12	H	COC_6H_5	COC_6H_5	H	H	COC_6H_5	-	5.61 (6.0)	-	32 (8)
13	COOH	CH_3	C_6H_5	C_6H_5	H	H	-	-	4.65	33
14	COOH	H	C_6H_5	C_6H_5	H	H	7.70	6.85	-4.37	33
15	NO_2	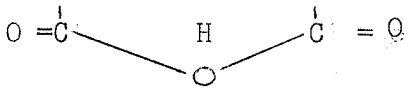			H	H	9.0	6.0	6.7	53

TABLE 3.2 (continued)

Compound	R	R'	S	S'	T	T'	J_{cis}	J_{trans}	J_{gem}	Reference
16	COOH	H	$CH=C(CH_3)_2$	H	CH_3	CH_3	8.7	-	-	Chapter II
17	H	COOH	$CH=C(CH_3)_2$	H	CH_3	CH_3	-	5.4	-	Chapter II
18	CH_3	CH_3	H	$S-C_6H_5$	H	H	8.5	5.	5	35
19	CH_3	CH_3	Cl	H	H	H	7.39	4.10	-5.98	Chapter IV
20	Cl	Cl	O-R	H	H	H	7.8	5.0	-8.8	Chapter V
21	C_6H_5	COOH	H	H	H	H	ST = Ca. 9.6 S'T'= Ca. 9.8	6.9	-4.0	Chapter VI
22	C_6H_5	C_6H_5	H	H	H	H	9.55	6.42	-	Chapter VI
23	H	H	H	NH_2	H	H	ST = 6.6 TR T'R' = 12.5	ST' =3.6 TR' =7.5	-5.5	Chapter VII

compared to a previous angle of 118°.[14] The smaller angle improves the agreement between J_{trans} and the predicted value. For an angle of 118° the dihedral angle is very nearly 147°, giving a predicted value of 6.4 cps, while for 114° the dihedral angle is about 144°, giving a predicted value of 5.9 cps.

However, apart from the fact that the theory assumes sp^3 hybridization and is, furthermore, one which is to be used as a rough guide only, substituent effects may be of some importance. Glick and Bothner-By[17] some time ago suggested that in ethyl compounds the average vicinal coupling constant was a linear function of the electronegativity: J (cps) = 8.4 - 0.4E, where E is the Huggins electronegativity of the substituent. A slightly different relation, based on more extensive data, has been recently given by Banwell and Sheppard.[38] They have found it to be valid for more heavily substituted ethanes. In both relations the dependence on electronegativity is about ten times smaller than in vinyl compounds.[18,19]

Although there is a variation of vicinal coupling constants with the substituent for the cyclopropanes it does not clearly depend on the electronegativity of the substituent. Thus, for compounds 9 and 14 the substituent is the carboxyl group and $J_{cis} + J_{trans}$ = 15.88 and 13.55 cps, respectively. The neighbor groups are carboxyl groups in the one case and phenyl groups in the other. In compound 15 $J_{cis} + J_{trans}$ = 15.0 cps and the trend is in the opposite direction to that expected from the behaviour of ethanes. In the latter compound

there may be a certain amount of distortion of the molecule. Probably for all these compounds the high degree of substitution involves enough distortion of the molecule to obscure any small linear dependence of the coupling constants on the electronegativity of the substituent. Compounds 1 and 23, the only monosubstituted molecules in Table 3.2, do show a substituent effect on vicinal couplings which appears to be appreciable and in the right direction.

It has been suggested that the cyclopropane ring has some π - electron character,[39] but it appears that, if present, it does not contribute noticeably to the coupling. Otherwise there should be a large substituent electronegativity effect as in ethylenic compounds.[18, 19] Also, appreciable coupling to the methyl substituents through four bonds would be expected as is usually observed when the C-C bond has appreciable π-character.[40]

ii. Geminal Couplings

In the five cases in Table 3.2 where it has been determined, J_{gem} is of opposite sign to the vicinal couplings. Chapters IV, VI and VII discuss the determination of the relative signs between spin couplings by double resonance experiments and by the analysis of complex systems. In almost all cases, with the exception of certain ethylenes and epoxide groupings, the opposite sign of the geminal and vicinal couplings is true also in other systems.[41-45] The agreement between theory and experiment for vicinal couplings leads to the conclusion that these are positive as required by theory.

Then geminal couplings through two bonds are negative, at least in sp^3 systems. This sign convention is at present being disputed by Musher.[46] However, it is still suggested that all geminal coupling constants in Table 3.2 are negative, as predicted by the Dirac vector model.[47]

The magnitudes are smaller than those found in tetrahedral systems but similar to the one found in propylene oxide, although it is zero in propylene sulfide.[29] J_{gem} has the same sign as the vicinal coupling constants in a series of epoxides with an average value of 5.7 cps.[27,30] J_{gem} therefore goes through about zero for the heterocyclic sulfides and becomes negative for the cyclopropanes. The H-C-H angles in both ethylene oxide and ethylene sulfide are almost equal[26] and the relation between J_{gem} and this angle is no longer justified,[36] especially since J_{gem} is almost certainly negative in sp^3 systems. The reason for the change in sign of J_{gem} on going from the oxide to cyclopropane remains to be explained.

For compounds 7, 8, 9 and 15 the sum of the three couplings is fairly constant, as noted by Graham and Rogers.[32] But if J_{gem} is negative for these compounds, then the sum varies between 4.8 and 11.1 cps and this regularity no longer holds.

B. Chemical Shifts

These were determined either for the pure compounds or in solvents which have large solvent effects. Detailed discussion is

therefore not in order. Some instructive points may, however, be made about the mixture of cis- and trans-1-chloro-2-methyl-2-cyano-cyclopropane carboxylates. An analysis by gas chromatography of this mixture gave approximately 20 per cent trans ester.[48] From peak heights 20.5 ± 0.5% was found for the less abundant component, which is assumed to be the trans isomer.

Graham and Rogers[32] found the proton trans to the two carboxyl groups in cyclopropane-1,1,2-tricarboxylic acid to be more shielded than the cis proton. On that basis the proton trans to the carboxymethyl and cyano groups (proton B) in the cis ester can be assigned to the peaks centred at 53.5 cps in Figure 3.5. The shielding difference is presumably due to magnetic anisotropy effects since electronegativity effects should be the same for both protons. On interchanging the chlorine and the carboxymethyl group, proton A is shifted to high field by 27.2 cps and proton B to low field by 33.5 cps. The difference between these values could then be attributed to the anistropy of the chlorine.

Two weaknesses in this argument are clear. First, although the dielectric constant of benzene is low, field effects arising from the difference in dipole moment of the two isomers could be appreciable.[49] Second, the solvent effect due to the magnetic anisotopy of the benzene may be large.[50] If the benzene molecules pack around the solute molecules in such a way as to avoid electron-rich centres[51] then proton B in the cis isomer should experience the highest solvent

shift to high field. The size of this shift is possibly as large as 0.5 ppm or even more.[50]

The conclusion is, of course, that before any definite statements about substituent effects can be made, systematic studies must be carried out in a number of well-chosen solvents. Dipole moments of the solutes are also needed. Due to the limited solubility of carboxyl-substituted cyclopropanes in electrically and magnetically inert solvents, the synthesis of a series of cyclopropane derivatives with other groups is indicated. That appreciable substituent effects are present is seen from the chemical shift of cyclopropane at 13.2 cps with respect to tetramethylsilane.[52]

CHAPTER IV

RELATIVE SIGNS OF THE GEMINAL AND VICINAL COUPLING CONSTANTS BY DOUBLE RESONANCE

1. Introduction

The proton - proton spin coupling constants obtained from high resolution NMR spectroscopy are usually determined with an ambiguity in signs. Two methods are available to determine the relative signs of these coupling constants, the exact analysis of a strongly coupled three or more spin system and the double irradiation technique.[54,55] This latter method was used to determine the relative signs between the geminal and vicinal couplings in a cyclopropane derivative in this chapter while the method of exact analysis is used in Chapters VI and VII.

Recent studies of the relative signs of spin coupling constants in substituted ethanes have shown that the geminal and vicinal coupling constants are opposite in sign,[41-45,56,57] in disagreement with the theoretical calculations.[7,36] It has now been established, following suggestions by Karplus,[58] that the one bond C-H coupling has the same sign as the three bond H-C-C-H vicinal coupling constants[59] and has the opposite sign to the two bond H-C-H geminal coupling[60] in substituted ethanes. Since the directly bonded C-H coupling constants are almost certainly positive, that is, the antiparallel nuclear spin state corresponds to a more stable state than the parallel orientation, it may be concluded that J_{gem}

is negative and $J_{\underline{vic}}$ is positive. This would in effect agree with the Dirac vector model.[47] Buckingham and McLauchlan have determined the absolute sign of the coupling constant in p-nitrotoluene by a new NMR technique.[61] This coupling is positive, in agreement with that which can be deduced on the assumption that the $C^{13}H$ coupling is positive. A recent theoretical study by Musher on this subject gives results which are of the opposite sign designation.[46] To see whether these results would be the same for substituted cyclopropanes, Freeman's double resonance technique[62] was used on 1-chloro-2,2-dimethylcyclopropane.

2. Double Nuclear Magnetic Resonance of an ABX System

The multiplet structure that is observed between groups of magnetically equivalent nuclei in the spectra of liquid samples has been shown to be due to a scalar coupling $J\ \underline{I}\cdot\underline{S}$.[63] For this coupling to be observed the nuclei must have different chemical shifts. The effect of this coupling can be made to disappear if one of the groups is subjected to a second radiofrequency field H_2 at ν_2 such that $\gamma H_2 \gg 2\pi |J|$. The new form of the resonance of the other groups may be examined simultaneously by means of the usual weak radio-frequency field H_1 at ν_1.

Evans[54] has shown how double resonance may be used to obtain the relative signs of the spin coupling constants on the three spin system of the thallium diethyl cation, and Freeman has extended the method for use with proton - proton couplings.[55] As in the analytical

method the molecule under investigation must contain at least three non equivalent nuclei or groups of nuclei with spin interactions to determine the relative signs of the couplings. Appendix II gives the general analysis of the transition energies for a three spin system under double irradiation.[64] The method of Freeman for the spin decoupling of an ABX system is discussed below.

A. Double Irradiation, J_{AB} and J_{BX} of Like Sign

If it is assumed that all three coupling constants in an ABX system are positive, then it is possible to tabulate the spin states of the proton neighbors for each of the twelve observed transitions numbered in Figure 4.1. For the two possible spin orientations, $m = +\frac{1}{2}$, is represented by α, and $m = -\frac{1}{2}$ by β. For each of the observed A transitions m_X and m_B values can be assigned for a particular choice of the signs of J_{AB} and J_{AX}, as illustrated in Figure 4.2. With a positive coupling constant α_i will cause the low-field resonance and β_i the high-field resonance. For a negative coupling where the spins of the nuclei tend to be parallel, β_i is to low field and α_i is to high field. In Table 4.1 the A, B, and X transitions are given with respect to the spin states of the proton neighbors, assuming that all the coupling constants are positive and that $|J_{BX}| > |J_{AB}| > |J_{AX}|$.

Now, it is possible to irradiate the system at a frequency intermediate between lines 5 and 6 with a power high enough to destroy J_{AX} and yet low enough to avoid perturbing transitions 7 and 8.

Figure 4.1 First order spectrum of an ABX system.

Figure 4.2 First order spectrum of the A nucleus coupled to two other nuclei of spin $\frac{1}{2}$.

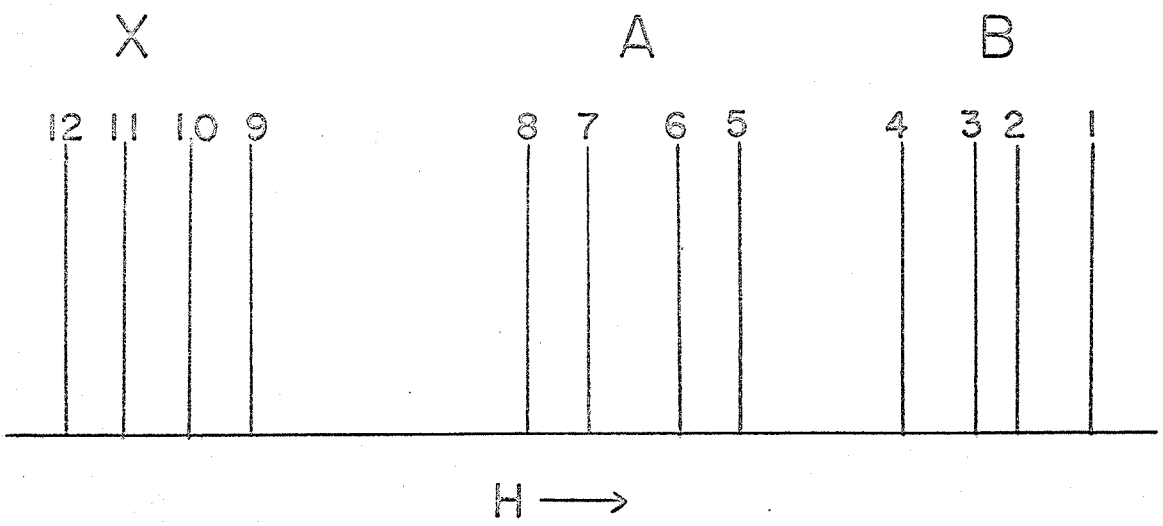
X
A
B
12 11 10 9
8 7 6 5
4 3 2 1
H ⟶

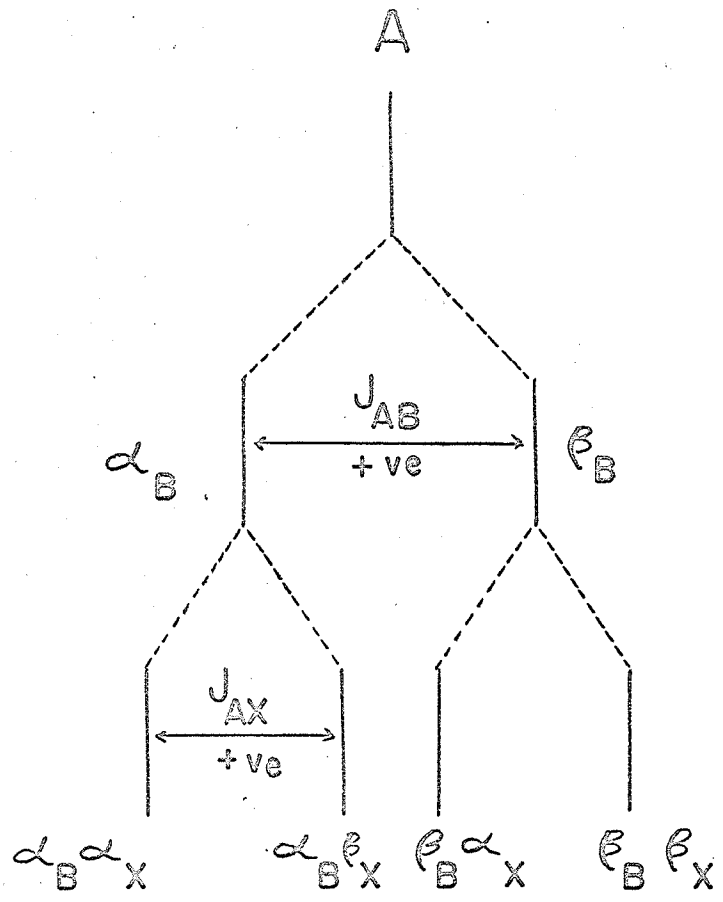
A
J_{AB}
+ ve
α_B
β_B
J_{AX}
+ ve
$\alpha_B\alpha_X$
$\alpha_B\beta_X$
$\beta_B\alpha_X$
$\beta_B\beta_X$

TABLE 4.1

SPIN STATES FOR THE PROTON NEIGHBORS IN AN ABX SYSTEM WITH J_{AB}, J_{AX}, J_{BX} POSITIVE

	12	11	10	9	8	7	6	5	4	3	2	1
A	α	β	α	β					α	β	α	β
B	α	α	β	β	α	α	β	β				
X					α	β	α	β	α	α	β	β

At the same time the X transitions are observed with the normal H_1 radiofrequency field. Here the transitions arising from the AX coupling which is dependent on spin β for the B proton are destroyed. From Table 4.1 this is transitions 9, 10. Thus for the situation where J_{AB} and J_{BX} have the same sign (here taken to be positive), transitions 9, 10 collapse to a single line. Transitions 11 and 12 should remain unchanged since these transitions result from those molecules where the proton B has spin state α, and these are not affected by the strong radiofrequency field. If these coupling constants were taken to be negative all the α's and the β's in Table 4.1 would be interchanged. The argument would be the same as above, so that only the relative signs and not the absolute signs are determined by this experiment.

B. Double Irradiation, J_{AB} and J_{BX} of Opposite Sign

Since the behaviour of the X spectrum when part of the A spectrum is strongly irradiated is independent of the sign of J_{AX}, the coupling constant being destroyed, the only other case to be considered is that when J_{AB} and J_{BX} are of opposite sign. The case is discussed where J_{AB} is taken to be negative and J_{BX} positive. As before, only the relative signs have any meaning and the reverse sign designation would follow the same argument.

Table 4.2 can be constructed in a similar fashion to Table 4.1. There is one main difference with J_{AB} negative; the relative positions of α_B, β_B for the A transitions and α_A, β_A for the B transitions are interchanged.

TABLE 4.2

SPIN STATES FOR THE PROTON NEIGHBORS IN AN ABX SYSTEM WITH J_{AB} NEGATIVE, J_{AX}, J_{BX} POSITIVE

	12	11	10	9	8	7	6	5	4	3	2	1
A	α	β	α	β					β	α	β	α
B	α	α	β	β	β	β	α	α				
X					α	β	α	β	α	α	β	β

Again the strong radiofrequency field H_2 is used to destroy the J_{AX} coupling between transitions 5 and 6 without affecting 7 and 8. From Table 4.2 it can be seen that the J_{AX} coupling which is destroyed

is dependent on proton B being in the α state. Observing the X spectral lines, transitions 11 and 12 would collapse to a single line while lines 9 and 10 would not be disturbed.

Thus when transitions 5 and 6 are irradiated in the A spectrum with the simultaneous observation of the X spectrum, the relative sign between the coupling constants J_{AB} and J_{BX} can be determined by observing which pair of peaks 9, 10 or 11,12 collapse. That is:

J_{AB}, J_{BX} same sign - 9,10 collapse

J_{AB}, J_{BX} opposite sign - 11, 12 collapse

C. Determination of the Relative Sign Between J_{AB}, J_{AX}

In a similar manner the relative sign between the coupling constants J_{AB} and J_{AX} may be obtained by irradiating the B transitions 1 and 2 with the strong radiofrequency field H_2 and observing the resultant X spectrum. If these couplings have the same sign, then transitions 9 and 11 collapse to a single line; if the couplings are opposite in sign transitions 10 and 12 collapse.

D. Double Resonance Techniques

There are basically two methods of performing the spin decoupling experiment, the "field sweep" and the "frequency sweep" methods. In the field sweep method the frequencies ν_1 and ν_2 are fixed and the spectrum is investigated by a slow magnetic field sweep.[62,65-67] Since H_2 is most effective when it is centred exactly on a multiplet pattern, its effectiveness must vary during the

magnetic field sweep, sometimes making the interpretation difficult.

The frequency sweep method[68] provides the simpler set of conditions from the point of view of interpretation. H_o is maintained constant, ν_2 is set to be near resonance for the group to be strongly irradiated, while ν_1 is slowly varied to display the resonance of the second group. Unfortunately, with the majority of spectrometer systems currently available, it is technically difficult to stabilize the magnetic field H_o. For this reason most decoupling experiments use the field sweep method. This is done here.

3. Experimental

The sample of 1-chloro-2,2-dimethylcyclopropane was a gift from Dr. G. L. Closs. The physical constants of this compound are given in his paper.[8] No impurities were found in the proton resonance spectrum and the compound was not purified further. 1-chloro-2,2-dimethylcyclopropane was analyzed as a one-to-five solution in benzene on a DP 60 Mcps spectrometer by the usual high resolution techniques. Tetramethylsilane was used as internal reference. The solution was sealed in a thin walled tube to avoid any changes in concentration between the single resonance and double resonance experiments. At 60 Mcps the three spin system for the ring protons may be calculated by the ABX approximation. Ten spectra calibrated by the sideband modulation technique were recorded with the magnetic field in the increasing and decreasing

directions and the averages used in evaluating the molecular parameters.

The equipment for the double resonance experiment was constructed and used as described by Freeman.[62] The X spectrum was centred on the oscilloscope and the radiofrequency power increased until it was sufficiently strong to destroy the coupling constants. Field modulation less than the chemical shift between the X and the AB regions was applied and the field swept slowly to display the normal AB part of the spectrum with the lock-in-detector. When the phase control on the radiofrequency receiver was adjusted and the modulation level reduced so that the lines were not broadened by saturation, a normal spectrum as in Figure 4.4 was obtained. Spin decoupling was then accomplished by increasing the modulation frequency gradually to the calculated decoupling frequencies.

4. Results

The results of the ABX analysis in benzene solution are given in Table 4.3.[69] Figure 4.3 shows the experimental and calculated spectrum of 1-chloro-2,2-dimethylcyclopropane in benzene solution at 60 Mcps.

To determine the relative signs by double irradiation, the transitions of this ABX system were carefully measured and labelled according to their origin as the ratio of the coupling constant to the chemical shift approached zero, assuming $|J_{BX}| > |J_{AB}| > |J_{AX}|$.

Figure 4.3 Proton resonance spectrum of 1-chloro-2,2-dimethyl-cyclopropane at 60 Mcps in benzene; calibration is to low field of internal TMS.

1-CHLORO-2,2-DIMETHYLCYCLOPROPANE

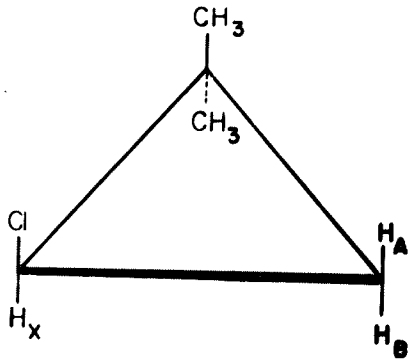

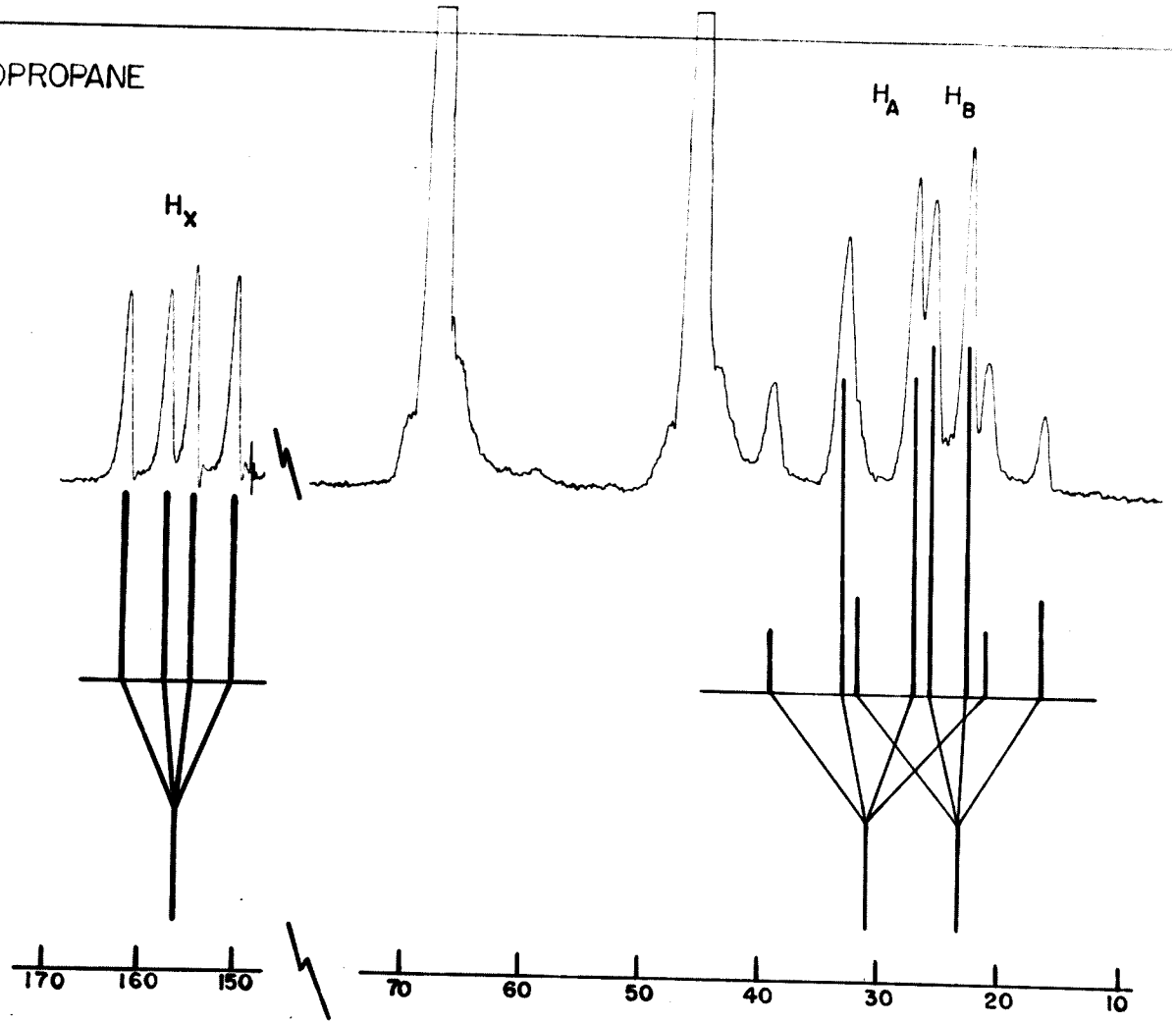

Figure 4.4 Proton resonance of AB part of the spectrum of 1-chloro-2,2-dimethylcyclopropane at 60 Mcps, with transitions numbered to correspond to that given in Figure 4.1.

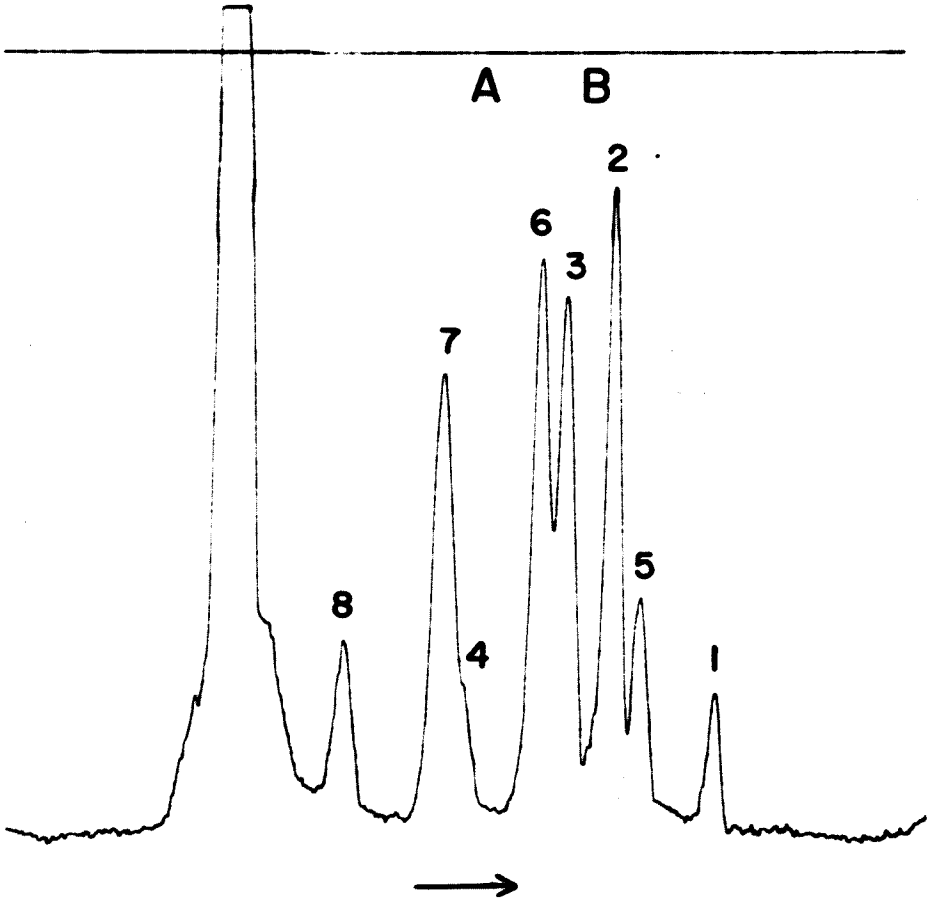
A
B
2
6
3
7
8
4
5
1

TABLE 4.3

ABX ANALYSIS OF 1-CHLORO-2,2-DIMETHYLCYCLOPROPANE

Coupling Constants	Chemical Shifts#
J_{AB} = 5.98 ± .17 cps*	H_A: 30.9 cps
J_{AX} = 4.11 ± .17 cps	H_B: 22.9 cps
J_{BX} = 7.39 ± .17 cps	H_X: 156.3 cps

*Root mean square deviation.
#At 60 Mcps with respect to internal TMS.

The decoupling frequencies were calculated for the two possibilities, namely, where the geminal and vicinal couplings have the same sign and the opposite sign. It was convenient to apply the high amplitude radiofrequency field to the X transitions and observe the results in the AB spectrum. With the reverse procedure ambiguous results were obtained, probably due to the simultaneous disturbance of more than one pair of transitions. The results for the double resonance experiment are given in Table 4.4.

The numbering of the A and B transitions to correspond with that of Freeman is shown in Figure 4.4. The B transitions are numbers 1 - 4 and the A transitions 5 - 8. The peak to low field of the AB region corresponds to one of the methyl substituent resonances. The X transitions which are not shown in this diagram are numbers 9 - 11, as in Figure 4.1. Figures 4.5 and 4.6 show the

TABLE 4.4

DOUBLE RESONANCE OF 1-CHLORO-2,2-DIMETHYLCYCLOPROPANE

Signs of J_{AB} and J_{BX}	Decoupling Frequency Calculated	Experimental
Same	124.5 cps	
Opposite	116.5 cps	118 ± 1 cps
Signs of J_{AB} and J_{AX}		
Same	132.2 cps	
Opposite	138.4 cps	140 ± 1 cps

change in the AB region when the X transitions are irradiated with the strong radiofrequency given below the spectrum. The magnetic field was swept in the forward and reverse directions as indicated by the arrows in these figures. Here again the resonance from one of the methyl groups may be seen to low field of the AB region. Figure 4.5 shows the spectrum when a decoupling frequency is applied for the situation where the couplings J_{AB} and J_{BX} have the same and the opposite sign. If J_{AB} and J_{BX} have the same sign and transitions 11, 12 are irradiated, lines 7, 8 should collapse approximately to a single peak for a decoupling frequency of 124.5 cps. If J_{AB} and J_{BX} have the same sign and transitions 9, 10 are irradiated, then lines 7, 8 should collapse with a decoupling frequency of 116.5 cps.

Figure 4.5 Nuclear double resonance spectra of AB region when a decoupling frequency of a) 124.1 cps and b) 118.5 cps is applied to the X transitions. Spectra have been recorded with the magnetic field in the forward and reverse directions.

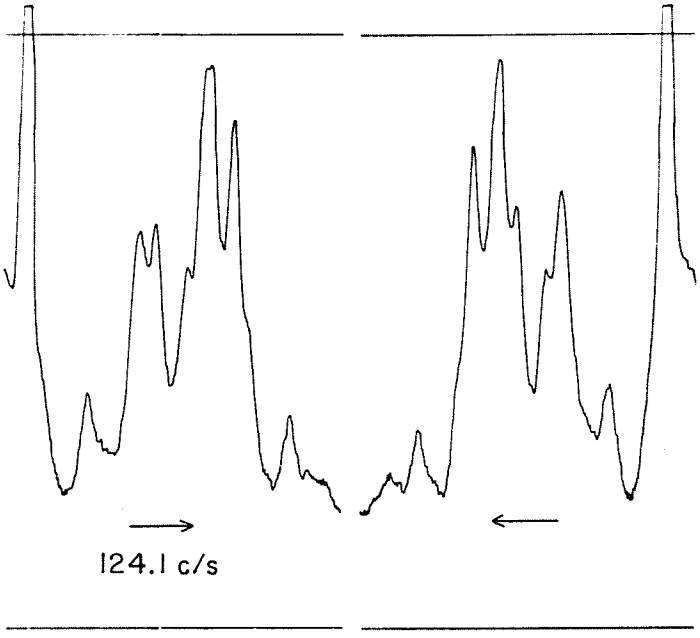
124.1 c/s

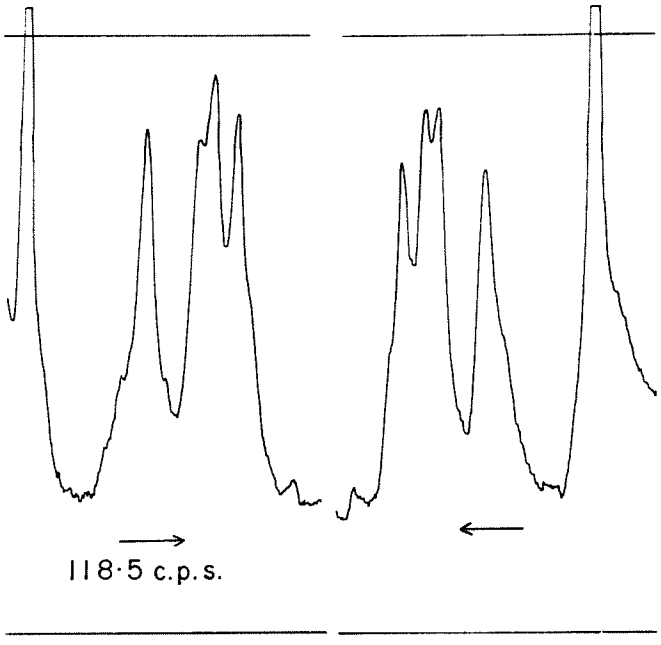
118·5 c.p.s.

Figure 4.6 Nuclear double resonance spectra of AB region when a decoupling frequency of a) 133.0 cps and b) 140.1 cps is applied to the X transitions. Spectra have been recorded with an increasing and decreasing magnetic field.

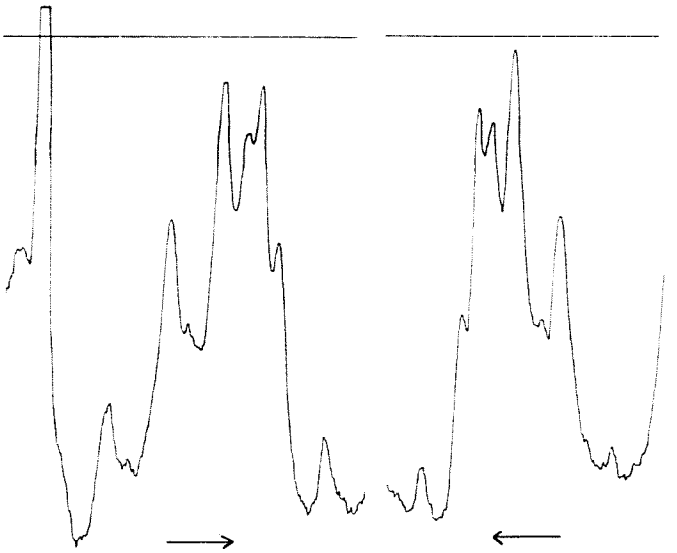
133·0 c.p.s.

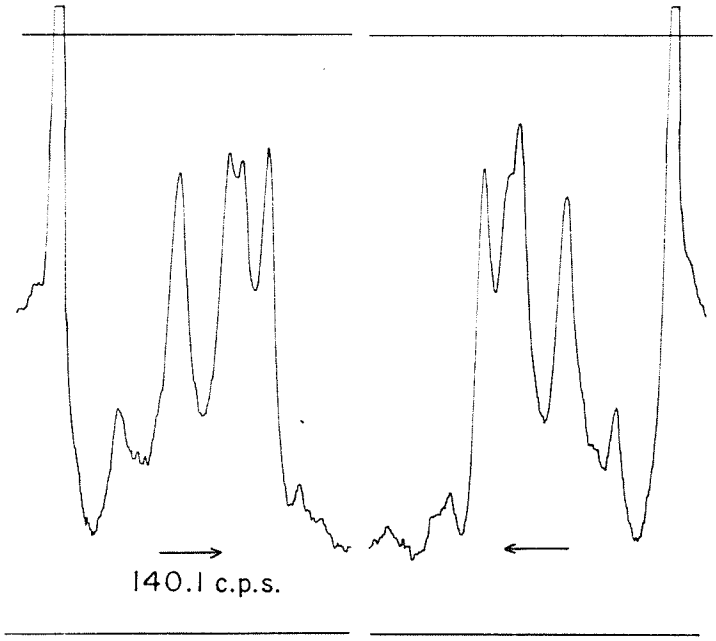
140.1 c.p.s.

In Figure 4.6 the two possibilities for the coupling constants J_{AB} and J_{AX} are examined. If J_{AB} and J_{AX} have the same sign and the strong radiofrequency field is applied between transitions 9, 11 then lines 1, 3 would collapse for a decoupling frequency of 132.2 cps. If these two couplings are opposite in sign lines 1, 3 would collapse when the field is placed between transitions 10, 12 at a frequency of 138.4 cps.

The decoupling occurred gradually near to those frequencies listed in Table 4.4 for the case with opposite signs and then remained collapsed for a further increase of about 1 cps in the modulation frequency. The agreement between the observed and calculated decoupling frequencies is sufficiently good to show that the geminal coupling constant J_{AB} is opposite in sign to the vicinal couplings J_{AX} and J_{BX}.

5. Conclusions

From the results of the double resonance study on 1-chloro-2,2-dimethylcyclopropane it can be concluded that the geminal coupling for substituted cyclopropanes is opposite in sign to the vicinal couplings. In analogy to ethanes the geminal coupling constant is negative and the vicinal couplings are positive for cyclopropanes. A similar conclusion has been indicated by the direct analysis of the proton spectra of cyclopropanecarboxylic acid[34] and 2,2-diphenylcyclopropanecarboxylic acid[33] at low magnetic fields.

CHAPTER V

TEMPERATURE AND SOLVENT EFFECTS ON THE PROTON MAGNETIC RESONANCE SPECTRUM OF BIS (2,2-DICHLOROCYCLOPROPYL) ETHER

1. Introduction

The proton magnetic resonance spectrum of bis (2,2-dichlorocyclopropyl) ether, the structure of which is shown in I, consists of two slightly shifted ABX systems arising from the meso and d,l isomers. The chemical shifts of the three protons in each ABX spectrum relative to one another and to an internal reference depend markedly on solvent and temperature. The experimental data has been examined in terms of internal relation effects, effective inversion of the oxygen atom and association effects. It appears that the latter is consistent with experiment.

BIS (2,2-DICHLOROCYCLOPROPYL) ETHER

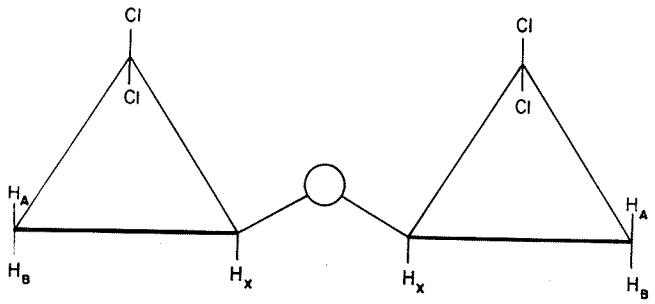

I

2. Solvent Effects in NMR

The screening constant which is observed in NMR is the sum of a screening constant for the isolated molecule, σ_{gas}, and a contribution from the medium, $\sigma_{solvent}$, where

$$\sigma_{solvent} = \frac{H_o - H}{H} ,$$

H_o is the field strength for the resonance of an isolated gaseous molecule and H is the field for resonance in the medium.

The solvent screening constant may be divided into four different contributions to $\sigma_{solvent}$:[70]

$$\sigma_{solvent} = \sigma_b + \sigma_a + \sigma_w + \sigma_E$$

where σ_b is due to the bulk magnetic susceptibility of the medium; σ_a arises from the anisotropy in the molecular susceptibility of solvent molecules; σ_w is that part of the contribution between the solvent and solute due to the van der Waals forces; and σ_E is the "polar" or "reaction field" effect.[49]

A. Bulk Magnetic Susceptibility, σ_b

In the measurement of chemical shifts in high resolution spectroscopy either internal or external references may be used. With an external reference a correction involving the difference between the bulk diamagnetic susceptibilities of the reference and the solvent must be applied to the measured chemical shift. The solvent molecules surrounding the solute interact with the resonant nuclei and cause a change in the chemical shift. In a magnetic field

the solvent molecules will be diamagnetically polarized, which may in turn contribute to the magnetic field at the nucleus and thus the screening constant σ. This secondary field depends upon both the type of medium and the shape of the sample container.

With an external reference there is a different medium surrounding the solute molecules in comparison to the reference molecules and consequently the diamagnetic contribution to their screening constants are different. For an internal reference in a solution, the solute and reference are surrounded by the same medium and are affected to the same extent by the diamagnetic contribution. The relative positions of the reference and solute resonances are not affected since they are both shifted by the same amount.

B. Anisotropy in the Susceptibility of the Solvent, σ_a

Aromatic solvents tend to produce high-field shifts in the solute due to their disk shape and their large diamagnetic anisotropy. This large anisotropy of the aromatic molecule results from the circulation of the mobile π-electrons induced by the magnetic field. In benzene, for example, the six mobile π-electrons behave much like charged particles free to move on a circular wire. Applying a magnetic field perpendicular to the ring produces a circulation of electrons and a diamagnetic moment opposed to the primary field, as shown in Figure 5.1. From the diagram it is evident that protons situated near the sides of the ring resonate at a lower field due to the negative contribution to the screening

constant. Protons at a point directly above or below the plane of the

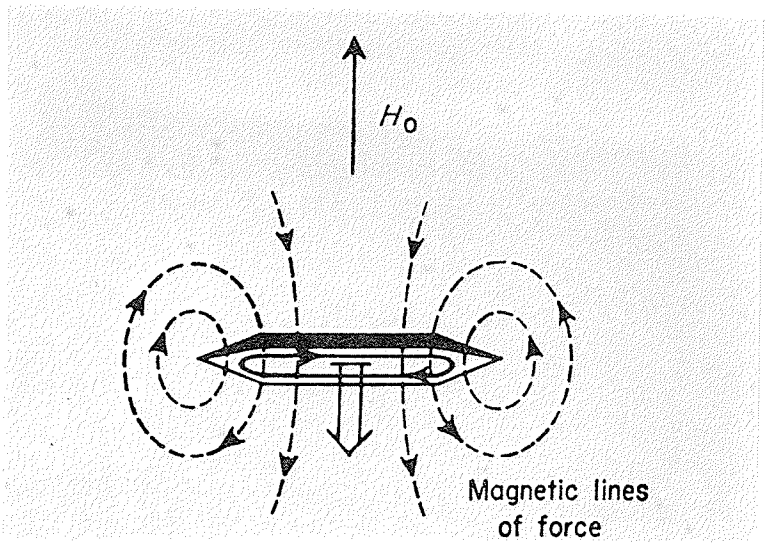

Figure 5.1 Current and magnetic lines of force induced in benzene by a primary field H_o.

ring experience a high-field shift since the secondary magnetic field in this position is opposed to the primary field. Because benzene is disk-shaped there is a greater probability that a solute molecule would be above or below the ring rather than in the plane of the ring. Thus after averaging over all possible orientations there is a net shift of the proton signal to high field. If there is a preferred orientation between benzene and the solute there may be a larger shift to high field.

For rod-shaped solvent molecules such as carbon disulfide, whose largest diamagnetic susceptibility is along the axis of the rod, the solute would also tend to lie above or below the rod rather

than at either end most of the time. This would lead to low-field shifts for the solute protons since the primary magnetic field would be reinforced in this position.

C. van der Waals Forces, σ_W, and the Polar Effect, σ_E

Interactions between molecules perturb their electronic structure and the resultant distortion leads to a solvent-dependent nuclear screening constant σ_W.

When a polar molecule is dissolved there is another contribution, σ_E, to the shielding constant. The polar molecule polarizes the surrounding medium and this leads to an electric field, called the reaction field, at the solute. The different protons in a molecule may have various values of σ_E.

3. Experimental

The spectra were recorded on a Varian DP 60 Mcps spectrometer. A sample of about 0.1 gm. of bis (2,2-dichlorocyclopropyl) ether was obtained from Dr. Bernard T. Gillis.[71] The spectra were taken at room temperature in carbon tetrachloride, benzene, carbon disulfide, and in a series of mixed solvents of benzene and carbon disulfide. Measurements were made with benzene as solvent over a temperature range of +18°C. to +138°C. using a temperature probe built by Mr. G. Ensell of the National Research Council.[72]

Since carbon disulfide offers a wide liquid range for temperature studies the spectrum was studied from -85°C. to +101°C. in this solvent. The solution with the mixed solvent 0.59 mf carbon disulfide and 0.41 mf benzene was also observed from +18°C. to +132°C. The solutions were prepared by dilution with 0.5 ml of reagent grade solvent and represent an ether concentration of about 8 mole percent in benzene, 7 mole percent in carbon tetrachloride and 5 mole percent in carbon disulfide. The ether was isolated by evaporation of the solvent from each solution and used again. Tetramethylsilane was the internal reference in all solutions. Other solvents such as cyclohexane and n-hexane, useful for the comparison of chemical shifts, were not used because of the interference of their proton resonances in the region of interest.

The results represent an average of ten calibrated spectra for those taken at room temperature and of six to eight spectra at other temperatures. Spectra were taken with an increasing and decreasing magnetic field sweep.

Temperatures were measured with a pre-calibrated Varian G-11A recorder using a thermocouple placed near the sample in the exit stream of the spinning and heating gas. The temperature control was approximately ± 1°C. over the period of time necessary to run the calibrated spectra.

4. Results

Figures 5.2 and 5.3 show the proton resonance spectrum in benzene at room temperature and at 138°C. Figures 5.4 and 5.5 show the room temperature spectrum in carbon disulfide and carbon tetrachloride, respectively, and Figures 5.6, 5.7 and 5.8 in the mixed benzene-carbon disulfide solvents. From the relative intensities of the two ABX spectra one isomer (M) is seen to be about twice as abundant as the other isomer (L). The former is probably the meso isomer[73] although there is no way of deciding this from the spectrum.

The chemical shifts relative to internal TMS and the prcton coupling constants are given in Tables 5.1, 5.2 and 5.3.[74] Graphs of the chemical shifts as a function of temperature in benzene and in a mixed benzene-carbon disulfide solution are shown in Figures 5.9, 5.10 and 5.11. In Figure 5.12 the variation of the chemical shifts with temperature for the protons of the M isomer in carbon disulfide is shown. Figure 5.13 shows the chemical shifts of the protons of the M isomer as a function of the benzene concentration in the mixed solvent system. The shifts of the protons in the L isomer could not always be obtained with any accuracy because of overlapping peaks.

For the benzene solution the shift between the benzene peaks and the TMS peaks was 430.4 $\pm$ 0.1 cps at 18°C. and 431.0 $\pm$ 0.2 cps at 102°C. For the mixed solvent 0.59 mf carbon disulfide and 0.41 mf benzene these shifts were 429.1 $\pm$ 0.1 cps at 18°C. and 429.6 $\pm$ 0.1 cps at 145°C.

Figure 5.2 Proton resonance spectrum at 60 Mcps of bis (2,2-dichlorocyclopropyl) ether in benzene at 18°C; calibration is to low field of internal TMS.

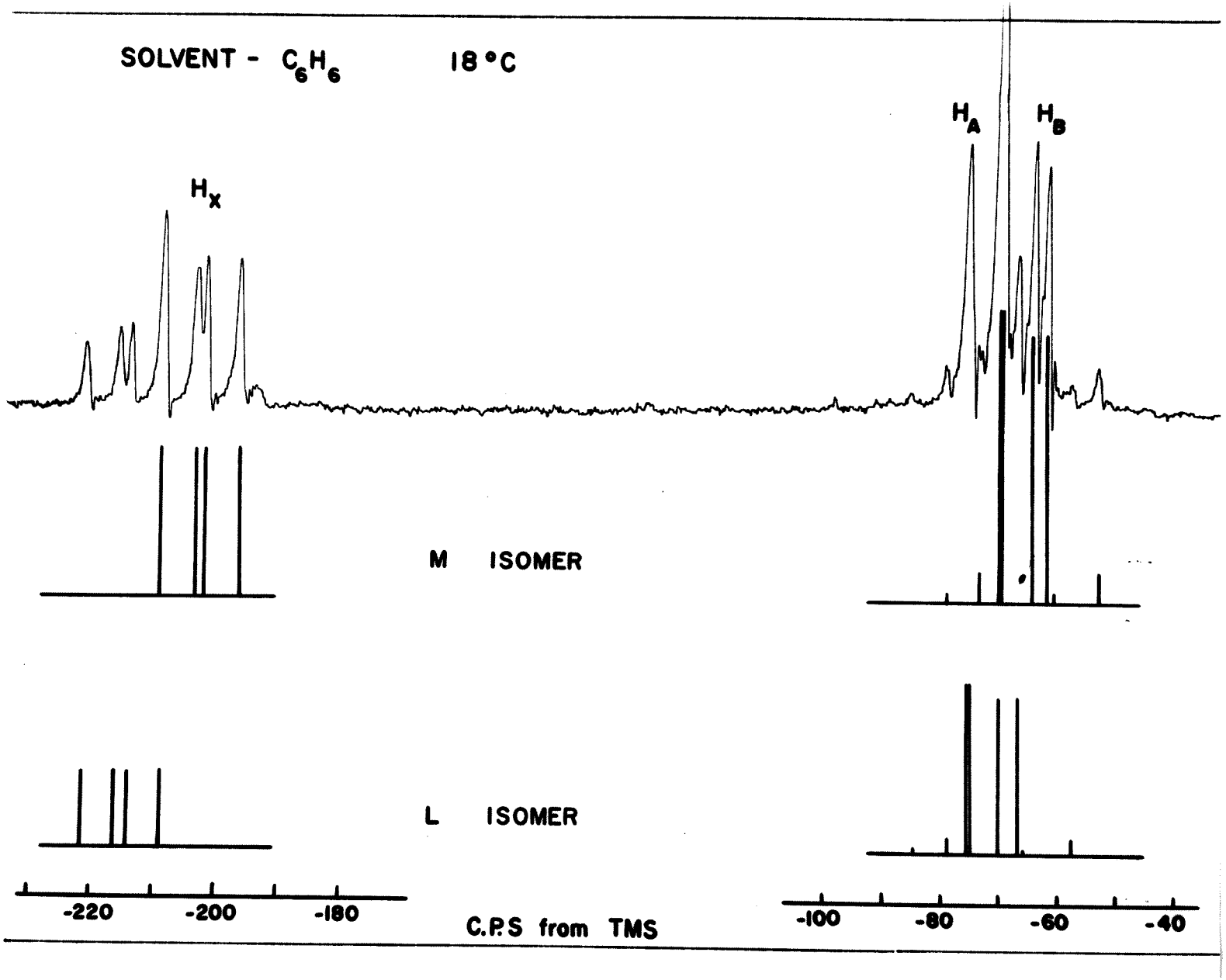
SOLVENT - C_6H_6
18 °C
H_A
H_B
H_X
M ISOMER
L ISOMER
-220
-200
-180
-100
-80
-60
-40
C.P.S from TMS

Figure 5.3 Proton resonance spectrum at 60 Mcps of bis (2,2-dichlorocyclopropyl) ether in benzene at 138°C; calibration is to low field of internal TMS.

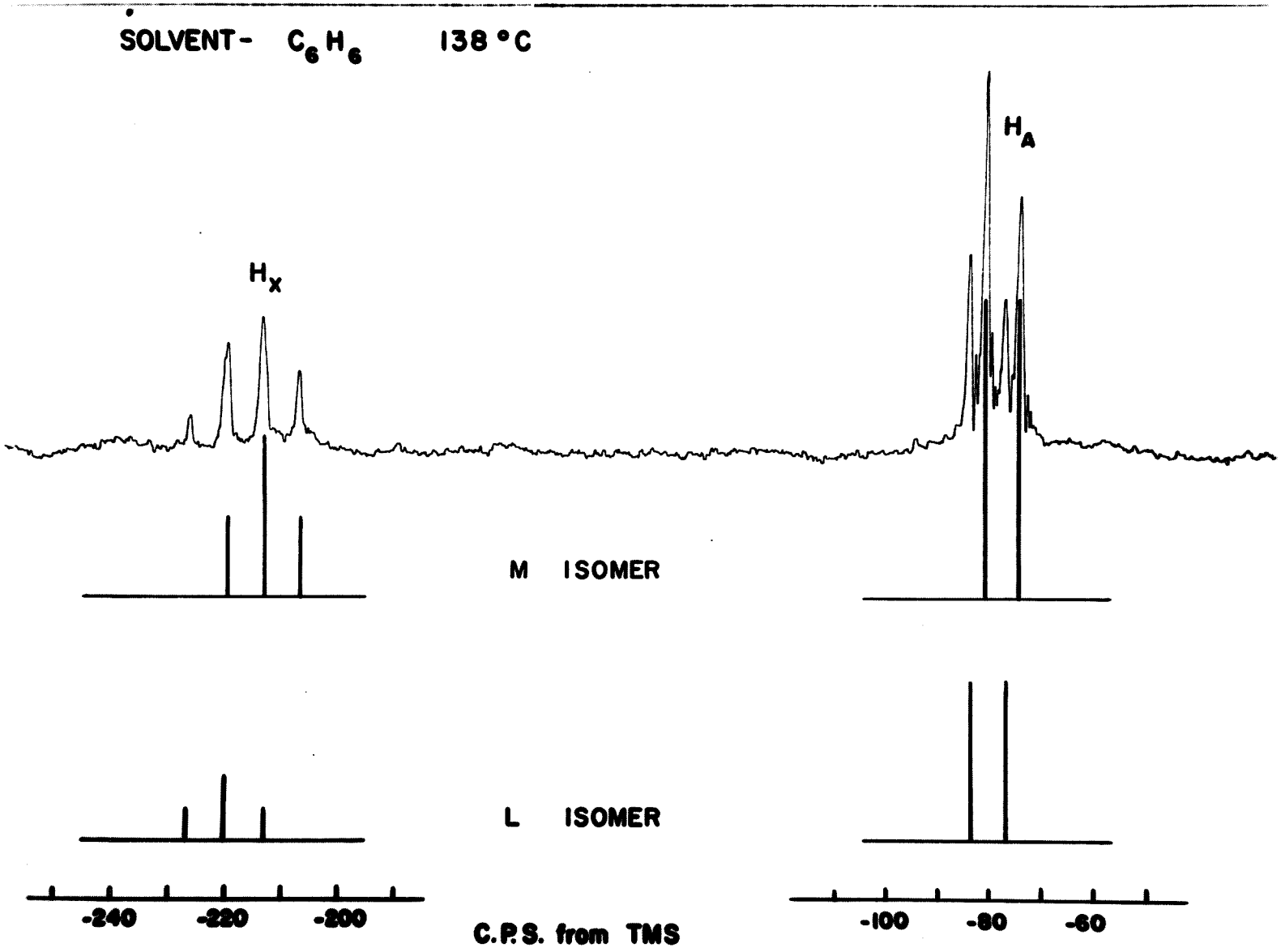
SOLVENT- C_6H_6 138 °C
H_A
H_X
M ISOMER
L ISOMER
-240
-220
-200
-100
-80
-60
C.P.S. from TMS

Figure 5.4 Proton resonance spectrum at 60 Mcps of bis (2,2-dichlorocyclopropyl) ether in carbon disulfide at 18°C; calibration is to low field of internal TMS.

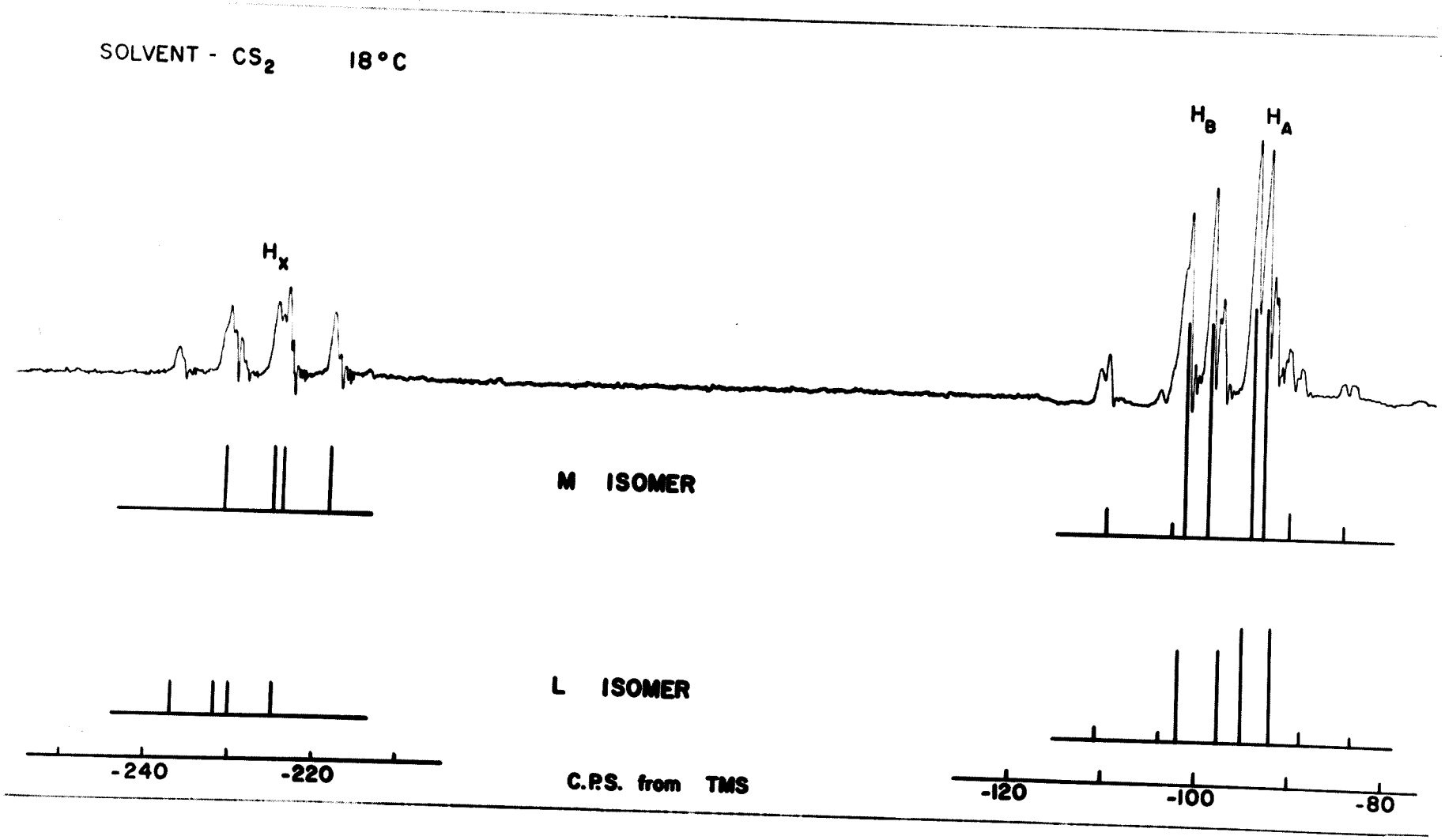
SOLVENT - CS_2 18°C
H_B
H_A
H_X
M ISOMER
L ISOMER
-240
-220
C.P.S. from TMS
-120
-100
-80

Figure 5.5 Proton resonance spectrum at 60 Mcps of bis (2,2-dichlorocyclopropyl) ether in carbon tetrachloride at 18°C; calibration is to low field of internal TMS.

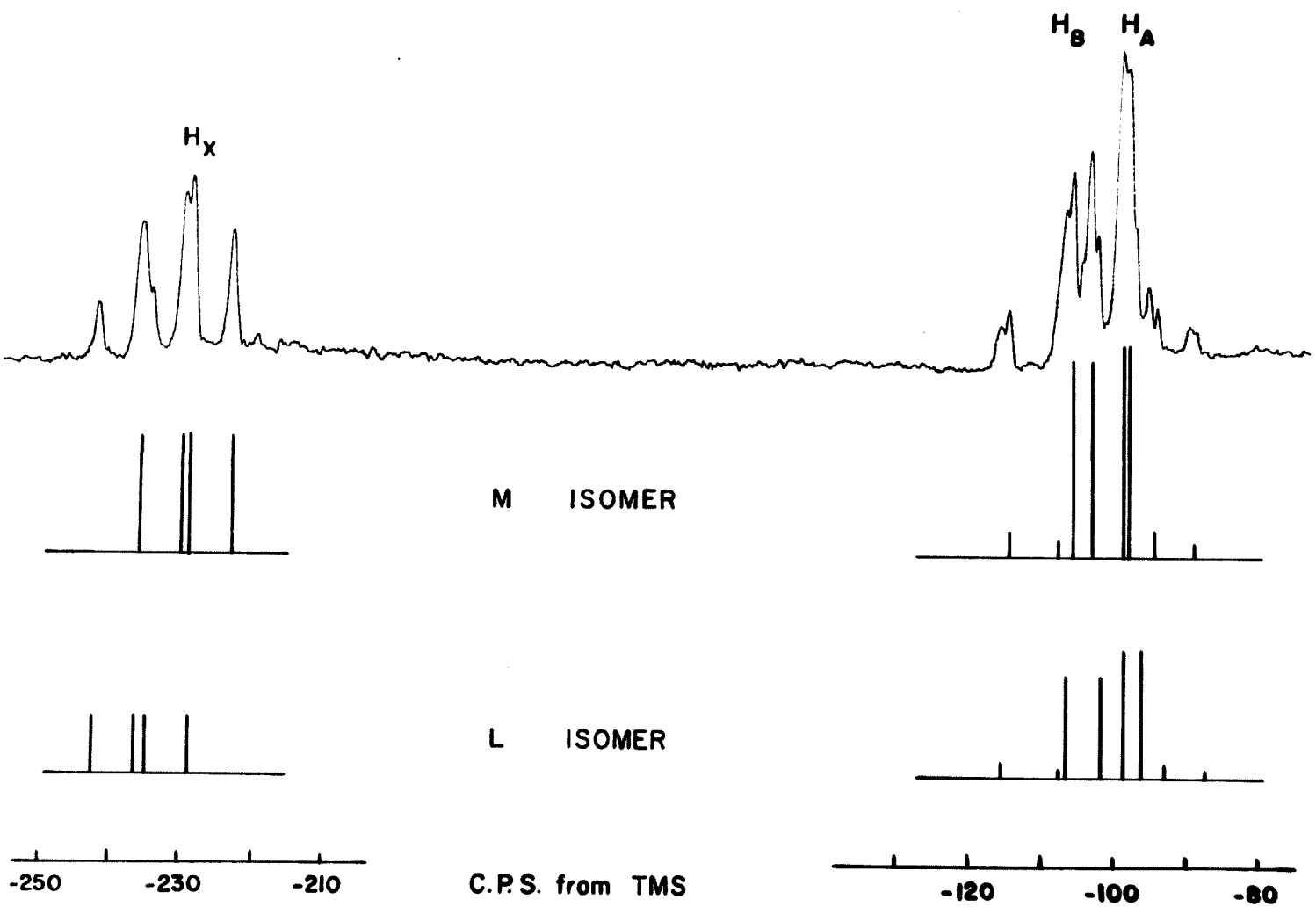
SOLVENT - CCl_4
18° C
H_B
H_A
H_X
M ISOMER
L ISOMER
-250
-230
-210
C.P.S. from TMS
-120
-100
-80

Figure 5.6 Proton resonance spectrum at 60 Mcps of bis (2,2-dichlorocyclopropyl) ether in the mixed solvent 0.03 mf C_6H_6, 0.97 mf CS_2 at 18°C; calibration is to low field of internal TMS.

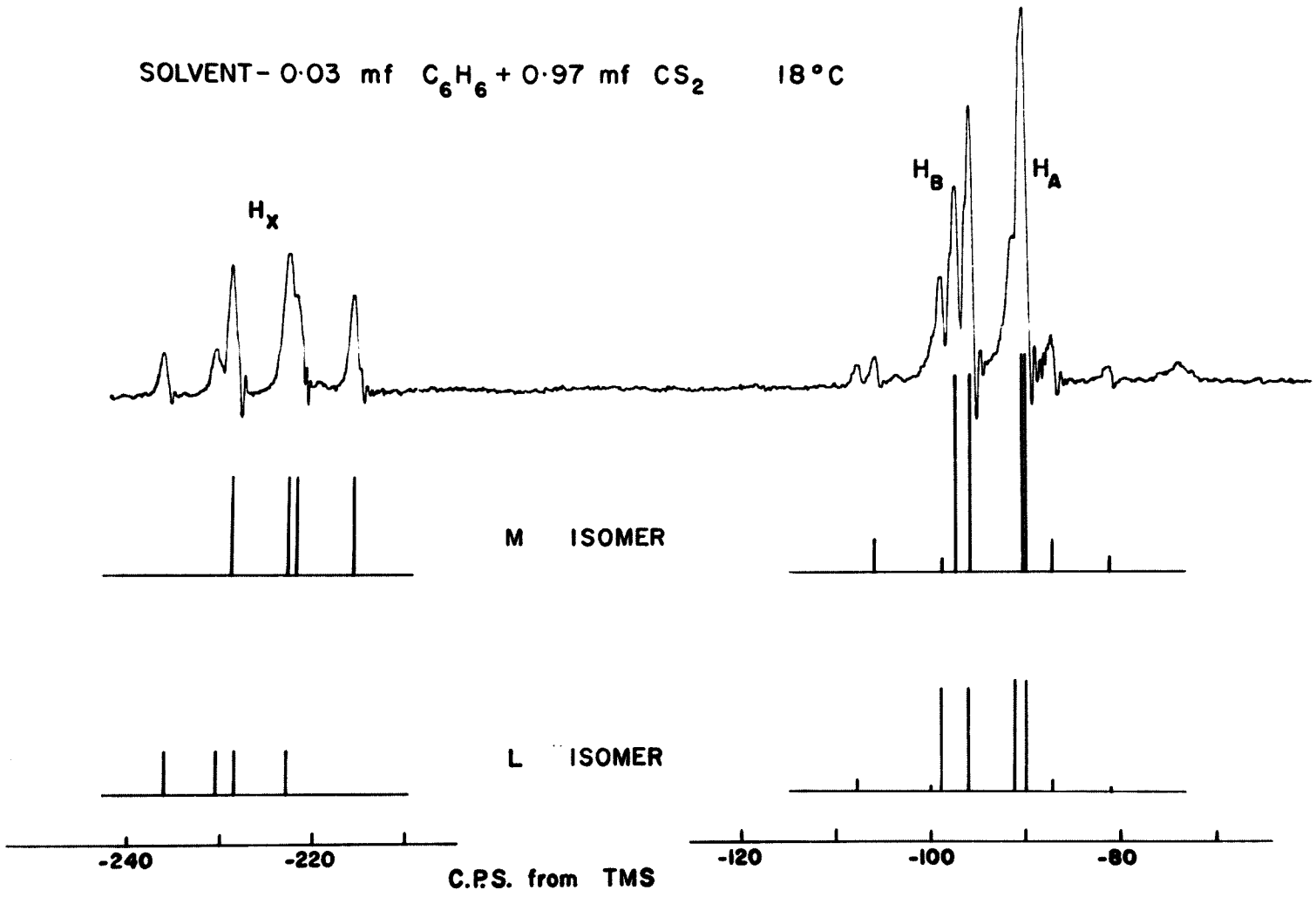
SOLVENT - 0·03 mf C_6H_6 + 0·97 mf CS_2 18°C
H_X
H_B
H_A
M ISOMER
L ISOMER
-240
-220
-120
-100
-80
C.P.S. from TMS

Figure 5.7 Proton resonance spectrum at 60 Mcps of bis (2,2-dichlorocyclopropyl) ether in the mixed solvent 0.08 mf C_6H_6, 0.92 mf CS_2 at 18°C; calibration is to low field of internal TMS.

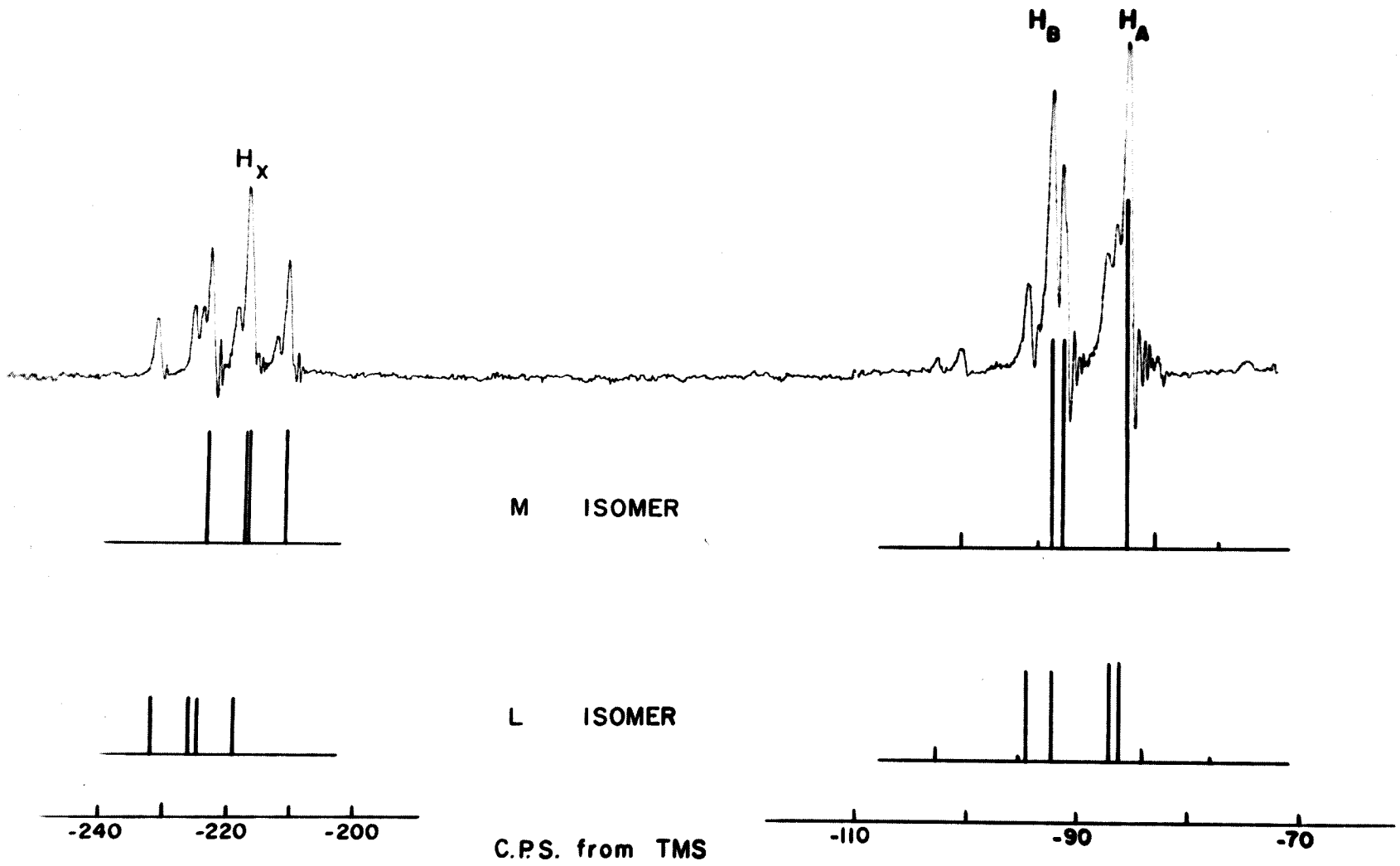
SOLVENT - 0·08 mf C_6H_6 + 0·92 mf CS_2 18°C
H_B
H_A
H_X
M ISOMER
L ISOMER
-240
-220
-200
-110
-90
-70
C.P.S. from TMS

Figure 5.8 Proton resonance spectrum at 60 Mcps of bis (2,2-dichlorocyclopropyl) ether in the mixed solvent 0.41 mf C_6H_6, 0.59 mf CS_2 at 18°C; calibration is to low field of internal TMS.

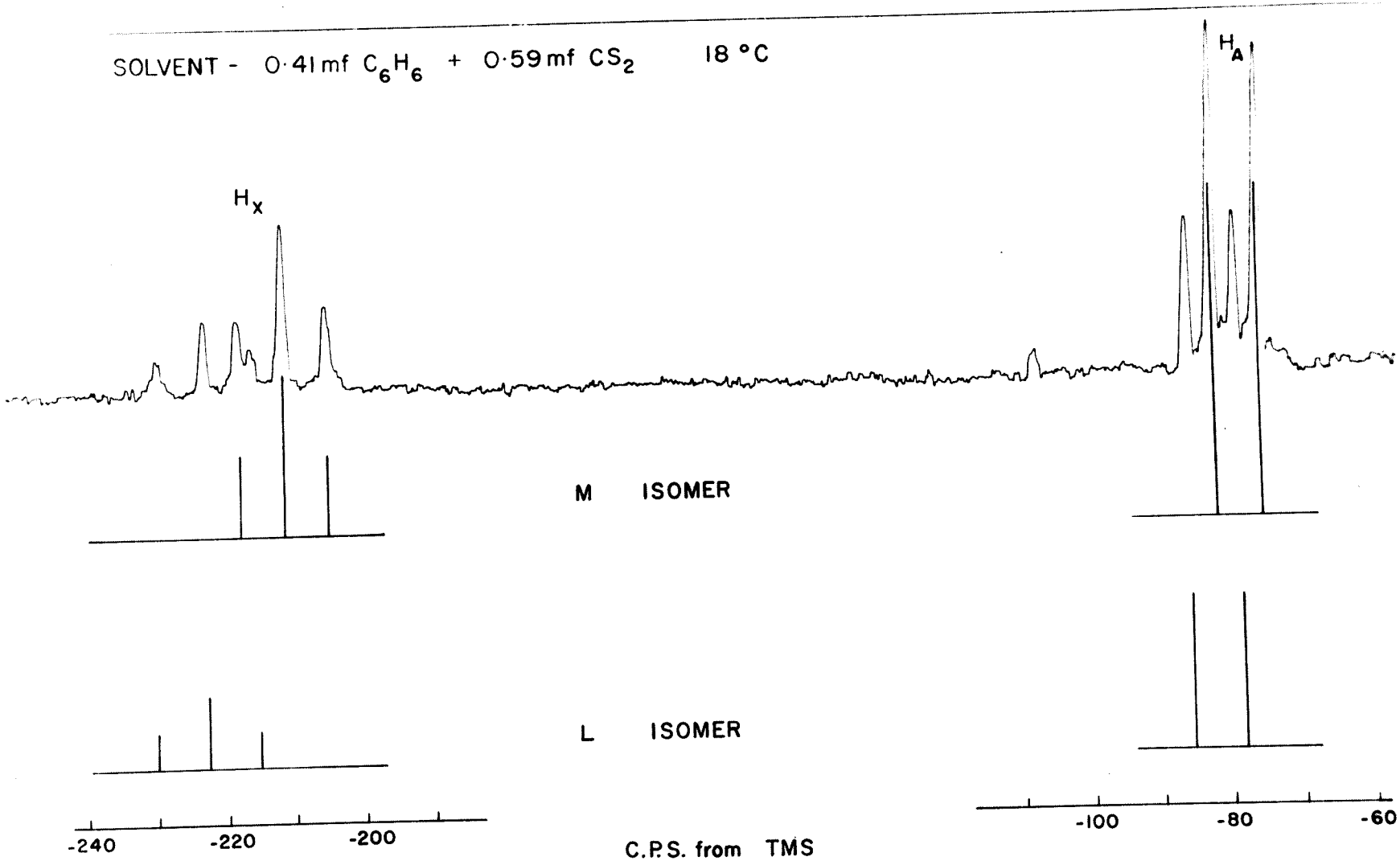
SOLVENT - 0·41mf C_6H_6 + 0·59mf CS_2 18 °C
H_A
H_X
M ISOMER
L ISOMER
-240
-220
-200
-100
-80
-60
C.P.S. from TMS

TABLE 5.1

Coupling constants and proton chemical shifts in c.p.s. in benzene solution

	M Isomer						L Isomer				
Temp (°C)	J_{gem}	J_{cis}	J_{trans}	ν_A *	ν_B *	ν_X *	J_{cis}	J_{trans}	ν_A *	ν_B *	ν_X *
18	-8.88 ± .12	8.19	4.65	68.4	63.6	203.2	-	-	-	-	216.0
36	-8.96 ± .12	7.89	4.85	70.6	66.2	204.7	-	-	-	-	216.5
51	-8.97 ± .10	7.90	4.82	71.3	67.5	206.3	-	-	-	-	217.1
66	-8.88 ± .09	8.22	4.60	72.7	69.8	207.6	8.76	4.45	76.9	73.7	217.6
81	-8.91 ± .10	8.53	4.42	73.6	71.6	209.1	8.39	4.74	78.1	75.2	218.4
98	-8.92†	8.40	4.58	75.1	73.2	210.5	8.60	4.73	78.5	76.6	219.0
121	-8.92†	8.13	4.76	76.8	75.1	212.2	8.52	4.86	79.9	78.1	219.6
136	-	$\frac{J_{cis} + J_{trans}}{2} = 6.53$		77.4		213.3	$\frac{J_{cis} + J_{trans}}{2} = 6.57$		80.2		220.2
(Average)	-8.92	8.18	4.67				8.57	4.70			

* At 60 Mc/s to low field of TMS as internal reference

† Average value of J_{gem} used for the analysis.

TABLE 5.2

Coupling constants and proton chemical shifts in c.p.s. in carbon disulfide solution

	M Isomer						L Isomer
Temp (°C)	J_{gem}	J_{cis}	J_{trans}	ν_A *	ν_B *	ν_X *	J_{gem}
101	-8.57 ± .17	7.38	5.39	95.0	101.2	226.2	-8.57 ± .17
91	-8.53 ± .17	7.28	5.54	94.8	101.0	225.9	-8.53 ± .17
69	-8.51 + .21	7.34	5.58	95.3	101.5	226.1	-8.51 ± .21
46	-8.53 ± .08	7.49	5.42	95.4	101.6	226.1	-8.53 ± .08
18	-8.53 ± .08	7.66	5.27	95.9	101.8	226.2	-8.59 ± .11
5	-8.69 ± .09	7.75	4.95	96.3	102.1	226.1	-8.76 ± .08
-16	-8.65 ± .13	7.75	4.86	96.6	102.5	226.3	-8.75 ± .11
-32	-8.62 ± .12	7.89	4.71	97.0	102.9	226.2	-8.71 ± .13
-38	-8.64 ± .12	7.83	4.83	97.3	103.1	226.4	-8.69 ± .12
-49	-8.68 ± .10	7.96	4.88	97.5	103.3	226.5	-8.82 ± .12
-61	-8.64 ± .10	8.16	4.52	98.0	103.8	226.4	-8.73 ± .11
-85	-8.81 ± .14	7.74	4.72	97.6	103.4	226.6	-8.81 ± .14
(Average)	-8.62	7.69	5.06				-8.67

* At 60 Mc/s to low field of TMS as internal reference

TABLE 5.3

Coupling constants and proton chemical shifts in c.p.s.

		M Isomer						L Isomer					
Solvent	Temp (°C)	J_{gem}	$\frac{J_{cis} \text{ or } J_{trans}}{2}$	J_{cis} + J_{trans}	ν_A *	ν_B *	ν_X *	J_{gem}	$\frac{J_{cis} \text{ or } J_{trans}}{2}$	J_{cis} + J_{trans}	ν_A *	ν_B *	ν_X *
CCl_4	18	-8.88 ± .18	7.99	5.16	98.2	104.0	216.6	-8.95 ± .14	-	-	-	-	-
0.97 mf CS_2 0.03 mf C_6H_6	18	-8.56 ± .11	7.42	5.44	91.2	95.7	222.1	-8.62 ± .16	8.27	5.01	88.8	95.4	229.5
0.92 mf CS_2 0.08 mf C_6H_6	18	-8.54 ± .12	6.89	5.75	86.6	90.4	217.4	-8.67 ± .11	8.06	5.14	87.4	92.6	225.7
0.59 mf CS_2 0.41 mf C_6H_6	18	-	6.45 ± .13		78.3		211.5	-	6.57 ± .14		81.6		222.5
0.59 mf CS_2 0.41 mf C_6H_6	85	-	6.50 ± .09		83.1		215.0	-	6.63 ± .16		88.8		-
0.59 mf CS_2 0.41 mf C_6H_6	132	-	6.49 ± .07		85.7		217.6	-	-		-		-

* At 60 Mc/s to low field of TMS as internal reference

Figure 5.9 Plot of proton resonance shifts for M isomer of bis (2,2-dichlorocyclopropyl) ether in benzene (in cps at 60 Mcps) against temperature; calibration is to low field of internal TMS.

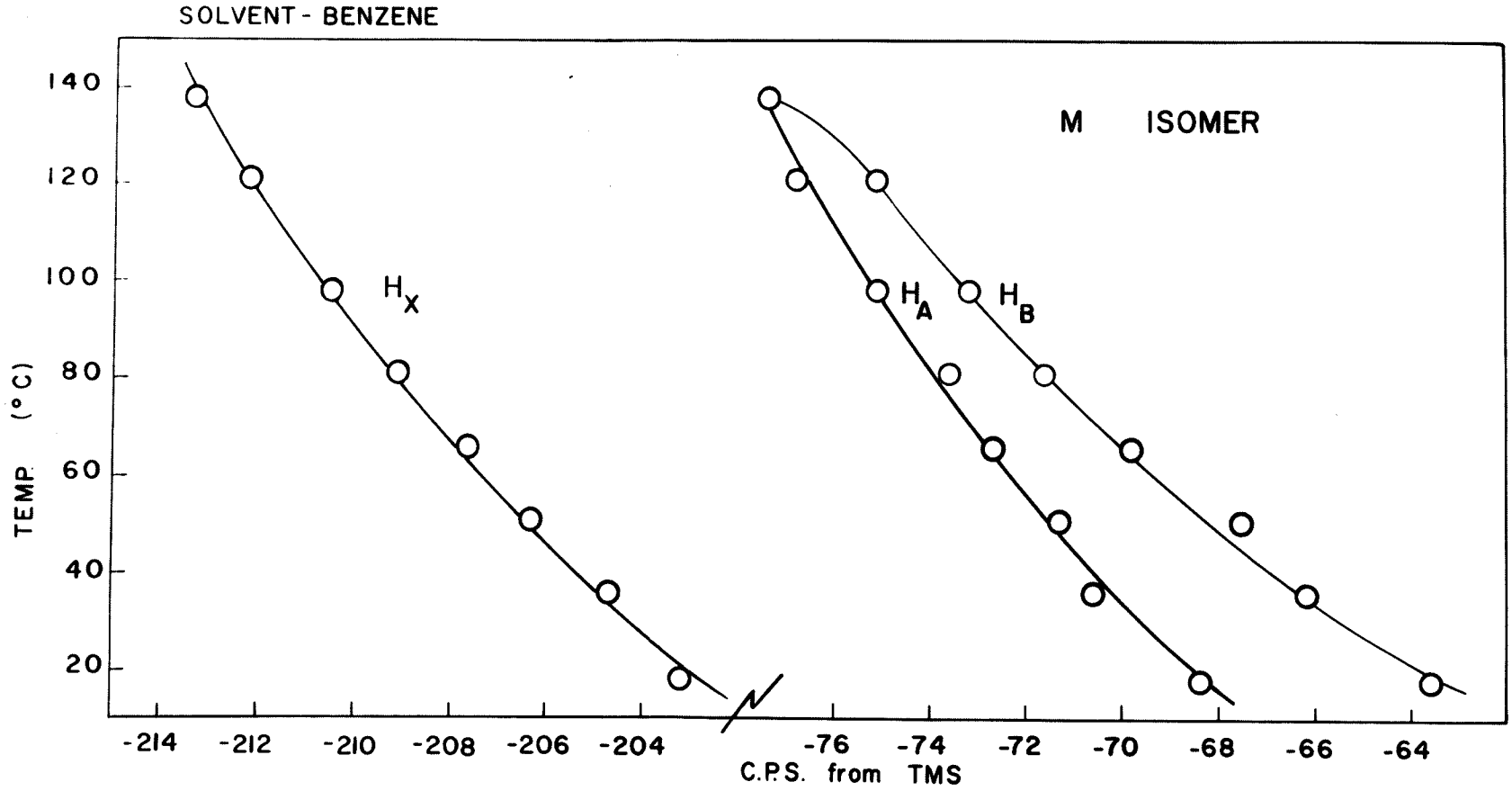
SOLVENT - BENZENE
M ISOMER
H_X
H_A
H_B
TEMP (°C)
140
120
100
80
60
40
20
-214
-212
-210
-208
-206
-204
-76
-74
-72
-70
-68
-66
-64
C.P.S. from TMS

Figure 5.10 Plot of proton resonance shifts for L isomer of bis (2,2-dichlorocyclopropyl) ether in benzene (in cps at 60 Mcps) against temperature; calibration is to low field of internal TMS.

Figure 5.11 Plot of proton resonance shifts for M isomer of bis (2,2-dichlorocyclopropyl) ether in the mixed solvent 0.41 mf C_6H_6, 0.59 mf CS_2 (in cps at 60 Mcps) against temperature; calibration is to low field of internal TMS.

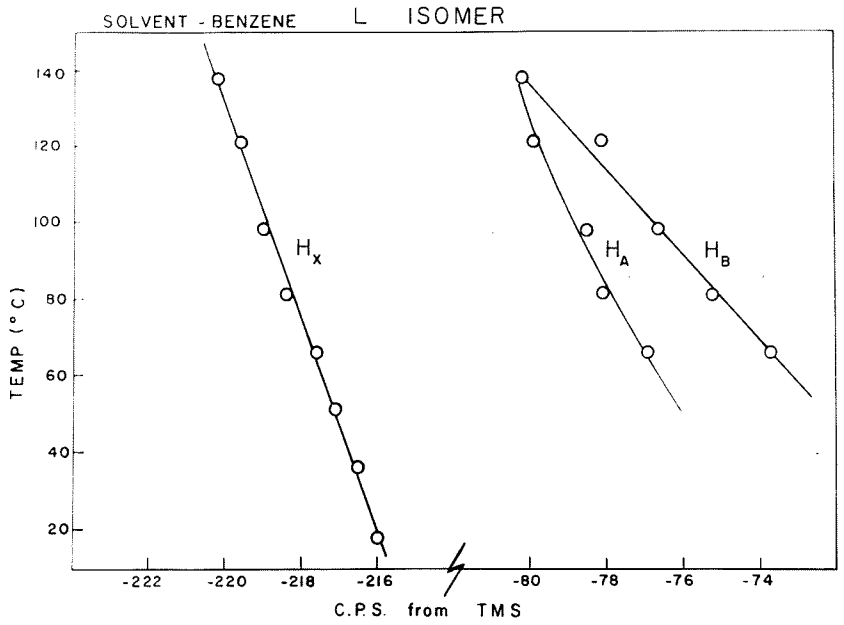
SOLVENT - BENZENE
L ISOMER
TEMP (°C)
140
120
100
80
60
40
20
H_X
H_A
H_B
-222
-220
-218
-216
-80
-78
-76
-74
C.P.S. from TMS

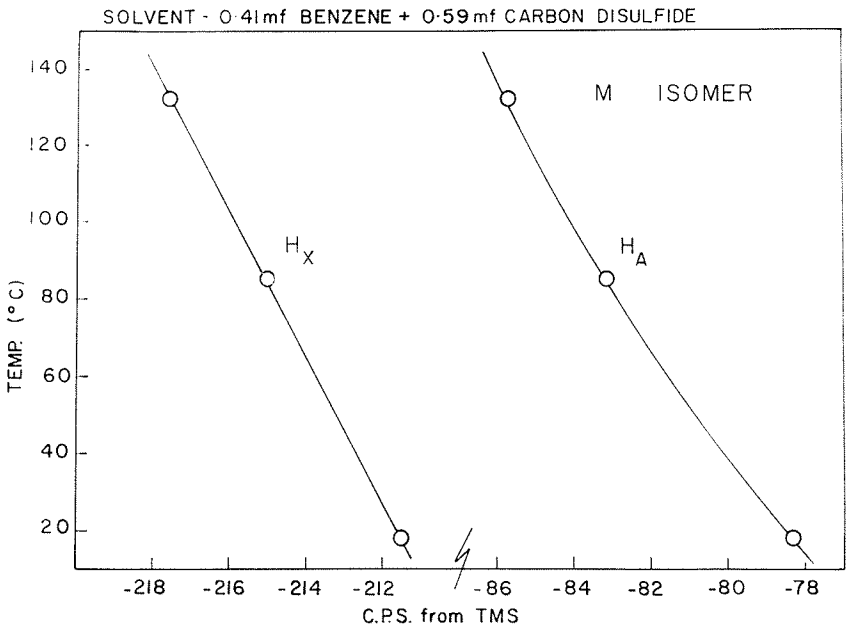
SOLVENT - 0·41mf BENZENE + 0·59mf CARBON DISULFIDE
M ISOMER
TEMP. (°C)
140
120
100
80
60
40
20
H_X
H_A
-218
-216
-214
-212
-86
-84
-82
-80
-78
C.P.S. from TMS

Figure 5.12 Plot of proton resonance shifts for the M isomer of bis (2,2-dichlorocyclopropyl) ether in carbon disulfide (in cps at 60 Mcps) against temperature; calibration is to low field of internal TMS.

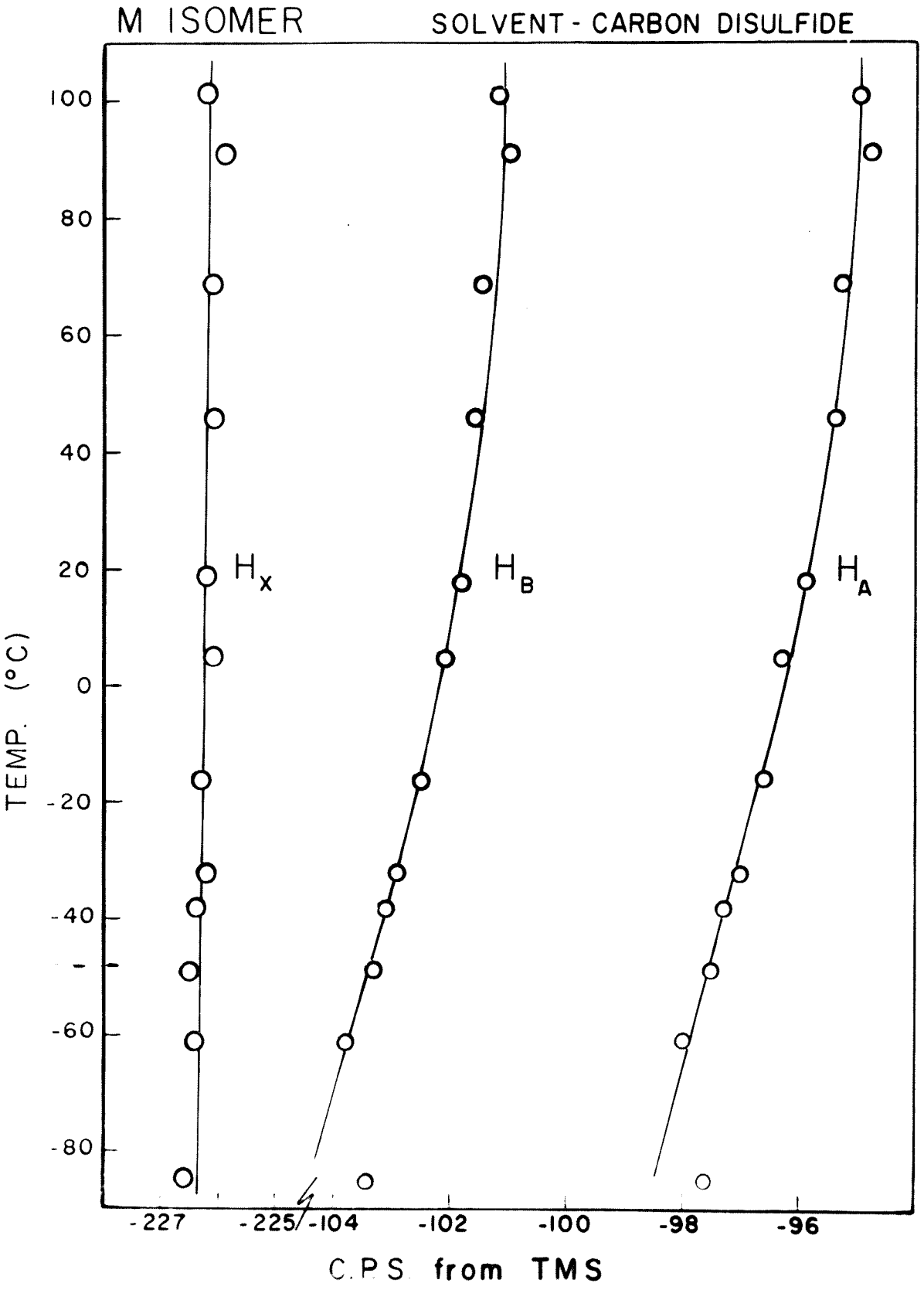
M ISOMER
SOLVENT - CARBON DISULFIDE
100
80
60
40
20
0
-20
-40
-60
-80
TEMP. (°C)
H_X
H_B
H_A
-227
-225
-104
-102
-100
-98
-96
C.P.S from TMS

Figure 5.13 Plot of proton resonance shifts for M isomer of bis (2,2-dichlorocyclopropyl) ether (in cps at 60 Mcps) against mole fraction benzene at 18°C; calibration is to low field of internal TMS.

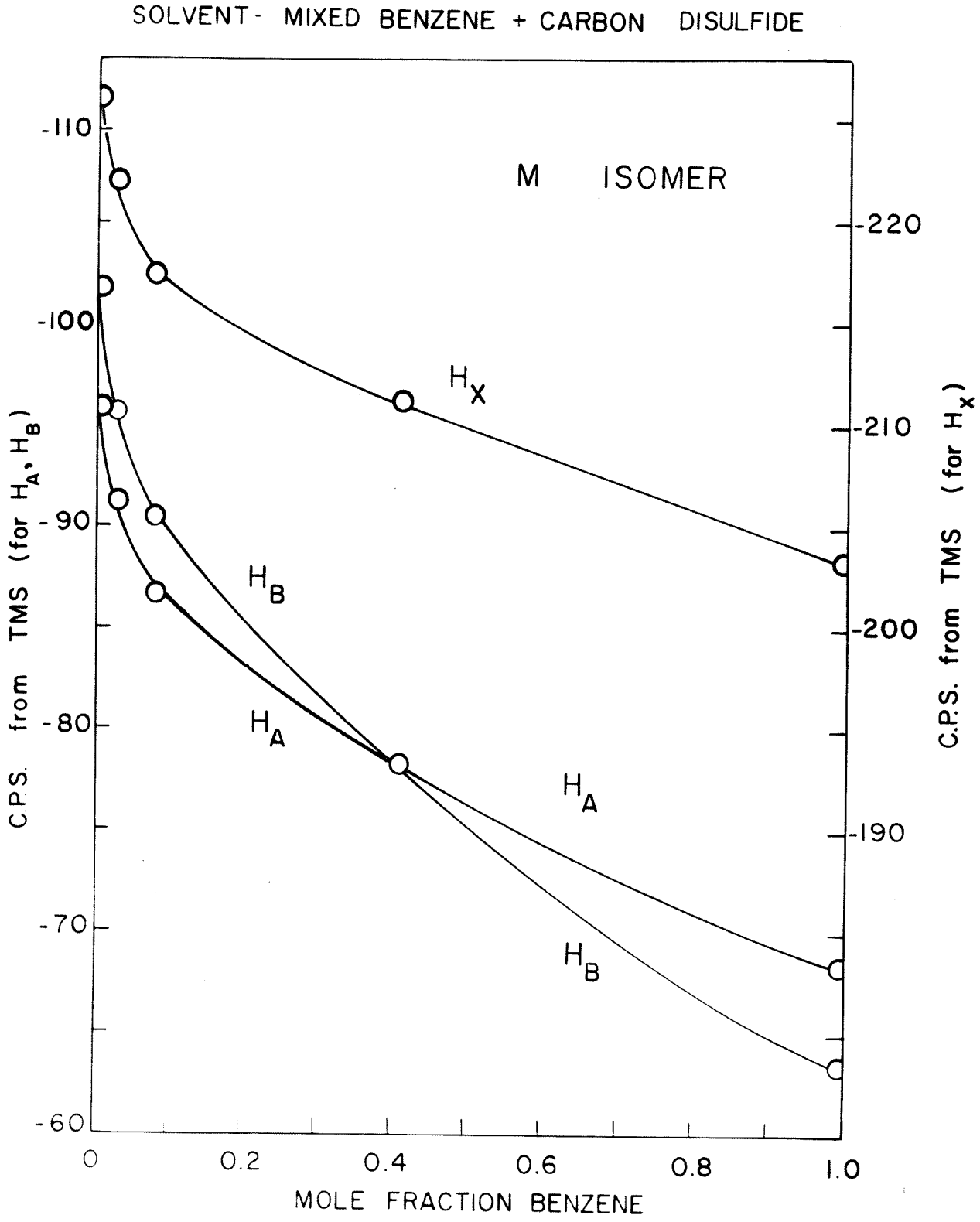
SOLVENT- MIXED BENZENE + CARBON DISULFIDE
M ISOMER
H_X
H_B
H_A
H_A
H_B
-110
-100
-90
-80
-70
-60
-220
-210
-200
-190
C.P.S. from TMS (for H_A, H_B)
C.P.S. from TMS (for H_X)
0
0.2
0.4
0.6
0.8
1.0
MOLE FRACTION BENZENE

5. Discussion

A. Coupling Constants

From a series of measurements (Chapter IV) it is almost certain that proton coupling constants in cyclopropane derivatives are negative. The vicinal couplings are then positive with the trans smaller than the cis (Chapters II and III). The labelling in Figure 5.1 and in the other figures and tables assumes this relationship and that the B proton resonates at a higher field than the A proton in benzene solution.

From the tables for isomer M: $J_{AB} = J_{gem} = -8.77 \pm 0.25$ cps; $J_{AX} + J_{BX} = 12.8 \pm 0.2$ cps with $J_{AX} = J_{trans} = 5.0 \pm 0.5$ cps and $J_{BX} = J_{cis} = 7.8 \pm 0.5$ cps. For the L isomer: $J_{AB} = J_{gem} = -8.7 \pm 0.2$ cps; $J_{AX} + J_{BX} = 13.0 \pm 0.2$ cps with $J_{AX} = J_{trans} = 4.8 \pm 0.5$ cps and $J_{BX} = J_{cis} = 8.2 \pm 0.5$ cps. The individual errors in J_{AX} and J_{BX} are considerably larger than their sum because of the way in which these quantities depend on peak separations.[75] For those solutions where the shift between A and B protons was zero the average of J_{AX} and J_{BX} could be determined quite accurately and was equal to half the sums given above, within experimental error. Also, within error, the couplings are independent of solvent and temperature.

B. Chemical Shifts and Internal Rotational Effects

The internal rotational motions of the molecules about the carbon-oxygen bonds is indicated schematically in Figure 5.14, where R represents the substituted cyclopropyl group. From Dreiding molecular models it appears unlikely that rotations about these bonds

would result in an averaging process such that the shifts of the A and B protons would become identical. This hypothesis is supported by the shift behaviour of these two protons as a function of temperature in carbon disulfide and in benzene. The dielectric constants of these

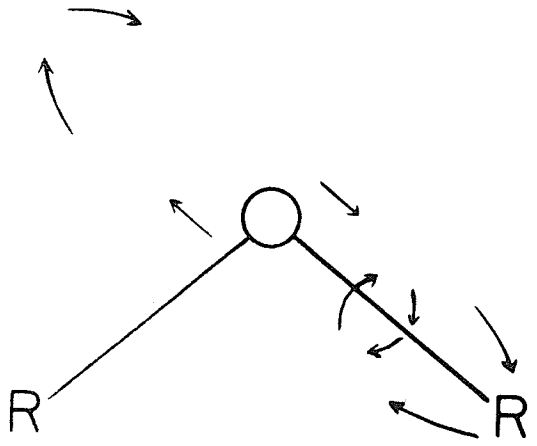

Figure 5.14 Schematic representation of the internal rotational motions of the molecules about the carbon-oxygen bonds; R represents the substituted cyclopropyl group.

two solvents are almost identical and the population of the various rotational isomers should have the same temperature dependence in the two solvents. As can be seen in the tables, this is not the case at all.

Similar objections can be levelled against a more complex motion consisting of combined rotation and an effective inversion of the oxygen atom.

C. Chemical Shifts and Association in Benzene

Association between benzene and polar molecules has been investigated for relatively simple molecules by a number of workers.[70,76-81] Such an association usually results in a high-field shift of the solute protons due to the disk-shaped molecules of the diamagnetically anisotropic benzene.[70] A temperature increase should break up the association and result in a shift to low field of the solute proton peaks. This is exactly what is found. If the A and B protons have different association shifts, as is reasonable, the high-temperature shift equivalence must be looked upon as accidental.

The temperature dependence of the shifts in carbon disulfide as shown in Figure 5.12 is consistent with very weak association between the rod-shaped anisotropic carbon disulfide molecules and the solute. Such an association results in a low-field shift[70] and as the temperature increases a high-field shift is predicted. This is what is found, although it is small (1 - 3 cps) and therefore consistent with very weak association.

In this discussion dispersion (van der Waals) effects and density effects have been ignored. However, the use of an internal

reference minimizes these effects since they are small and therefore almost the same for the solute and the reference. Reaction field effects[49] should be almost the same in both carbon disulfide and benzene. The excess shifts which are observed, therefore, can be put down to specific interactions with the solvent. The negligible change with temperature of the benzene peaks relative to the TMS peaks indicates no drastic change in the packing of molecules which do not specifically interact.

It is postulated that the complex formation between the ether and benzene can be represented by

$$A\text{-}H + B \rightleftharpoons A\text{-}H \ldots B$$

with an equilibrium constant

$$K = \frac{[A\text{-}H \ldots B]}{[A\text{-}H]\,[B]} = \exp\left(\frac{\Delta S}{R}\right) \exp\left(\frac{-\Delta H}{RT}\right)$$

Where [A - H] is the concentration of the ether, [B] is the concentration of the benzene and [A - H ... B] is the concentration of the complex. ΔS is the entropy of formation and ΔH the heat of formation of the complex. If K is written in units of mole fraction (mf) and it is assumed that the shifts differ by a negligible amount from those of an infinitely dilute solution, the benzene concentration becomes unity.

Then

$$\frac{p}{1-p} = \frac{[A - H \ldots B]}{[A - H]} = \exp\left(\frac{\Delta S}{R}\right) \exp\left(\frac{-\Delta H}{RT}\right) \qquad (1)$$

where p is the fraction of the ether in the complex form. The measured shift of the solute protons δ is the weighted mean of the shift of the unassociated solute δ_u and that in the complex δ_c. Then

$$\delta = p\,\delta_c + (1 - p)\,\delta_u \qquad (2)$$

From equations (1) and (2) δ can be found as a function of ΔH, ΔS, δ_c and δ_u and the known temperature.

Following Abraham[81] it may be argued that at a high temperature where $\Delta H \ll kT$, all the solute protons would be in the unassociated form. In this state the shift from internal TMS would be due to the different chemical nature of the solute and reference and to the reaction field of the benzene. Since carbon disulfide and benzene have almost the same dielectric constant the high temperature shift in carbon disulfide can be taken as the unassociated shift δ_u. Any small effects due to slight differences in dispersion forces have been ignored. The high temperature shift in carbon disulfide was taken in order to eliminate association effects with this solvent as far as possible. This effect is very small since at most a 3 cps shift with respect to internal TMS was found over a 200°C. range (Table 5.2).

At low temperature, $\Delta H \gg kT$, all the solute molecules would be associated with the benzene and the shift would now be δ_u plus that due to complex formation. δ_u is taken to be the origin and all

the chemical shifts are measured from it.

Then it follows that $\delta = p\ \delta_c$ and that

$$\delta = \delta_c \left[1 + \exp\left(\frac{-\Delta S}{R}\right) \exp\left(\frac{\Delta H}{RT}\right)\right]^{-1} \qquad (3)$$

which is the equation given by Abraham.[81] δ is now a function of three unknowns only.

Equation (3) has been applied to the most abundant isomer M where the individual proton shifts are most reliable. δ_u is taken from Table 5.2. The experimental points in Figure 5.9 can be fitted with the following values for the parameters within the error limits given:

Proton	δ_u (cps)	δ_c (cps)	ΔH (cal.)	ΔS (e.u.)
H_X	-226.2	52 ± 2	-1700 ± 50	$-6.2 \pm .1$
H_B	-101.2	88 ± 5	-1700 ± 100	$-6.2 \pm .1$
H_A	- 95.0	64 ± 5	-1700 ± 100	$-6.2 \pm .1$

The values are reasonable in that ΔH and ΔS are the same for all three protons while δ_c is different. δ_c depends on the structure of the complex and may therefore very well be different for protons situated at different positions in the solute molecule.

Equation (3) was not applied to the isomer L chemical shift in Figure 5.10 since a reliable value of δ_u was not available.

6. Conclusions

Hydrogen bonding has been postulated to explain interactions of methyl iodide and iodoform with toluene[81] and of chloroform with mesitylene.[76] Whether the interaction found for this ether with benzene can be similarly explained is open to speculation. It is felt that an association such that the benzene molecules tend to avoid electron rich centres (oxygen and chlorine) is probably just as reasonable if not preferable.[51] H_X would then be expected to have the smallest association shift as has been found. It is interesting to note that the dilution shifts of protons A and B in the mixed solvent (Figure 5.11) have a ratio $H_A/H_B = 0.71$ while the ratio of the association shifts is 0.73. Since the former are measured against internal TMS they should also be a measure of the association dependence of the proton shifts.

CHAPTER VI

A_2B_2 SPECTRA OF CYCLOPROPANE DERIVATIVES

1. Introduction

The analysis of A_2B_2 spectra has been discussed in some detail,[82-90] especially in regard to unsaturated ring systems.[89,90] Here the probable A_2B_2 spectra for 1,1-disubstituted cyclopropanes are discussed and illustrated with an example. This discussion is applicable also to A_2B_2 arrangements in other fixed saturated ring systems.[57,91] From the collection of proton coupling constants in cyclopropanes given in Chapter III,[31] and from spin decoupling experiments in Chapter IV,[69] it is known that the probable range of values is -4 to -8 cps for J_{gem}, 4 to 8 cps for J_{trans} and 7 to 11 cps for J_{cis}, depending on the substituents. A similar approach to that which Martin and Dailey[89] applied to disubstituted benzenes is used except that the parameters are expressed in units of Δ , the chemical shift.

The shifts and coupling constants are given for the protons in 1-phenylcyclopropylcarboxylic acid in solution in carbon disulfide, chloroform and benzene as an example of the A_2B_2 analysis. The ring protons in 1-phenylcyclopropylcarbinol were found to be equivalent in different solvents, with insignificant coupling to the protons in the methylene and phenyl groups.

Some of the proton coupling constants were also obtained for the symmetrically substituted 1,1-diphenylcyclopropane using A_2X_2

analysis on the C^{13}--H_2 sidebands from the ring protons.

2. Experimental

1-Phenylcyclopropylcarboxylic acid was studied as a 6 mole percent solution in carbon disulfide, 7 mole percent solution in chloroform, and an 8 mole percent solution in benzene. 1-Phenylcyclopropylcarbinol was investigated as a 20 mole percent solution in benzene and chloroform and 10 mole percent and 15 mole percent solution in carbon disulfide. Tetramethylsilane was used as the internal reference. Small quantities of these compounds were a gift from Dr. James W. Wilt. Their physical properties are given in his paper.[92] No impurities were observable in the proton spectra.

The spectra were obtained on a Varian DP 60 Mcps spectrometer at room temperature. The results represent an average of ten spectra run forward and reverse. Corresponding A and B transitions were found to be symmetrical with respect to the centre of the spectrum to within $\pm$ 0.05 cps. The possible error in each line position is not more than $\pm$ 0.1 cps.

1,1-Diphenylcyclopropane was studied as a 1:1 solution in carbon disulfide. The proton resonances of the phenyl substituents and the cyclopropyl ring were calibrated with respect to internal tetramethylsilane. The C^{13}--H_2 satellites from the cyclopropyl protons were measured using the C^{12}--H_2 resonance as reference. This compound contained only the natural abundance of the C^{13} isotope.

3. Computation of the Spectra

The ring proton systems for unsymmetrically 1,1-disubstituted cyclopropanes are of the A_2B_2 type, consisting of two pairs of equivalent spins. The secular equation of this system is given in the literature[83] and is shown in Table I, Appendix III.

Since the system has C_{2V} symmetry and the spin operator $F_Z = \sum I_Z$ commutes with the Hamiltonian, the 16 X 16 secular determinant may be reduced to eight subdeterminants of which only one, the 4 X 4 symmetric subdeterminant with $F_Z = 0$, is of order greater than 2 X 2. Therefore all but four of the eigenfunctions may be determined explicitly.[83]

The spectrum consists of two 12-line groups, symmetric about a central point so that only one half of the spectrum need be discussed. The frequencies and intensities of the lines in one half-spectrum are given in Table II, Appendix III, using the parameters K, L, M, N, and Δ which are defined in part A below. The frequencies and intensities of the transitions which may be solved explicitly, lines 1, 3 and 9-12, are given in terms of these molecular parameters. The other six transitions, numbered 2, 4, and 5-8, involve the quantities P_m and c_{mn} which arise from the diagonalization of the 4 X 4 subdeterminant. The parameter P_m is the difference between the energy of eigenfunction mS_o' and that of the base function mS_o, to which it reverts in the limit of large internal chemical shift. The parameters c_{mn} arise from the calculation of the eigenvectors of the 4 X 4 subdeterminant.

The analysis is further simplified if the AB chemical shift is large with respect to the coupling constants. For this situation the 4 X 4 can be reduced to 2 X 2 subdeterminants so that all the frequencies and intensities of the transitions can be given explicitly.[93] The coupling constants are defined as in I:

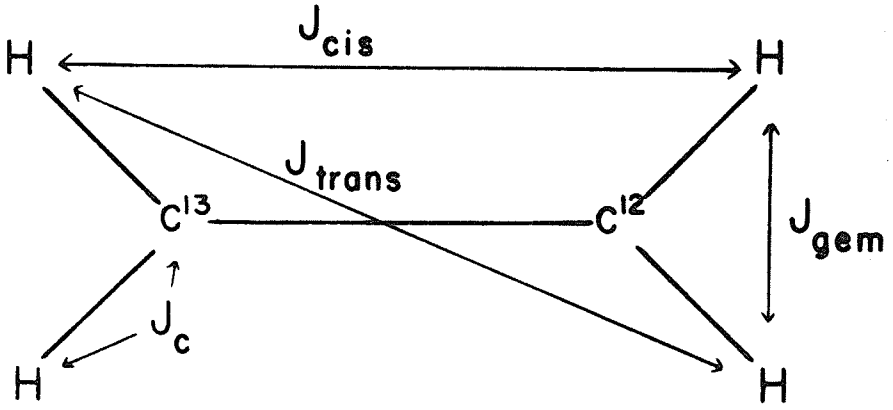

I

The energies and intensities of the C^{13}--H_2 transitions in a slightly perturbed A_2X_2 spin system can be given as in Table III, Appendix III.[26] There are four distinct coupling constants for such a system. In addition to the two vicinal and one geminal coupling constants, there is the coupling between the C^{13} spin and its attached protons, called J_c, which gives rise to the sidebands in the first place. Because of the size of these coupling constants this spin system can best be

described by a slightly perturbed A_2X_2 system. In 1,1-diphenylcyclopropane the two cis coupling constants are equal so that transitions 9, 10 and 11,12 from Table III, Appendix III are always degenerate. There are thus a maximum of ten allowed transitions for each of the A and the X resonances.

A. A_2B_2 Analysis

i) General

For the A_2B_2 systems under consideration there are four coupling constants as in II, where J_A and J_B are the two cis couplings. The parameters Δ , K, L, M, and N are also defined.

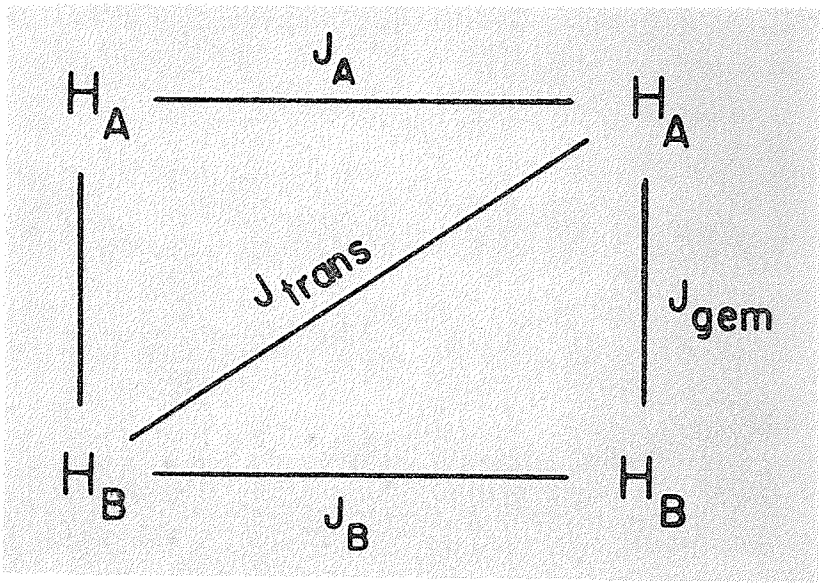

II

$$\Delta = \eta_{H_o} (\sigma_B - \sigma_A)$$

$$K = J_A + J_B \qquad N = J_{\underline{gem}} + J_{\underline{trans}}$$

$$M = J_A - J_B \qquad L = J_{\underline{gem}} - J_{\underline{trans}}$$

The secular equation and energy transitions have been tabulated in Appendix III. The substitution of -L for L does not alter the secular equation and that of -M for M merely interchanges the labelling of certain transitions, so that the signs of L and M cannot be obtained from the spectrum. The spectrum is, however, sensitive to the relative signs of K and N.[90] K here is defined to be positive since it is the sum of two cis coupling constants.[59] N may then be negative for $|J_{gem}| > |J_{trans}|$ and positive for $|J_{gem}| < |J_{trans}|$. It is almost certain that $J_{gem} < 0$ and that $J_{trans} > 0$,[31,59,69] and hence, L must be less than 0 which makes it possible to assign values to J_{gem} and J_{trans} from the spectrum. J_A and J_B will differ by hardly more than 1 cps in these systems.[31] Therefore there is no specific information as to the relative signs of L and M so that J_A and J_B cannot be distinguished from the spectra.

The eigenvalues and eigenvectors of the 4 X 4 determinant of the secular equation were computed on an IBM 1620. The theoretical spectra were obtained for all combinations of the parameters in units of the chemical shift Δ :

K = 0.4, 0.6, 0.8, 1.0, 1.2, 1.5

L = 0.3, 0.4, 0.5, 0.6

N = -0.1, 0, 0.1, 0.2

M = 0, 0.01, 0.02, 0.04

These values correspond to the most probable values of the coupling constants,[31,57,91] together with the values of Δ which would give

rise to intelligible spectra. Some of the computed spectra are presented in Figures 6.1 to 6.9. Since the spectra are symmetric about the centres, only the high-field halves are shown. A bracket around transition 8 indicates that it now comes from the low-field proton transitions.

ii) The Effect of the Parameters K, L, M, N

The effect of the relative signs of the coupling constants and the magnitudes and signs of the parameters K, L, M, N upon the A_2B_2 spectra has been discussed in detail by Grant et al for unsaturated ring systems.[90] The changes which occur specifically for 1,1-disubstituted cyclopropanes are outlined.

a) Parameter K

The K parameter does not change the positions of lines 1 and 3 nor those of the antisymmetric set of transitions 9-12. It does however influence the positions of the symmetric set 5-8, line 2, and to a small extent line 4. Transition 2, at a position of $\Delta + \frac{1}{2}N - \frac{1}{2}C_N - P_1$ moves toward the outer edge of the B spectrum as K increases until $\left| K \left|\right> \right| - \Delta - \frac{1}{2}N \right|$. At this point the value of P_1 reverses sign, bringing line 2 back into the interior of the spectrum. These changes in the spectrum can be seen in Figures 6.1, 6.3, 6.5 and 6.7, for $L = 0.3\Delta$ and $N = -0.1$, 0, 0.1, and 0.2Δ. The parameter K may be approximated from the spectra as the differences $\nu_8 - \nu_7 = \nu_6 - \nu_5$.

b) Parameter L

The change in the spectrum with an increase in the value of L from 0.3Δ to 0.6Δ can be seen in Figures 6.2, 6.4, 6.6 and 6.8. Both the antisymmetric transitions 9 through 12 and the symmetric transitions 5 through 8 are affected by an increase in L. As L increases the difference $\nu_8 - \nu_7 = \nu_6 - \nu_5$ becomes less and less a reasonable approximation to the value of K. Transitions 2 and 4 also shift with an increase in L, but 1 and 3 are unaffected. When $|L| \gg |M|$, L may be obtained almost exactly from the spectrum as the difference between lines 9,11 or 10,12. This is very likely the case for 1,1-disubstituted cyclopropanes.

c) Parameter N

Lines 1 to 4 are most affected by a change of N. As N decreases to zero lines 1 and 3 coalesce at the chemical shift position and interchange positions when N becomes negative. The most important change as N goes from a positive to a negative value is that of lines 2 and 4. These two lines are in reverse order but not reverse position in the spectrum, so that the sign of N can be distinguished from the appearance of the spectrum as shown in Figures 6.1 and 6.5, 6.2 and 6.6. This indicates the relative sign between $J_{\underline{gem}}$ and $J_{\underline{trans}}$ in substituted cyclopropanes. The antisymmetric transitions 9 to 12 are unaffected by a change of N. The symmetrical quartet 5 to 8 is also not significantly changed over the small range for which N has been varied.

d) Parameter M

The M parameter affects only the positions of the anti-symmetrical set 9 to 12 for any given value of L. As a first approximation the value of M may be taken as the difference between lines 9 and 10 or 11 and 12. As M increases from zero lines 11,12 and 9,10 separate, as Figure 6.9 indicates. Since $M = J_A - J_B$ is of the order of 1 cps or less,[31] the spectra presented in Figures 6.1 to 6.8 have all been calculated assuming a small, and rather arbitrary, value of $M = 0.01\,\Delta$.

Figure 6.1 The variation of the spectrum with a change in the parameter K is presented for N = -0.1, L = 0.3, and M = 0.01. The high-field B transitions of the symmetrical A_2B_2 spectrum are illustrated with the magnetic field in units of the chemical shift from the centre of the spectrum. The bracket around transition 8 indicates in this and all succeeding diagrams that it is an A transition overlapping in the B spectrum. The intensities of transitions 5 and 9 have been doubled relative to the intensities of the other transitions. The parameters K, L, N, M are given in units of the chemical shift Δ .

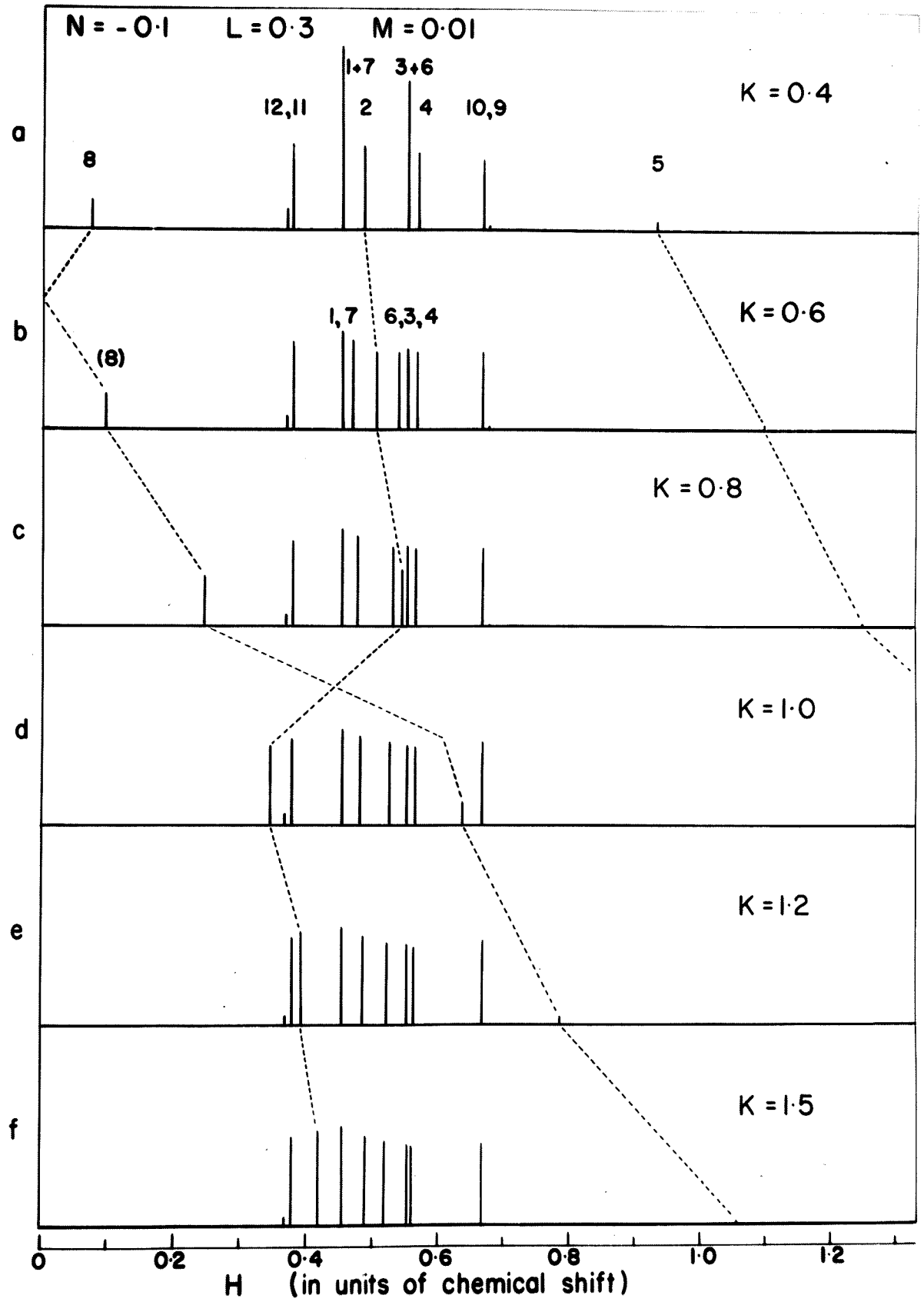
N = -0·1
L = 0·3
M = 0·01
a
K = 0·4
8
12,11
1+7
2
3+6
4
10,9
5
b
K = 0·6
(8)
1, 7
6,3,4
c
K = 0·8
d
K = 1·0
e
K = 1·2
f
K = 1·5
0
0·2
0·4
0·6
0·8
1·0
1·2
H (in units of chemical shift)

Figure 6.2 Starting with the spectrum presented in Figure 6.1(b), the spectral changes due to the parameter L are shown for N = -0.1, K = 0.6, and M = 0.01. The changes in the spectrum when varying L from 0.3 to 0.6 for the other values of the parameter K in Figure 1 are the same as that given here for the case of K = 0.6.

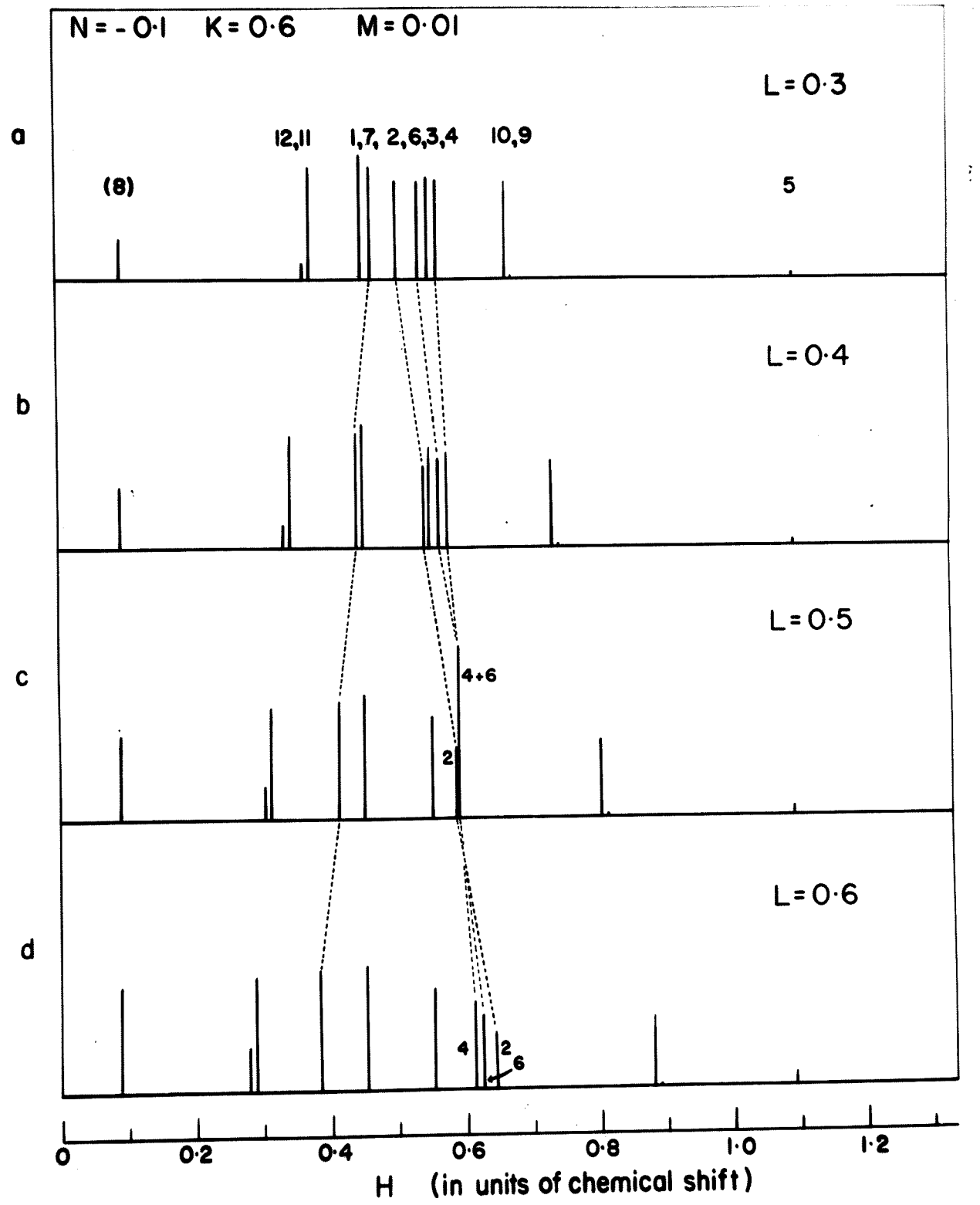
N = - 0·1 K = 0·6 M = 0·01
a
L = 0·3
12,11
1,7, 2,6,3,4
10,9
(8)
5
b
L = 0·4
c
L = 0·5
4+6
2
d
L = 0·6
4
2
6
0
0·2
0·4
0·6
0·8
1·0
1·2
H (in units of chemical shift)

Figure 6.3 The variation of the spectrum with a change in the parameter K is presented for N = 0, L = 0.3 and M = 0.01.

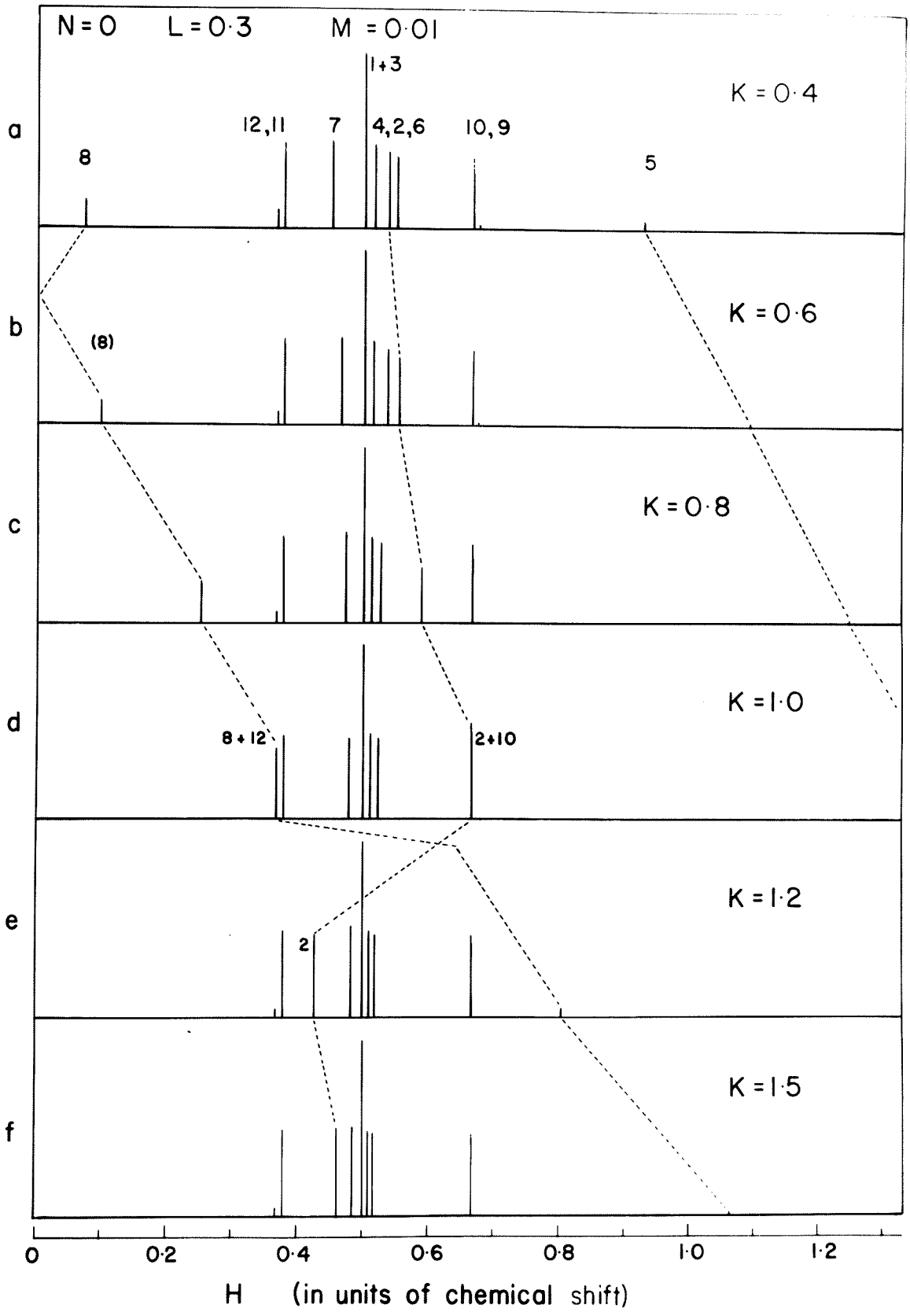
N = 0 L = 0·3 M = 0·01
a
K = 0·4
1+3
12,11
7
4,2,6
10,9
8
5
b
K = 0·6
(8)
c
K = 0·8
d
K = 1·0
8+12
2+10
e
K = 1·2
2
f
K = 1·5
0
0·2
0·4
0·6
0·8
1·0
1·2
H (in units of chemical shift)

Figure 6.4 Starting with the spectrum presented in Figure 6.3(b) the spectral changes due to the parameter L are shown for N = 0, K = 0.6, and M = 0.01. The changes in the spectrum when varying L from 0.3 to 0.6 for the other values of the parameter K in Figure 6.3 are the same as that given here for the case of K = 0.6.

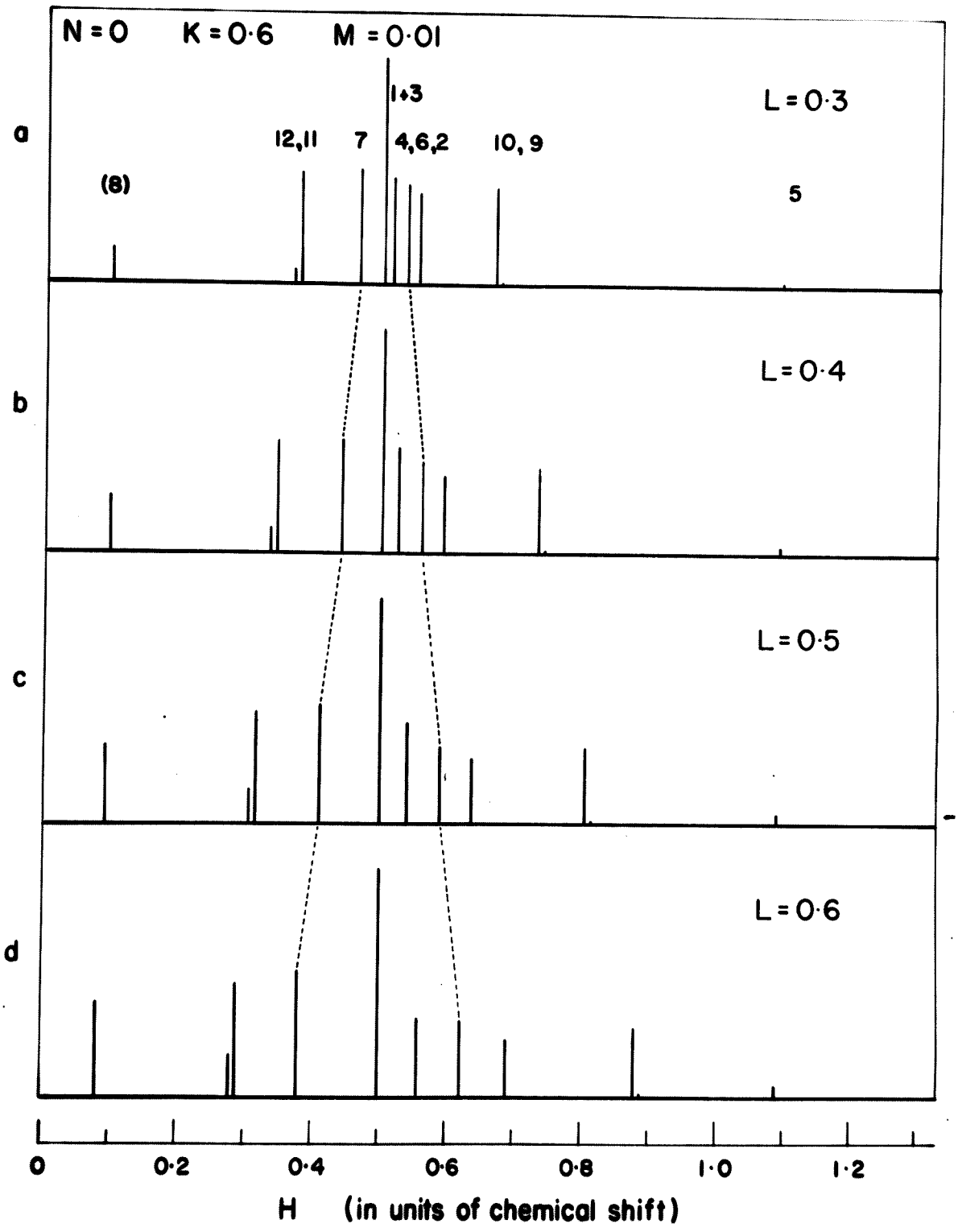
N = 0 K = 0·6 M = 0·01
a
L = 0·3
1+3
12,11
7
4,6,2
10, 9
(8)
5
b
L = 0·4
c
L = 0·5
d
L = 0·6
0
0·2
0·4
0·6
0·8
1·0
1·2
H (in units of chemical shift)

Figure 6.5 The variation of the spectrum with a change in the parameter K is presented for N = 0.1, L = 0.3, and M = 0.01. A comparison of corresponding spectra in this diagram and Figure 6.1 illustrates the spectral change for N negative, $\left|J_{\underline{gem}}\right| > \left|J_{\underline{trans}}\right|$, and N positive, $\left|J_{\underline{gem}}\right| < \left|J_{\underline{trans}}\right|$.

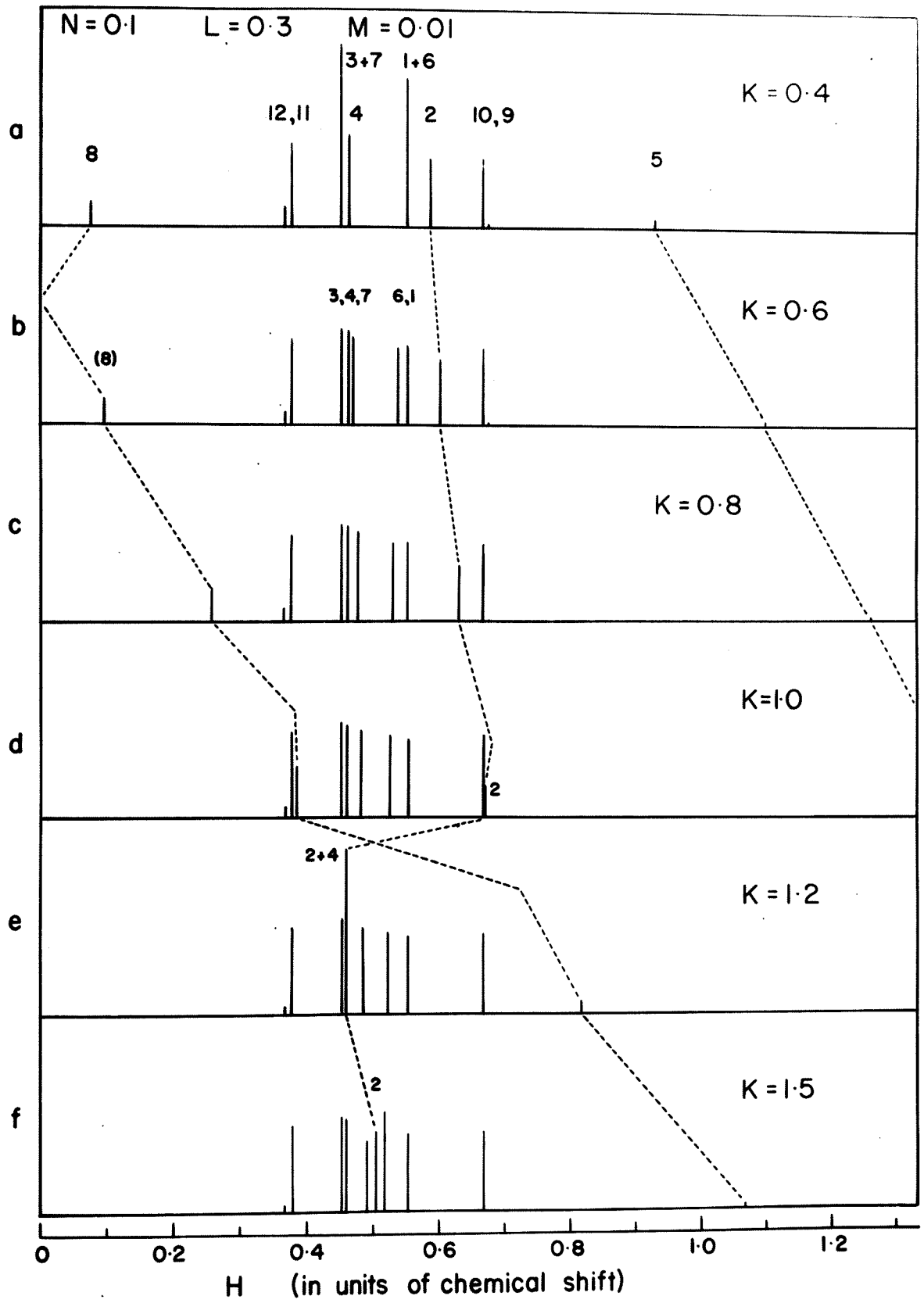
N = 0·1
L = 0·3
M = 0·01
a
8
12,11
3+7
4
1+6
2
10,9
5
K = 0·4
b
(8)
3,4,7
6,1
K = 0·6
c
K = 0·8
d
2
K=1·0
e
2+4
K = 1·2
f
2
K = 1·5
0
0·2
0·4
0·6
0·8
1·0
1·2
H (in units of chemical shift)

Figure 6.6 Starting with the spectrum presented in Figure 6.5(b), the spectral changes due to the parameter L are shown for N = 0.1, K = 0.6, and M = 0.01. Here also, a comparison with the corresponding spectra in Figure 6.2 illustrates the difference for a negative and positive value of N. The changes in the spectrum when varying L from 0.3 to 0.6 for the other values of the parameter K in Figure 6.5 are the same as that given here for the case of K = 0.6.

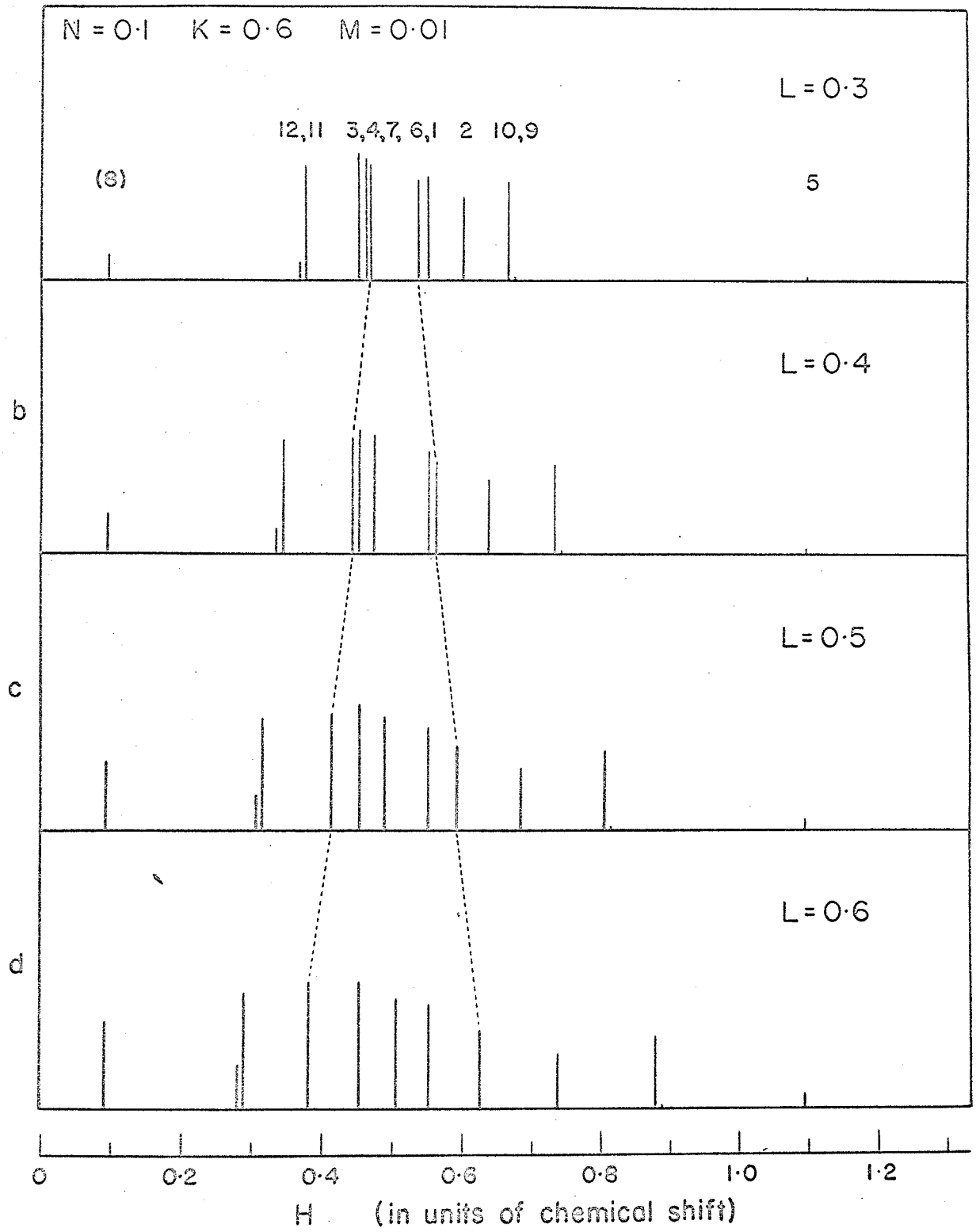
N = 0·1 K = 0·6 M = 0·01
L = 0·3
12,11 3,4,7, 6,1 2 10,9
(8)
5
b
L = 0·4
c
L = 0·5
d
L = 0·6
0
0·2
0·4
0·6
0·8
1·0
1·2
H (in units of chemical shift)

Figure 6.7 The variation of the spectrum with a change in parameter K is presented for N = 0.2, L = 0.3, and M = 0.01.

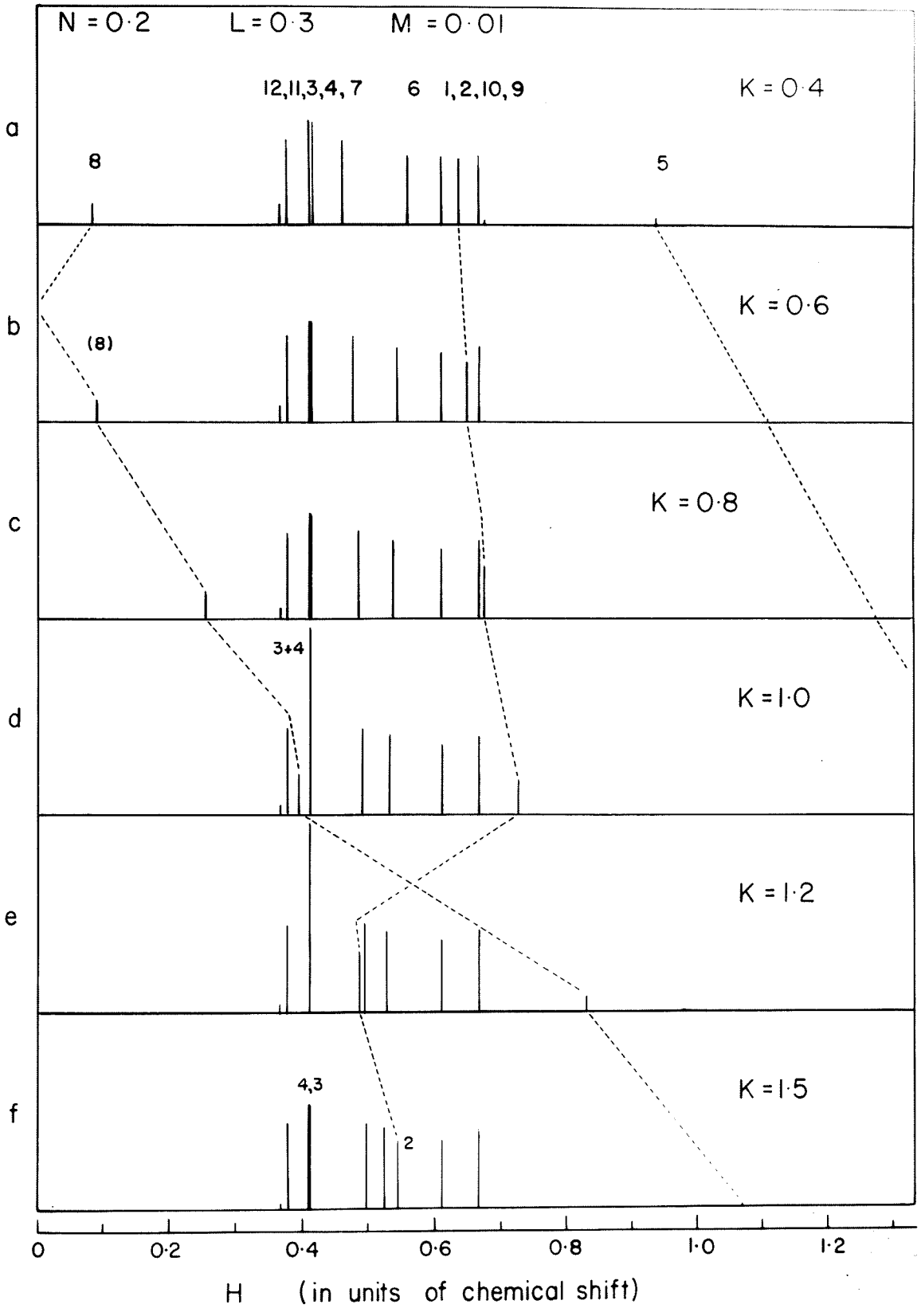
N = 0·2
L = 0·3
M = 0·01
12,11,3,4,7
6
1,2,10,9
K = 0·4
a
8
5
b
K = 0·6
(8)
c
K = 0·8
3+4
d
K = 1·0
e
K = 1·2
f
4,3
2
K = 1·5
0
0·2
0·4
0·6
0·8
1·0
1·2
H (in units of chemical shift)

Figure 6.8 Starting with the spectrum presented in Figure 6.7(b) the spectral changes due to the parameter L are shown for N = 0.2, K = 0.6, and M = 0.01. The changes in the spectrum when varying L from 0.3 to 0.6 for the other values of the parameter K in Figure 6.7 are the same as that given here for the case of K = 0.6.

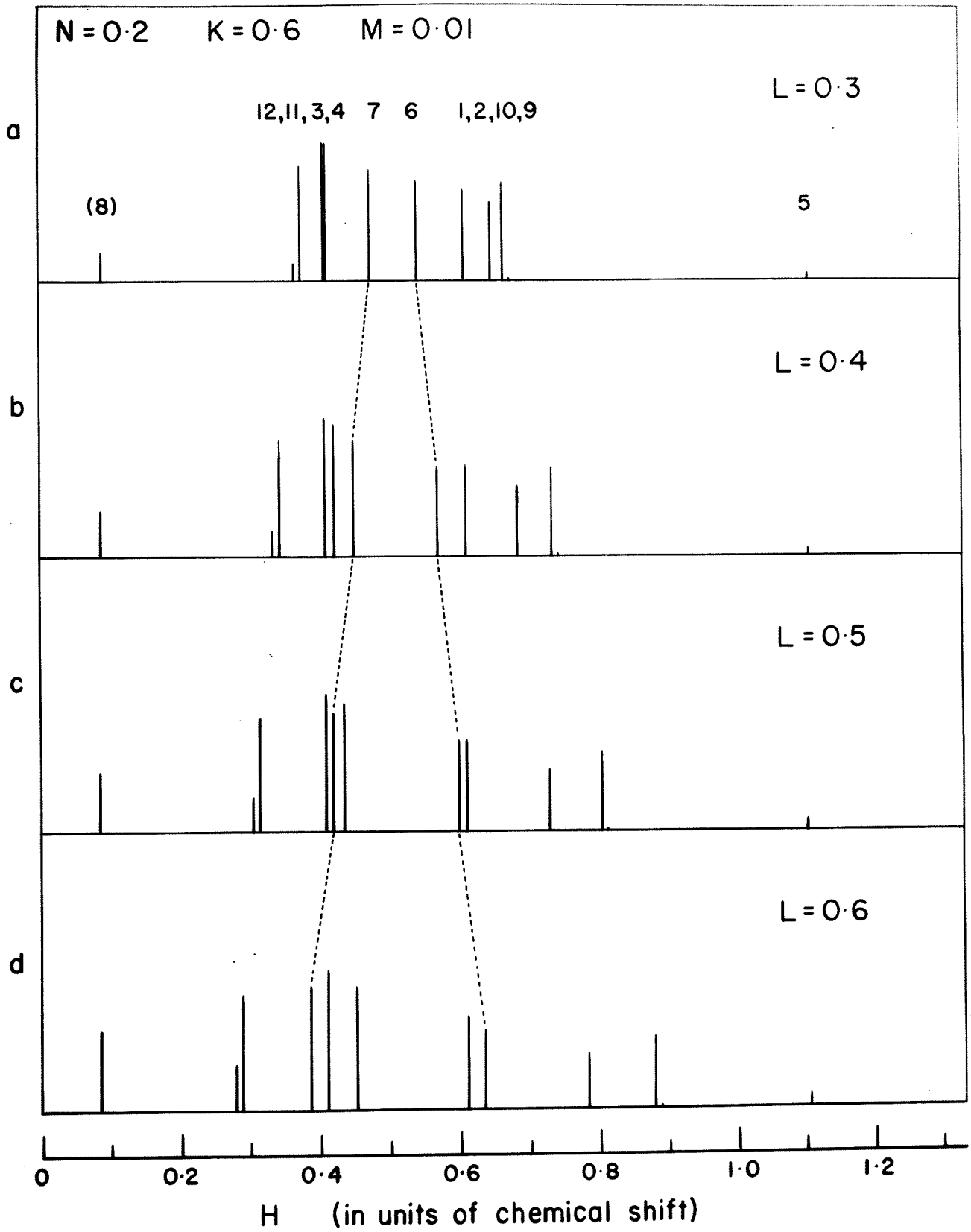
N = 0·2
K = 0·6
M = 0·01
a
L = 0·3
12,11,3,4
7
6
1,2,10,9
(8)
5
b
L = 0·4
c
L = 0·5
d
L = 0·6
0
0·2
0·4
0·6
0·8
1·0
1·2
H (in units of chemical shift)

Figure 6.9 The effect of the parameter M on the A_2B_2 spectrum is illustrated. The spectrum in Figure 6.3 (a) corresponds to that in (b) here. Since the parameter M for 1,1-disubstituted cyclopropanes appears to be small, all the spectra in Figures 6.1 to 6.8 were arbitrarily calculated for $M = 0.01\Delta$. For other values of M only transitions 9-12 in the preceding figures would change as illustrated here.

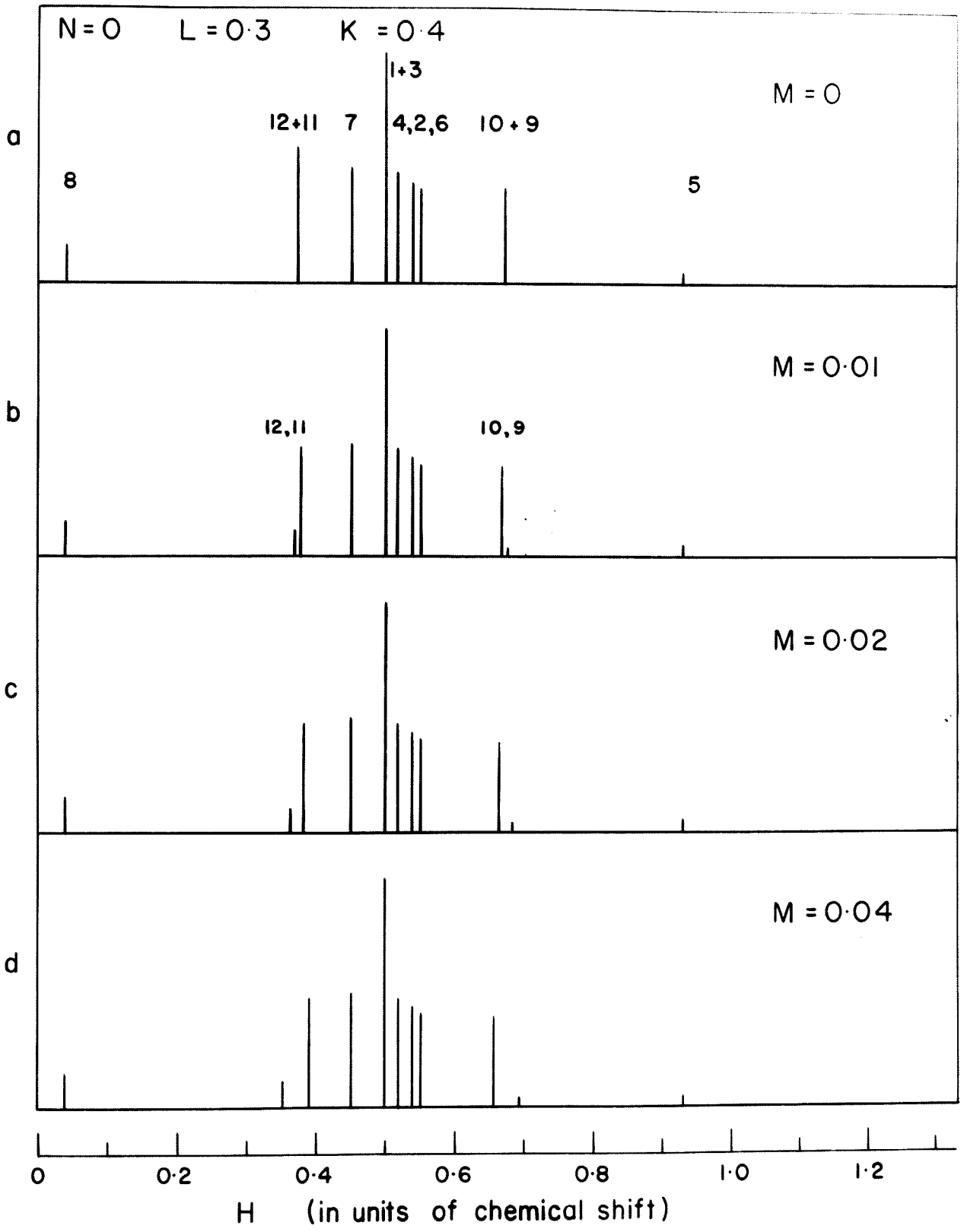
N = 0 L = 0·3 K = 0·4
a
M = 0
1+3
12+11
7
4,2,6
10 + 9
8
5
b
M = 0·01
12,11
10,9
c
M = 0·02
d
M = 0·04
0
0·2
0·4
0·6
0·8
1·0
1·2
H (in units of chemical shift)

iii) Analysis of Spectra

The A_2B_2 spectra for cyclopropane derivatives can be conveniently analyzed using the transition frequencies of Martin and Dailey[89] given in Table II, Appendix III. The use of symmetry and of the spin operator leaves only one 4 X 4 determinant which cannot be solved explicitly. The transitions which arise from this subdeterminant are lines 2,4 and 5-8. These lines contain the quantities P_m and c_{mn} which must be obtained from the numerical solution of the 4 X 4.

Since the frequencies and intensities of the remaining transitions are given explicitly in terms of the molecular parameters Δ , L, N, and M, the main problem is the identification of these lines in an experimental spectrum. The value of N may be obtained from the difference of lines 1 and 3 and the chemical shift from the position of either 1 or 3 with respect to the centre of the spectrum. L and M may be calculated from lines 9 to 12. When $|L| \gg |M|$, as would normally be true for these spectra, the parameter L may be obtained from $\nu_9 - \nu_{11} = \nu_{10} - \nu_{12}$. M will be approximately $\nu_9 - \nu_{10} = \nu_{11} - \nu_{12}$. These two parameters can then be adjusted to fit the experimental and theoretical spectra to within the accuracy desired.

One parameter, K, remains to be evaluated. The values obtained for Δ , N, and L are used to solve the 4 X 4 numerically with the method of successive approximations to find the value of K.

The lines which vary the most with a change in K, lines 2 and 8, are a good means of identifying the correct value of K. If a fit between the experimental and theoretical transitions cannot be obtained using N as a positive quantity, then the calculations should be repeated for N negative.

B. A_2X_2 Analysis

Since the energy transitions in an A_2X_2 system can be given explicitly, as in Table III, Appendix III, the analysis is relatively straightforward. From the known magnitudes of the coupling constants in cyclopropanes the relative order of the lines in the spectrum may be found. With this assignment of lines the vicinal coupling constants are obtained from the calibrated spectrum. The geminal coupling constant cannot be found for this case since transitions 4 and 7 of the quartet 4-7, from which J_{gem} is calculated, are very weak and not observable in the spectrum.

4. Results

A. 1-Phenylcyclopropylcarboxylic Acid

The values obtained for the chemical shifts with respect to internal TMS and the coupling constants for 1-phenylcyclopropylcarboxylic acid are given in Table 6.1. Figure 6.10 shows the proton resonance spectrum in benzene with the calculated spectrum below. The phenyl and carboxyl proton resonances were approximately 440 cps and 740 cps to low field of internal TMS, respectively. They are not discussed further.

TABLE 6.1

CHEMICAL SHIFTS AND COUPLING CONSTANTS OF 1-PHENYCYCLOPROPYLCARBOXYLIC ACID IN CPS

Solution	Chemical Shifts*		Parameters				J_{gem}	J_{trans}	J_A*		J_B*	
	H_A*	H_B*	L	N	K	M#			M = 0	M = 0.4	M = 0	M = 0.4
6 mole % in CS_2	93.7	68.1	±10.89	+3.00	+19.3	±0.2	-3.89	6.89	9.65	9.85	9.65	9.45
8 mole % in C_6H_6	89.1	52.8	±10.96	+3.00	+19.4	±0.2	-3.99	6.97	9.7	9.9	9.7	9.5
7 mole % in $CHCl_3$	98.8	74.3	±10.95	+2.89	+19.4	±0.2	-4.03	6.92	9.7	9.9	9.7	9.5

*At 60 Mcps to low field from internal TMS.

*The protons H_A, H_B and their respective coupling constants cannot be distinguished in the analysis and are designated arbitrarily.

#Value of M could be of the order of 0 to 0.4 cps.

Figure 6.10 Proton resonance spectrum at 60 Mcps of 1-phenyl-cyclopropylcarboxylic acid, 8 mole % in benzene; calibration is to low field of internal TMS. The calculated spectrum below illustrates the overlap of transition 8 from the B region into the A region. Protons A and B are assigned arbitrarily and cannot be distinguished from the spectrum alone. The calculated spectrum assumes $J_{\underline{gem}}$ to be of opposite sign to $J_{\underline{cis}}$ and $J_{\underline{trans}}$.

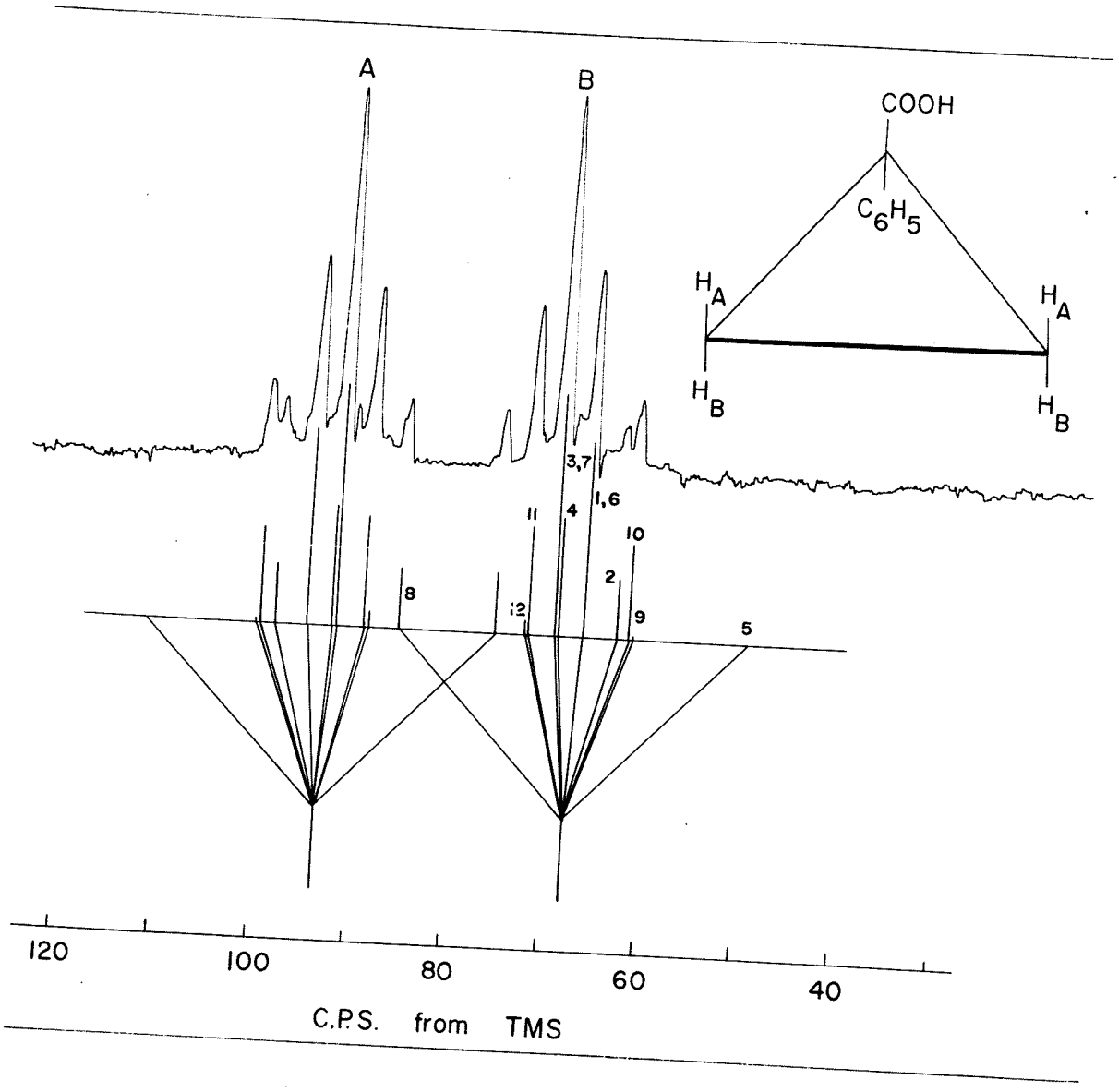
A
B
COOH
C_6H_5
H_A
H_A
H_B
H_B
3,7
1,6
11
4
10
2
8
12
9
5
120
100
80
60
40
C.P.S. from TMS

The parameters give a fit of the theoretical and experimental lines to within ±0.1 cps, which is as good as the uncertainty in the measurements. The parameter M could not be evaluated since no splitting of lines 11, 12 and 9, 10 was observed. This does not necessarily indicate that M = 0 since there appears to be sufficient coupling of the cyclopropyl protons with the phenyl substituent to broaden the lines slightly. This could mask any splitting of up to 0.4 cps. The spectrum in Figure 6.10 was calculated assuming M = 0.2 cps. Line 5 was not observed in the spectrum due to its low intensity and the broadening by the phenyl group.

The designation of protons H_A and H_B in Figure 6.10 is assigned arbitrarily and could be reversed. J_A cannot be distinguished from J_B, especially since their values are very similar. From the spectrum alone J_{gem} and J_{trans} cannot be distinguished. However, J_{gem} is almost certainly negative and J_{trans} positive.[31,59,69] A satisfactory fit to the observed spectrum could only be obtained with opposite signs for J_{gem} and J_{trans}.

B. 1-Phenylcyclopropylcarbinol

This compound, the structure of which is given in III, was expected to have an A_2B_2 spectrum but in the four solutions in Table 6.2 the ring protons were isochronous. They were not sufficiently coupled to either substituent to give an observable splitting of the single resonance peak. No coupling was observed between the methylene and hydroxyl protons, indicating exchange of the hydroxyl protons at a rate sufficient to obscure the expected splitting of about 5 cps.[94]

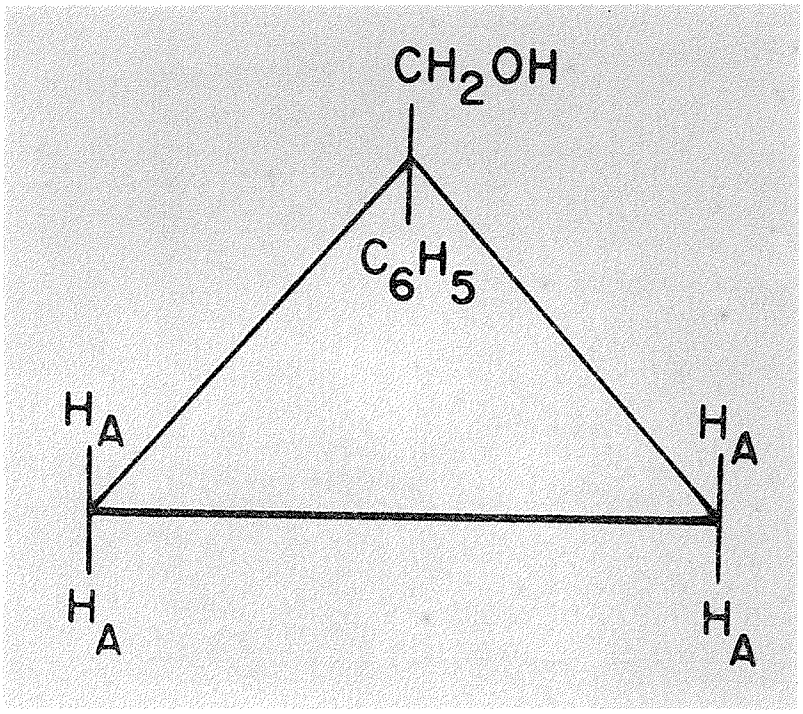

III

The shifts of all protons relative to internal TMS are given in Table 6.2.

C. 1,1-Diphenylcyclopropane

From the A_2X_2 analysis of the C^{13}--H_2 sidebands of the ring protons, the coupling constants were found to be:

$J_{\underline{cis}}$ = 9.55 cps.

$J_{\underline{trans}}$ = 6.42 cps.

$J_{C^{13}-H}$ = 162.2 cps.

In a 1:1 carbon disulfide solution the chemical shifts with respect to internal TMS were 68.6 cps and 422 cps to low field for the cyclopropyl and phenyl protons, respectively.

TABLE 6.2

PROTON CHEMICAL SHIFTS* OF 1-PHENYLCYCLOPROPYLCARBINOL IN SOLUTION

Solution	Ring Protons	$-CH_2-$	-OH	C_6H_5
10 mole % in CS_2	39.7	200.2	186.2	427
15 mole % in CS_2	38.6	199.6	203.6	425.6
20 mole % in C_6H_6	41.1	206.3	179.1	400#
20 mole % in $CHCl_3$	43.7	205.9	180.7	425#

*In cps at 60 Mcps to low field from internal TMS.

#Phenyl resonance hidden by solvent peak.

5. Discussion

A. 1-Phenylcyclopropylcarboxylic Acid

From the A_2B_2 analysis of this compound, a fit between the experimental and the theoretical spectrum could only be obtained with the geminal coupling constant of opposite sign to the vicinal couplings. This is in agreement with the results presented in Chapter IV.

In Table 6.1 it can be seen that the H_B protons shift more to high field than do the H_A protons when the solvent is changed from

carbon disulfide to benzene. If it could be decided which side of the cyclopropane ring is avoided by the benzene solvent molecule, a definite assignment of H_A and H_B could be made. From previous experience with benzene as a solvent (Chapters III and V), it is suggested that the carboxyl group would cause a closer packing of the benzene molecules about the protons trans to it. The H_B protons as given in Table 6.1 would then be trans to the carboxyl group. A series of studies to establish preferences of this type is indicated.

Because of the magnetic anisotropy of both the C = O bond and the benzene ring, coupled with the possibility of rapid motion of both groups about the bonds to the cyclopropyl ring, it is difficult to speculate further on the relative shifts of the H_A and H_B protons in carbon disulfide itself. However, from Tables 6.1 and 6.2 it is clear that substitution of a carboxyl group for the hydroxymethyl group causes a large low-field shift for both H_A and H_B. If this is attributed to the anisotropy of the C = O bond, it may be reasonable that the protons cis to it (H_A) should be the most affected. This assignment would then agree with that suggested above from benzene solvent effects.

In chloroform both protons shift to low field and since the carboxyl group may be expected to introduce a considerable dipole moment, it is suggested that this is a reaction field effect.[49]

B. 1-Phenylcyclopropylcarbinol

Since all the cyclopropyl ring protons are isochronous no

coupling constants can be obtained from the spectrum. However, the chemical shifts in the various solutions merit some discussion. The phenyl proton shifts are almost solvent independent. This is also nearly the case for the protons on the cyclopropyl ring. By way of contrast, the similarly placed protons in bis (2,2-dichlorocyclopropyl) ether show a difference of about 0.5 ppm in carbon disulfide and benzene solutions (Chapter V). Relative to internal TMS the shift is to high field in benzene. In the latter case it has been shown that the shift is markedly temperature dependent, indicating association effects. Association effects in the present case must be very small. In fact, there is a small shift to low field when the solvent is changed from carbon disulfide to benzene. This is also true for the methylene protons. The dielectric constants of benzene and carbon disulfide are nearly the same and reaction field effect differences must therefore be very small.[49] These very odd shifts must be a result of a peculiar packing arrangement in solution which cannot, however, be more closely specified at present. The unexpected shifts in benzene solution are further emphasized by the almost identical shifts at the same concentration in chloroform. Further studies of the concentration and temperature dependence of these shifts are indicated.

The hydroxyl proton shifts in the two carbon disulfide solutions are reasonable since dilution would be expected to break up hydrogen bonding to other hydroxyl groups, thus causing a high-field shift.[95]

Again, hydrogen bonding to benzene solvent molecules is possible since this would also cause a shift to high field.[76]

C. 1,1-Diphenylcyclopropane

The values for the vicinal coupling constants are consistent with those obtained for other substituted cyclopropanes given in Chapter III, and were assigned with this prior knowledge of J_{cis} and J_{trans}. Also, the C^{13}--H coupling constant for this compound is similar to the value of 161 cps reported by Muller and Pritchard for cyclopropane itself.[20]

The Fermi contact contribution to the spin-spin coupling constant[96] between two nuclei is directly proportional to the product of the electron densities of the two bonding orbitals, through which they interact, at their respective nuclei. For atoms with hybridized bonding orbitals, the contact contribution is proportional to the percent s - character in the hybridized atomic orbital used in forming the bond. The magnitude of the C^{13}--H coupling constant should then be an indication of the amount of unsaturation in the bonds. A typical C^{13}--H coupling constant for a saturated sp^3 system is the value of 125 cps for methane and for a sp^2 system is 159 cps for benzene.[20] The C^{13} coupling constant obtained for cyclopropanes would then seem to indicate that the three membered ring has at least some degree of unsaturation or π-character.[97]

CHAPTER VII

THE PROTON MAGNETIC RESONANCE SPECTRUM OF CYCLOPROPYLAMINE; THE $A_2A'_2X$ CASE WITH STRONG CROSS-COUPLING: A PSEUDO FIRST-ORDER SPECTRUM WITH COMBINATION LINES

1. Introduction

Sometimes many of the theoretical transitions in high resolution NMR spectra effectively coalesce or may be too weak to observe. Since the analysis of the spectra usually reduces to the problem of assigning the observed peaks, there may be more than one assignment and, therefore, more than one set of coupling constants which fits the observed spectrum. Abraham and Bernstein have discussed this situation for the ABX, A_2X_2, and ABXY spectra in some detail.[16] In practice it is usually found that only sums or differences of coupling constants can be obtained from the observed pseudo first-order spectra. In general, such deceptively simple spectra are expected for the ABC...XYZ... systems when quantities of the type J_{AB}, J_{XY} are large compared to the chemical shift differences δ_{AB}, δ_{XY} plus quantities of the type $J_{AX} - J_{AY}$. Separations between the lines in each group are then given by the average of the constants of the type J_{AX}, J_{AY}. When the system has some symmetry the general statements have to be modified slightly.[16]

Examples of deceptively simple spectra are discussed in reference 16 and the misinterpretations in the literature which have resulted are also discussed. A similar discussion for the ABX case

was given by Schaefer,[98] by Grant and Gutowsky for the A_2B_2 case[99] and by Musher and Corey for the three spin system.[100]

In this chapter the ring proton spectrum of cyclopropylamine is discussed. The proton on the substituted carbon atom is shifted far enough to low field by the inductive effect of the amino group so that, in general, an A_2B_2X system is obtained at 60 Mcps. This case was first discussed by Richards and Schaefer.[101] By means of solvent effects a zero shift can be introduced between the A and B protons and hence an $A_2A'_2X$ system is obtained. A pseudo first-order spectrum is not found, however, but rather what may be described as a pseudo first-order spectrum with combination lines. As shall be shown, this is due to a strong cross-coupling between A and A' protons. Such a situation could have been qualitatively predicted from the discussion in reference 16. It appears that this example is the first of this type. It also appears that the existence of the few extra lines in the $A_2A'_2X$ spectrum places quite stringent limits on the values of the coupling constants. This is important in obtaining good starting values for the parameters in the computer solutions for systems as complex as a strongly coupled A_2B_2X.

2. Experimental

Proton spectra were taken on a Varian DP 60 Mcps spectrometer and calibrations were carried out by the sideband technique relative to internal tetramethylsilane (TMS). Spectra were taken in a number of solvents but in none of them except benzene were they strikingly

different from the standard spectrum in $CDCl_3$, recorded by Bhacca *et al.*[102] In benzene it was possible to obtain a spectrum of simple appearance at a concentration of about 1:4 benzene by volume. This concentration was very critical and the collapsed peaks were found to separate rapidly with concentration on either side of the critical one.

Spectra of this critical solution were run at various temperatures up to 131°C. Dissociation of the very weak complex formed with benzene (Chapter V) allowed the separation of the collapsed peaks to be followed in a sensitive way. In this way the assignment of the peaks could be checked and it was possible to obtain the relative order of the shifts of the two sets of equivalent protons in the uncollapsed region.

3. Results

The proton spectrum of the critical solution in benzene is shown together with the calculated spectrum in Figure 7.1. In Figure 7.2 the spectrum of the same solution at 64°C. is shown. The results of the $A_2A'_2X$ analysis on the ring proton system are given in the Discussion below, along with the explanation on how the values were obtained. The amino group proton resonance is not given in either Figure. Apart from a slight broadening of the neighbouring proton there was no evidence of any coupling with the ring protons by either the amine protons or the nitrogen nucleus.

Figure 7.1 Proton resonance spectrum at 60 Mcps of cyclopropylamine in benzene at room temperature. Calibration is in cps with respect to $\nu_o (1 - \sigma_A)$ and $\nu_o (1 - \sigma_X)$ which are at 162 cps and 123.2 cps to low field of internal TMS, respectively. In the calculated spectrum, the two large pseudo triplets in the A region are drawn to one-third the intensity of the other transitions. The amino group resonance at 84.8 cps to low field of internal TMS is not shown.

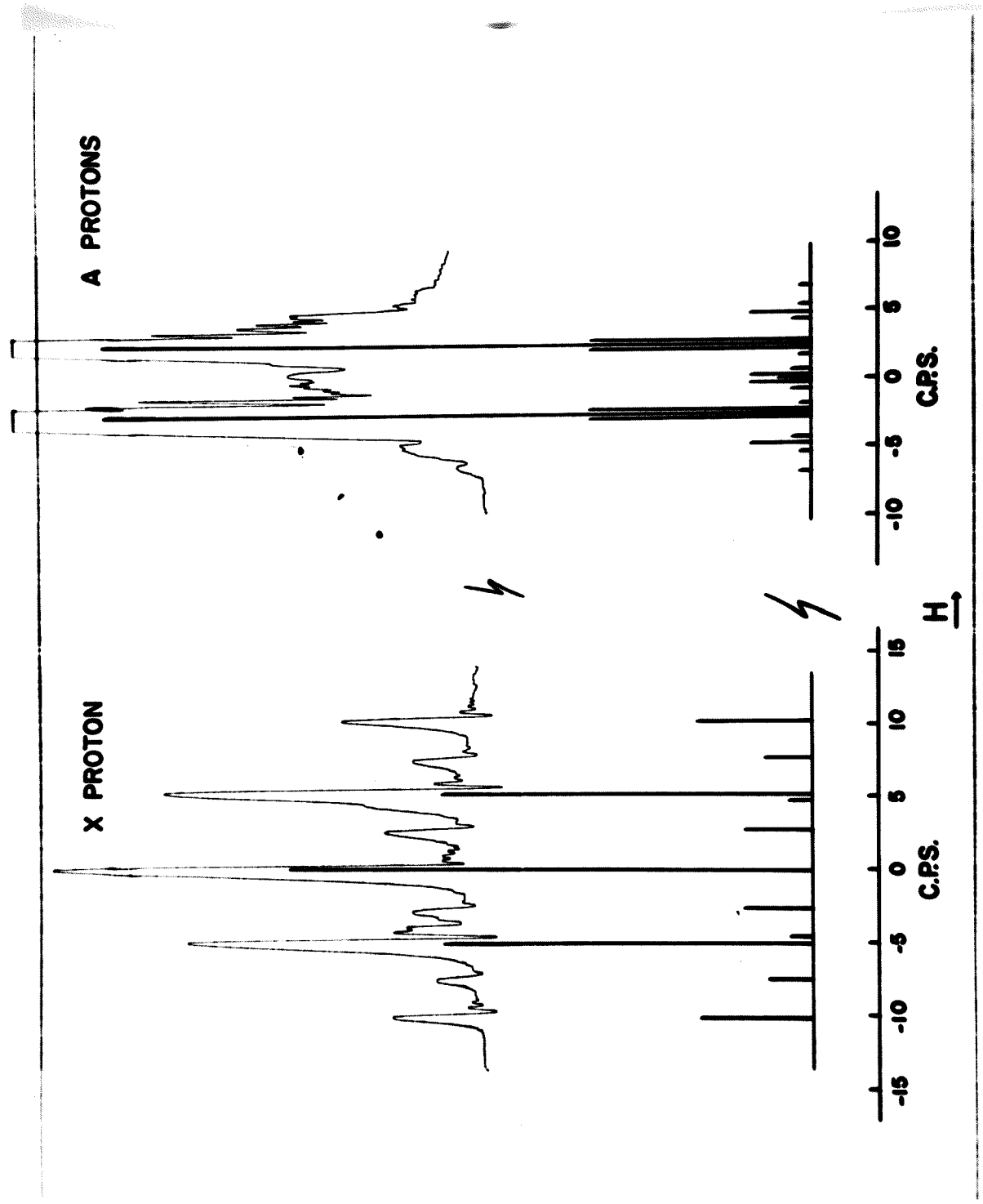
A PROTONS
X PROTON
C.P.S.
-15
-10
-5
0
5
10
15
C.P.S.
-10
-5
0
5
10
H

Figure 7.2 Proton resonance spectrum at 60 Mcps of cyclopropylamine in benzene at 64°C.; calibration is to low field of internal TMS. The amino group resonance at 90 cps is not shown. The transitions of the X proton which do not vary in position on introduction of a shift between A_2 and A_2' are indicated by the arrows.

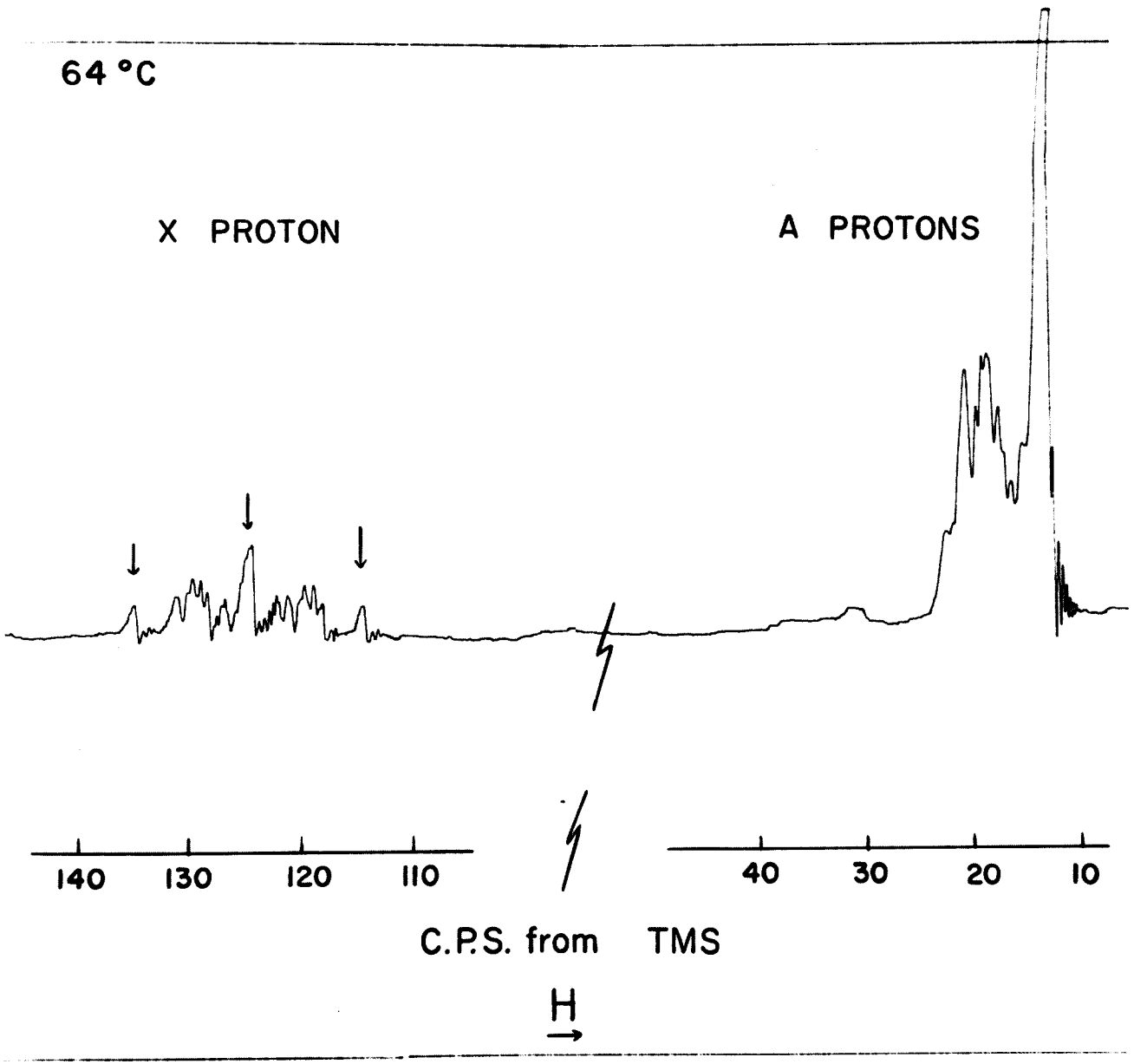
64 °C
X PROTON
A PROTONS
140
130
120
110
40
30
20
10
C.P.S. from TMS
H

4. Discussion

A. The Case $A_2A_2'X$

The critical solution spectrum of the ring protons corresponds to the case $A_2A_2'X$. The limiting case where the couplings from A_2 and A_2' to X are equal has already been discussed by Schaefer.[103] None of the possible 46 combination lines were considered in that treatment. Because some of these play a major role in this discussion and for reasons of clarity a rather general case, including the combination lines, is discussed here.

The ring proton system for the critical solution can be characterized as in I:

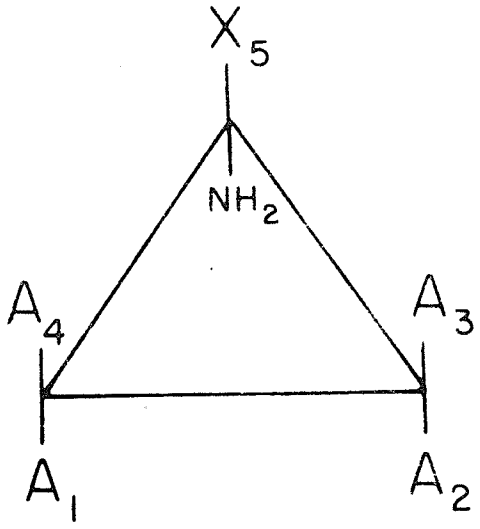

$H_A = H_{A'} = H_o(1 - \sigma_A)$;

$J_{12} \approx J_{34}$;

$J_{14} = J_{23}$

$J_{15} = J_{25}$; $J_{35} = J_{45}$

$J_{13} = J_{24}$

I

Here it is assumed that $J_{12} = J_{34}$. This is the only approximation made and from the analysis of cyclopropylcarboxylic acid[34] this

approximation is considered to be valid to at least 0.5 cps. Thirty-six of the line positions are independent of J_{12} and J_{34} and from the analysis it is clear that the error in many other line positions will be about half that of the difference in J_{12} and J_{34} or about 0.25 cps.

The matrix elements in the F_Z representation are given in Tables I and II, Appendix IV. In the $A_2A_2'X$ case for a five spin system the matrix is factored to eight 1 X 1, eight 2 X 2, and two 4 X 4 submatrices.

Positive quantities A, B, C, D and angles Θ, ϕ, ψ, γ are defined by:

$$\begin{aligned} 4A\cos 2\Theta &= J_{35} - J_{15}, & 4B\cos 2\phi &= J_{15} - J_{35}, \\ 2A\sin 2\Theta &= J_{23} + J_{13}, & 2B\sin 2\phi &= J_{23} + J_{13}, \\ 4C\cos 2\psi &= J_{35} - J_{15}, & 4D\cos 2\gamma &= J_{15} - J_{35}, \\ 2C\sin 2\psi &= J_{23} - J_{13}, & 2D\sin 2\gamma &= J_{13} - J_{23}. \end{aligned} \qquad (1)$$

The indicated orthogonal transformations were carried out on the eight 2 X 2 matrices and the stationary spin functions and energies are given in Tables III and IV, Appendix IV.

Selection rules allow a maximum of 110 transitions for the five nuclei. Of these, 46 are combination lines which were not considered in reference 103, but are taken into account here. Of the 46 combination lines 18 are zero intensity under all circumstances. This leaves 92 transitions for the general case. At this point the distinction between combination and other lines is dropped, since

for strong cross-coupling there is no longer a real distinction in the $A_2A_2'X$ limit.

The X protons give rise to a maximum of 36 lines of which 16 involve the two 4 X 4 submatrices. For the other 20 explicit energies and intensities are given in Table V, Appendix V. The A_2 and A_2' protons give rise to 56 lines of which 32 involve the 4 X 4 submatrices. Explicit energies and intensities for the other 24 are given in Table VI, Appendix IV.

B. The Proton Spectrum of Figure 7.1

i) The X Region

If the six weakest lines in the region are disregarded there are left five equally spaced lines with a separation of 5.10 cps. The intensities of these lines increase slightly towards high field indicating that the X approximation is not quite valid. However, $\nu_o(\sigma_A - \sigma_X) = 107.0$ cps compared with the largest off-diagonal element, expected to be about 12 cps. It is well known that the line positions are not nearly as sensitive to the spin functions as are the intensities, so that the analysis may still be carried out with some confidence.

A comparison of the line separations and the transition energies given in Table V, Appendix IV, indicates that the value $\left|J_{15} - J_{35}\right| = 10.2$ cps has been obtained. In a pseudo first-order spectrum these five lines would be expected to have intensities in the ratio 1:4:6:4:1. It is obvious that this is not so and, clearly,

the six weak lines derive their intensities from the inner three of the main lines.

In Table V, Appendix IV, eight lines are listed (lines 13 - 20) which become combination lines in the limit of a large chemical shift between the A_2 and A_2' protons. Lines 13 - 16 are assigned to the two pairs flanking the main peaks at ± 5.10 cps. From Equation (1) it immediately follows that A = B = 1.25 cps, and using the experimental intensities in Figure 7.1, the following limits can be placed on the parameters: $\frac{1}{4}(J_{35} - J_{15}) = 0.7$ --0.8 cps, $\frac{1}{2}(J_{23} + J_{13}) = 1.0$ -- 0.9 cps, $\phi - \theta = 41^\circ$ -- 44°.

It is assumed here that J_{23} is smaller and of opposite sign to J_{13} and that J_{15} and J_{35} are of the same sign with $J_{35} > J_{15}$. This agrees with a considerable set of data.[31,32,69,104] The same sign of J_{23} and J_{13} would simply interchange the constants A, B with C, D so that the relative signs of J_{23} and J_{13} cannot be obtained from the spectrum at this point. Opposite signs of J_{15} and J_{35} can, however, be ruled out here. If they did not have opposite signs then the spectrum would not be simple unless $\frac{1}{4}(|J_{35}| + |J_{15}|) \ll \frac{1}{2} |J_{23} - J_{13}|$ which is hardly likely. On the other hand, if J_{13} were very small (cross-coupling small) and $\frac{1}{4}|J_{35} - J_{15}| \ll \frac{1}{2} |J_{23}|$ then the spectrum would be completely first-order as has been shown, in effect, in reference 103.

From the additional demand that C and D be large enough to have $\sin^2(\Psi + \gamma) \leq 0.01$ (lines 17 - 20 in Table V, Appendix IV are

then unobservable), it follows that C = D = 6.5 -- 6.6 cps with $\frac{1}{2}\left|J_{13} - J_{23}\right|$ = 6.5 -- 6.6 cps. Hence, it is found that J_{23} = -5.5 ± 0.1 cps and $J_{13} = 7.5 \pm 0.1$ cps.

With this set of data the intensities and positions of all the lines in Table V, Appendix IV can be calculated. The positions of the two weak lines overlapping the main lines at $\pm$ 5.10 cps are still to be accounted for. Note that the pairs of lines at $\pm$ 10.2 cps are of unit intensity and should not vary in position on introduction of a shift between A_2 and A_2'. The same holds for the position of the six lines falling at 0 cps. In Figure 7.2 the spectrum verifies these statements. The separation of the three peaks in the X region is temperature independent.

ii) The A Region

The partial set of parameters derived from the X region allows the calculation of intensities and positions of the 24 lines in Table VI, Appendix IV. None of the lines deviate by more than 0.2 cps from the expected position at $\nu_o(1 - \sigma_A) \pm 2.55$ cps.

iii) The 4 X 4 Submatrices and J_{12}

To obtain the remaining transitions the 4 X 4 submatrices must be solved. The energy levels of the one differs from the energy levels of the other only by $\nu_o(1 - \sigma_X)$. Hence, four transitions between the two sets fall at $\nu_o(1 - \sigma_X)$, no matter what parameters are used for the solution, but the other transitions involving these eight energy levels depend on the input parameters. J_{15} and J_{35} enter

in the same way as in Equation (1). J_{23} and J_{13} enter independently and the values obtained above were used. J_{12} enters also, for the first time, and it is chosen as an adjustable parameter. The 4 X 4 submatrices were solved for the values of J_{12} = 8.0, 9.0, 10.0, 11.0, and 12.0 cps on an IBM 1620 computer. The positions of the weak lines at $\pm$ 4.6 cps in the X region were smooth and fairly sensitive functions of J_{12}, although their intensities were not very sensitive to J_{12}. In this way it was found that $J_{12} = 12.5 \pm 0.5$ cps, a reasonable value.[31]

The complete calculated spectrum of 92 lines is shown in Figure 7.1. Note that additional intensity accrues to the lines at $\nu_0(1 - \sigma_X) \pm$ 2.7 cps from transitions involving the 4 X 4 submatrices. Also note that all the lines separated by 0.25 cps or less have been collapsed in order to take the finite resolution of the observed spectrum into account. The agreement is thought to be satisfactory. It indicates also that J_{23} is indeed negative with respect to the vicinal couplings since it enters diagonally and off-diagonally into the 4 X 4 submatrices. In Figure 7.1 it is seen that the lines in the A region which fall off the $\pm$ 2.55 cps doublet calculated in pseudo first-order are relatively weak compared to the analogous lines in the X region. If the A region is run at an instrument gain such that the doublet just fills the recorder paper, no evidence of any other lines is noticeable.

The following sets of parameters in cps are probably reliable within the limits stated: $\nu_0(\sigma_A - \sigma_X) = 107.0$, $J_{34} \approx J_{12} = J_{\underline{cis}} =$

12.5 ± 0.5, $J_{14} = J_{23} = J_{\underline{gem}} = -5.5 \pm 0.3$, $J_{24} = J_{13} = J_{\underline{trans}} = 7.5 \pm 0.3$, $J_{15} + J_{35} = 10.2 \pm 0.1$, $J_{15} = J_{25} = J_{\underline{trans}} = 3.6 \pm 0.5$, $J_{35} = J_{45} = J_{\underline{cis}} = 6.6 \pm 0.5$. The last two values have been derived by considering the data in references 31, 32, 69, 104, which suggest that the ratio of $J_{\underline{cis}}$ to $J_{\underline{trans}}$ falls between 1.5 and 1.8, increasing as the electronegativity on the substituent increases.

C. The Solvent and Temperature Dependence of the Shift of the A and A' Protons

The effect of the benzene is to shift one pair of protons to high field more effectively than the other. For steric reasons[51,74] the protons trans to the NH_2 group are expected to be shifted more rapidly to high field by the anisotropy of the benzene molecules. If this is actually an association effect, similar to the one studied for bis(2,2-dichlorocyclopropyl) ether in Chapter V, then increasing temperature should cause the fastest low-field shift for these protons. In Figure 7.2 the low-field line of the intense doublet in the A region has split up while the high-field line has not. In Equation (1) each of the cosine expressions has added to it a shift term on the right-hand side for the A_2B_2X case. From the values of the coupling constants given above the values of A, B, C, and D can be calculated as a function of the shift between the A and A' protons. It follows easily that only A changes rapidly in the region of small shift. For instance, when the shift is 1 cps A has changed from 1.3 to 2.1 cps

while the others have changed by about 0.2 cps. Lines like 37 and 51 in Table VI, Appendix IV are expected to change their positions most rapidly and these are both originally centred on the low-field line on the intense doublet.

Now it is clear that in the limit of large shift the splitting in the group of lines arising from the protons *trans* to the amino group, i.e. *cis* to the X proton, would be largest: $J_{cis} > J_{trans}$. Hence, as the shift decreases to zero this group of lines collapses last. This set of lines appears at low field as shown above and moves to low field as the temperature increases. It has been shown, therefore, that it is the protons *trans* to the amino group which are most solvent dependent and experience the largest high-field shift on dilution in benzene. This is consistent with a preferred interaction with benzene molecules at this position.

The low-field shift of the *trans* protons can be understood in terms of Buckingham's electric field calculations.[49] The *cis* protons would also be shifted to low field by the dipole whose negative end points in the C--N direction, but due to the angular factor would be expected to be less, as observed. A quantitative estimate demands a knowledge of the magnitude of this dipole and also, perhaps, whether the contribution of the lone-pair on the nitrogen is important.

BIBLIOGRAPHY

REFERENCES FOR BIBLIOGRAPHY

1. J. A. Pople, W. G. Schneider, and H. J. Bernstein. High-Resolution Nuclear Magnetic Resonance. New York: McGraw-Hill, 1959.

2. L. M. Jackman. Applications of NMR Spectroscopy in Organic Chemistry. New York: Pergamon Press, 1959.

3. J. D. Roberts. Nuclear Magnetic Resonance. New York: McGraw-Hill, 1959.

4. J. D. Roberts. An Introduction to Spin-Spin Splitting in High Resolution Nuclear Magnetic Resonance Spectra. New York: W. A. Benjamin, 1961.

5. Varian Associates. NMR and EPR Spectroscopy. New York: Pergamon Press, 1960.

6. Reference 2, p. 86.

7. M. Karplus. J. Chem. Phys. 30, 11 (1959).

8. G. L. Closs and L. E. Closs. J. Am. Chem. Soc. 82, 5723 (1960).

9. H. M. Hutton and T. Schaefer. Can. J. Chem. 40, 875 (1962).

10. H. S. Gutowsky, D. W. McCall, and C. P. Slichter. Phys. Rev. 84, 589 (1951); E. L. Hahn and D. E. Maxwell. Ibid. 84, 1246 (1951).

11. M. Karplus, D. H. Anderson, T. C. Farrar, and H. S. Gutowsky. J. Chem. Phys. 27, 597 (1957).

12. M. Karplus and D. H. Anderson. J. Chem. Phys. 30, 6 (1959).

13. W. F. Ringk. Private communication.

14. O. Hassel and J. H. Viervoll. Acta. Chem. Scand. 1, 149 (1947).

15. O. Bastiansen and G. J. Lehmann. Tetrahedron Letters, 165 (1962).

16. R. J. Abraham and H. J. Bernstein. Can. J. Chem. 39, 216 (1961).

17. R. E. Glick and A. A. Bothner-By. J. Chem. Phys. 25, 362 (1956).

18. T. Schaefer. Can. J. Chem. 40, 1 (1962).

19. J. S. Waugh and S. Castellano. J. Chem. Phys. 35, 1900 (1961).

20. N. Muller and D. E. Pritchard. J. Chem. Phys. 31, 768 (1959).

21. T. Schaefer and W. G. Schneider. Can. J. Chem. 37, 2078 (1959).

22. S. Forsen and T. Norin. Acta. Chem. Scand. 15, 592 (1961)

23. F. A. L. Anet. Can. J. Chem. 39, 789 (1961).

24. R. V. Lemieux, R. K. Kullnig, H. G. Bernstein, and W. G. Schneider. J. Am. Chem. Soc. 80, 6098 (1958).

25. K. L. Williamson. J. Am. Chem. Soc. 85, 516 (1963).

26. F. S. Mortimer. J. Mol. Spect. 5, 199 (1960).

27. C. A. Reilly and J. D. Swalen. J. Chem. Phys. 34, 980 (1961).

28. C. Walling and P. S. Fredericks. J. Am. Chem. Soc. 84, 3326 (1962).

29. J. I. Musher and R. G. Gordon. J. Chem. Phys. 36, 3097 (1962).

30. D. D. Elleman and S. L. Manatt. J. Mol. Spect. 9, 477 (1962).

31. H. M. Hutton and T. Schaefer. Can. J. Chem. 41, 684 (1963).

32. J. D. Graham and M. T. Rogers. J. Am. Chem. Soc. 84, 2249 (1962).

33. J. I. Musher. Private communication.

34. K. Wiberg. Private communication.

35. U. Schöllkopf and G. J. Lehman. Tetrahedron Letters, 162 (1962).

36. H. S. Gutowsky, M. Karplus, and D. M. Grant. J. Chem. Phys. 31, 1278 (1959).

37. L. L. McCoy. J. Org. Chem. 25, 2078 (1960).

38. N. Sheppard. Private communication.

39. A. D. Walsh. Trans. Faraday Soc. 45, 179 (1949).

40. M. Karplus. J. Chem. Phys. 33, 1842 (1960).

41. K. A. McLauchlan and D. H. Whiffen. Proc. Chem. Soc., 144 (1962).

42. F. Kaplan and J. D. Roberts. J. Am. Chem. Soc. 83, 4666 (1962).

43. R. R. Fraser, R. U. Lemieux, and J. D. Stevens. J. Am. Chem. Soc. 83, 3901 (1961).

44. C. A. Reilly and J. D. Swalen. J. Chem. Phys. 35, 1522 (1961).

45. H. Finegold. Proc. Chem. Soc., 213 (1962).

46. J. I. Musher. J. Chem. Phys., to be published.

47. H. M. McConnell. J. Chem. Phys. 23, 2454 (1955).

48. L. L. McCoy. Private communication.

49. A. D. Buckingham. Can. J. Chem. 38, 300 (1960).

50. T. Schaefer and W. G. Schneider. J. Chem. Phys. 32, 1218 (1960).

51. T. Schaefer. Can. J. Chem. 39, 1864 (1961).

52. Reference 2, p. 52.

53. J. Smidt and Th. J. de Boer. Rec. Trav. Chim. 79, 1235 (1960).

54. J. P. Maher and D. F. Evans. Proc. Chem. Soc., 208 (1961).

55. R. Freeman and D. H. Whiffen. Mol. Phys. 4, 321 (1961).

56. R. R. Fraser. Can. J. Chem. 40, 1483 (1962).

57. H. S. Gutowsky and Cynthia Juan. J. Chem. Phys. 37, 120 (1962).

58. M. Karplus. J. Am. Chem. Soc. 84, 2458 (1962).

59. P. C. Lauterbur and R. J. Kurland. J. Am. Chem. Soc. 84, 3405 (1962).

60. F. A. L. Anet. J. Am. Chem. Soc. 84, 3767 (1962).

61. A. D. Buckingham and K. A. McLauchlan. Proc. Chem. Soc., 144 (1963).

62. R. Freeman. Mol. Phys. 3, 435 (1960).

63. N. F. Ramsey and E. M. Purcell. Phys. Rev. 85, 143 (1952); N. F. Ramsey. Ibid. 91, 303 (1953).

64. B.D.N. Rao and J.D. Baldeschwieler. J. Chem. Phys. 37, 2473 (1962).

65. W. A. Anderson. Phys. Rev. 102, 151 (1956).

66. R. Kaiser. Rev. Sci. Inst. 31, 963 (1960).

67. J. Itoh and S. Sato. J. Phys. Soc. Japan. 14, 851 (1959).

68. D. W. Turner. J. Chem. Soc., 847 (1962).

69. H. M. Hutton and T. Schaefer. Can. J. Chem. 41, 1623 (1963).

70. A. D. Buckingham, T. Schaefer, and W. G. Schneider. J. Chem. Phys. 32, 1227 (1960).

71. B. T. Gillis and K. F. Schimmel. J. Org. Chem. 27, 1071 (1962).

72. Reference 1, p. 73.

73. E. L. Eliel. Stereochemistry of Carbon Compounds. New York: McGraw-Hill, 1962, p. 138.

74. H. M. Hutton and T. Schaefer. Can. J. Chem. 41, 1857 (1963).

75. Reference 1, p. 132.

76. L. W. Reeves and W. G. Schneider. Can. J. Chem. 35, 251 (1957).

77. J. V. Hatton and R. E. Richards. Mol. Phys. 3, 253 (1960); Trans. Faraday Soc. 57, 28 (1961).

78. J. V. Hatton and W. G. Schneider. Can. J. Chem. 40, 1285 (1962).

79. R. E. Klinck and J. B. Stothers. Can. J. Chem. 40, 2329 (1962).

80. W. G. Schneider. J. Phys. Chem. 66, 2653 (1962).

81. R. J. Abraham. Mol. Phys. 4, 369 (1961).

82. H. M. McConnell, A. D. McLean, and C. A. Reilly. J. Chem. Phys. 23, 1152 (1955).

83. J. A. Pople, W. G. Schneider and H. J. Bernstein. Can. J. Chem. 35, 1060 (1957).

84. R. E. Richards and T. Schaefer. Trans. Faraday Soc. 54, 1280 (1958).

85. Reference 1, p. 138.

86. P. L. Cario. Chem. Rev. 60, 363 (1960).

87. B. Dischler and G. Englert. Z. Naturforsch. 16a, 1180 (1961).

88. K. B. Wiberg and B. J. Nist. Interpretation of NMR Spectra. New York: W.A. Benjamin, 1962.

89. J. Martin and B.P. Dailey. J. Chem. Phys. 37, 2594 (1962).

90. D. M. Grant, R. C. Hirst, and H. S. Gutowsky. J. Chem. Phys. 38, 470 (1963).

91. E. Lustig. J. Chem. Phys. 37, 2725 (1962).

92. J. W. Wilt and D. Roberts. J. Org. Chem. 27, 3430 (1962).

93. Reference 1, p. 140.

94. J. T. Arnold. Phys. Rev. 102, 136 (1956).

95. U. Liddel and N. F. Ramsey. J. Chem. Phys. 19, 1608 (1951).

96. Reference 1, Chapter 8.

97. R. Fuchs, C. A. Kaplan, J. J. Bloomfield and L. F. Hatch. J. Org. Chem. 27, 733 (1962); also see references there.

98. T. Schaefer. Can. J. Chem. 40, 1678 (1962).

99. D. Grant and H. S. Gutowsky. J. Chem. Phys. 34, 699 (1961).

100. J. I. Musher and E. J. Corey. Tetrahedron. 18, 791 (1962).

101. R. E. Richards and T. Schaefer. Proc. Roy. Soc. 246A, 429 (1958).

102. N. S. Bhacca, L. F. Johnson and J. N. Shoolery. NMR Spectra Catalog. National Press. 1962. Spectrum No. 37.

103. T. Schaefer. Can. J. Chem. 37, 882 (1959).

104. D. Seyferth, H. Yamazaki and D. L. Alleston. J. Org. Chem. 28, 703 (1963).

APPENDIX I

TABLE I

BASIC FUNCTIONS AND DIAGONAL MATRIX ELEMENTS FOR AN ABX SYSTEM

	Basic Function	F_Z	Diagonal Matrix Element $\mathcal{H}_{nn}$	Off-Diagonal Elements
1	$\alpha\alpha\alpha$	3/2	$\frac{1}{2}(\nu_A + \nu_B + \nu_X) + \frac{1}{4}(J_{AB} + J_{BX} + J_{AX})$	$\mathcal{H}_{23} = \mathcal{H}_{67} = \frac{1}{2} J_{BX}$
2	$\alpha\alpha\beta$	$\frac{1}{2}$	$\frac{1}{2}(\nu_A + \nu_B - \nu_X) + \frac{1}{4}(J_{AB} - J_{BX} - J_{AX})$	$\mathcal{H}_{34} = \mathcal{H}_{56} = \frac{1}{2} J_{AB}$
3	$\alpha\beta\alpha$	$\frac{1}{2}$	$\frac{1}{2}(\nu_A - \nu_B + \nu_X) + \frac{1}{4}(-J_{AB} - J_{BX} + J_{AX})$	$\mathcal{H}_{24} = \mathcal{H}_{57} = \frac{1}{2} J_{AX}$
4	$\beta\alpha\alpha$	$\frac{1}{2}$	$\frac{1}{2}(-\nu_A + \nu_B + \nu_X) + \frac{1}{4}(-J_{AB} + J_{BX} - J_{AX})$	
5	$\alpha\beta\beta$	$-\frac{1}{2}$	$\frac{1}{2}(\nu_A - \nu_B - \nu_X) + \frac{1}{4}(-J_{AB} + J_{BX} - J_{AX})$	
6	$\beta\alpha\beta$	$-\frac{1}{2}$	$\frac{1}{2}(-\nu_A + \nu_B - \nu_X) + \frac{1}{4}(-J_{AB} - J_{BX} + J_{AX})$	
7	$\beta\beta\alpha$	$-\frac{1}{2}$	$\frac{1}{2}(-\nu_A - \nu_B + \nu_X) + \frac{1}{4}(J_{AB} - J_{BX} - J_{AX})$	
8	$\beta\beta\beta$	$-3/2$	$\frac{1}{2}(-\nu_A - \nu_B - \nu_X) + \frac{1}{4}(J_{AB} + J_{BX} + J_{AX})$	

TABLE II

TRANSITION ENERGIES AND RELATIVE INTENSITIES FOR THE THREE NUCLEI ABX

Transition**	Energy*	Relative Intensity
1. $8 \longrightarrow 6'$	$\frac{1}{4}(-2\ J_{AB} - J_{AX} - J_{BX}) - D_-$	$1 - \sin 2\phi_-$
2. $7 \longrightarrow 4'$	$\frac{1}{4}(-2\ J_{AB} + J_{AX} + J_{BX}) - D_+$	$1 - \sin 2\phi_+$
3. $5' \longrightarrow 2$	$\frac{1}{4}(2\ J_{AB} - J_{AX} - J_{BX}) - D_-$	$1 + \sin 2\phi_-$
4. $3' \longrightarrow 1$	$\frac{1}{4}(2\ J_{AB} + J_{AX} + J_{BX}) - D_+$	$1 + \sin 2\phi_+$
5. $8 \longrightarrow 5'$	$\frac{1}{4}(-2J_{AB} - J_{AX} - J_{BX}) + D_-$	$1 + \sin 2\phi_-$
6. $7 \longrightarrow 3'$	$\frac{1}{4}(-2J_{AB} + J_{AX} + J_{BX}) + D_+$	$1 + \sin 2\phi_+$
7. $6' \longrightarrow 2$	$\frac{1}{4}(2J_{AB} - J_{AX} - J_{BX}) + D_-$	$1 - \sin 2\phi_-$
8. $4' \longrightarrow 1$	$\frac{1}{4}(2J_{AB} + J_{AX} + J_{BX}) + D_+$	$1 - \sin 2\phi_+$
9. $8 \longrightarrow 7$	$-\frac{1}{2}(J_{AX} + J_{BX})$	1
10. $5' \longrightarrow 3'$	$D_+ - D_-$	$\cos^2(\phi_+ - \phi_-)$
11. $6' \longrightarrow 4'$	$-D_+ + D_-$	$\cos^2(\phi_+ - \phi_-)$
12. $2 \longrightarrow 1$	$\frac{1}{2}(J_{AX} + J_{BX})$	1
13. $5' \longrightarrow 4'$	$-D_+ - D_-$	$\sin^2(\phi_+ - \phi_-)$
14. $6' \longrightarrow 3'$	$D_+ + D_-$	$\sin^2(\phi_+ - \phi_-)$

TABLE II (Notes)

*The energies of transitions 1. to 8. are relative to $\frac{1}{2}(\nu_A + \nu_B)$ and of transitions 9. to 14. to ν_X.

**The primed states 3', 4', 5', 6' result from the diagonalization of the 2 X 2 matrices.

Positive quantities D_+, D_- and angles ϕ_+, ϕ_- are defined by:

$$D_+ \cos 2\phi_+ = \tfrac{1}{2}(\nu_A - \nu_B) + \tfrac{1}{4}(J_{AX} - J_{BX})$$

$$D_+ \sin 2\phi_+ = \tfrac{1}{2}J_{AB}$$

$$D_- \cos 2\phi_- = \tfrac{1}{2}(\nu_A - \nu_B) - \tfrac{1}{4}(J_{AX} - J_{BX})$$

$$D_- \sin 2\phi_- = \tfrac{1}{2}J_{AB}$$

$$D_\pm = \tfrac{1}{2}\left\{\left[\nu_A - \nu_B \pm \tfrac{1}{2}(J_{AX} - J_{BX})\right]^2 + J_{AB}^2\right\}^{\frac{1}{2}}$$

APPENDIX II

NUCLEAR MAGNETIC DOUBLE RESONANCE OF A THREE SPIN SYSTEM

For the double resonance of a three spin ABC system,[64] the Hamiltonian in a coordinate system rotating about the Z axis with an angular velocity of $-\omega_2 k$ is given by:

$$\mathcal{H}_R = \mathcal{H}^{\circ}_R + \mathcal{H}'_R(t)$$

with $$\mathcal{H}^{\circ}_R = \sum_i{}' A_i I_Z(i) + \sum_{i<j}{}' J_{ij} I(i)\, I(j) + \sum_i{}' \nu_{2i} I_X(i)$$

$$\mathcal{H}'_R(t) = \sum_i{}' \nu_{1i}\left[I_X(i)\cos(\omega_1 - \omega_2)t - I_Y(i)\sin(\omega_1 - \omega_2)t\right]$$

where the summations are taken over the three interacting nuclei, J_{ij} is the spin-spin coupling constant between nuclei i and j, and

$$A_i = \nu_{0i} + \omega_2/2\pi \ ,$$

$$\nu_{0i} = -\gamma_i H_0/2\pi \ ,$$

$$\nu_{1i} = -\gamma_i H_1/2\pi \ ,$$

$$\nu_{2i} = -\gamma_i H_2/2\pi \ .$$

H_0 is the static magnetic field along the Z axis and H_1 and H_2 are the amplitudes of the weak and strong radiofrequency fields rotating at angular velocity $-\omega_1$ and $-\omega_2$, respectively.

Assuming that $\mathcal{H}'_R(t)$ is a small perturbation with respect to $\mathcal{H}^{\circ}_R$, the Hamiltonian can be solved for its stationary eigenvalues in the rotating frame. Table I gives the basis functions and the matrix elements of $\mathcal{H}^{\circ}_R$ for the ABC system. The energies and inten-

sities may be obtained in the usual manner after this 8 X 8 secular determinant has been diagonalized. The difference between the double resonance calculation and the single resonance calculation is due to the additional term $\sum \nu_{2i} I_X(i)$ in the $\mathcal{H}_R^\circ$ Hamiltonian. This term connects states with values of F_Z differing by one; F_Z is the Z component of the total spin angular momentum. F_Z no longer commutes with this Hamiltonian and the selection rule for single resonance transitions $\Delta F_Z = \pm 1$ breaks down.

The three spin system may be treated as an ABX system if the chemical shift of the irradiated X nucleus relative to A and B is large with respect to the coupling constants. This factors the secular determinant into two 2 X 2 and one 4 X 4 subdeterminants so that a solution in closed form is still not possible. With the AMX three spin approximation the secular determinant is reduced to four 2 X 2 determinants so that the energy transitions and relative intensities may be given explicitly. The diagonalized secular determinant is given in Table II for the case where the X nucleus is being irradiated with the strong radiofrequency field. From Table II the energies of transition for nucleus A or M may be calculated. The results for the A transitions are given in Table III. The positive quantities $D_\pm$, $F_\pm$ and angles $\Theta_\pm$, $\phi_\pm$ are defined as:

$$D_\pm = \tfrac{1}{2}\left\{\left[A_X \pm \tfrac{1}{2}(J_{AX} + J_{MX})\right]^2 + \nu_{2X}^2\right\}^{\frac{1}{2}},$$

$$F_\pm = \tfrac{1}{2}\left\{\left[A_X \mp \tfrac{1}{2}(J_{AX} - J_{MX})\right]^2 + \nu_{2X}^2\right\}^{\frac{1}{2}},$$

$$\tan 2\Theta_\pm = \nu_{2X} / \left[A_X \pm \tfrac{1}{2}(J_{AX} + J_{MX})\right],$$

$$\tan 2\phi_{\pm} = \nu_{2X} / [A_X \mp \tfrac{1}{2}(J_{AX} - J_{MX})],$$

In Table III, transitions 1 through 4 become the transitions in the single resonance spectrum in the limit $\nu_{2X} = 0$. Transitions 5 to 8 which are due to the double irradiation, vanish when $\nu_{2X} = 0$.

In a double irradiation experiment where $A_X = \frac{1}{2}J_{MX}$, $D_- = F_-$ and transitions 3 and 4 in Table III collapse to a single line $A_A - \frac{1}{2}J_{AM}$. If $A_X = -\frac{1}{2}J_{MX}$, then $D_+ = F_+$ and the transitions 1 and 2 centred about $A_A + \frac{1}{2}J_{AM}$ collapse. Assuming $J_{MX} > J_{AX}$, $A_X = \pm \frac{1}{2}J_{MX}$ corresponds to the irradiation at the centre of either the high-field doublet, or the low field doublet in the X spectrum. Thus with a given sign for A_X the doublet in the A spectrum which collapses to a single line depends on the sign of J_{AM} with respect to J_{MX}. This double resonance experiment thus gives the relative signs between J_{AM} and J_{MX}. By performing the same experiment on the resonances of another pair of nuclei in this three-spin system, the relative signs of all the coupling constants may be determined.

Although the method which has been outlined is most suitable for a first order spectrum, it may also be used to determine the relative signs of coupling constants for somewhat more strongly coupled systems.

TABLE I

BASIS FUNCTIONS AND MATRIX ELEMENTS FOR THE ABC SYSTEM
UNDER DOUBLE IRRADIATION

Number	Basis Function	Diagonal Elements
1	$\alpha\alpha\alpha$	$\frac{1}{2}(A_A + A_B + A_C) + \frac{1}{4}(J_{AB} + J_{AC} + J_{BC})$
2	$\alpha\alpha\beta$	$\frac{1}{2}(A_A + A_B - A_C) + \frac{1}{4}(J_{AB} - J_{AC} - J_{BC})$
3	$\beta\alpha\alpha$	$\frac{1}{2}(-A_A + A_B + A_C) + \frac{1}{4}(-J_{AB} - J_{AC} + J_{BC})$
4	$\beta\alpha\beta$	$\frac{1}{2}(-A_A + A_B - A_C) + \frac{1}{4}(-J_{AB} + J_{AC} - J_{BC})$
5	$\alpha\beta\alpha$	$\frac{1}{2}(A_A - A_B + A_C) + \frac{1}{4}(-J_{AB} + J_{AC} - J_{BC})$
6	$\alpha\beta\beta$	$\frac{1}{2}(A_A - A_B - A_C) + \frac{1}{4}(-J_{AB} - J_{AC} + J_{BC})$
7	$\beta\beta\alpha$	$\frac{1}{2}(-A_A - A_B + A_C) + \frac{1}{4}(J_{AB} - J_{AC} - J_{BC})$
8	$\beta\beta\beta$	$\frac{1}{2}(-A_A - A_B - A_C) + \frac{1}{4}(J_{AB} + J_{AC} + J_{BC})$

TABLE I (Notes)

Off-diagonal elements:

$$\mathcal{H}_{12} = \mathcal{H}_{34} = \mathcal{H}_{56} = \mathcal{H}_{78} = \tfrac{1}{2}\nu_{2C}$$

$$\mathcal{H}_{15} = \mathcal{H}_{26} = \mathcal{H}_{37} = \mathcal{H}_{48} = \tfrac{1}{2}\nu_{2B}$$

$$\mathcal{H}_{13} = \mathcal{H}_{24} = \mathcal{H}_{57} = \mathcal{H}_{68} = \tfrac{1}{2}\nu_{2A}$$

$$\mathcal{H}_{35} = \mathcal{H}_{46} = \tfrac{1}{2} J_{AB}$$

$$\mathcal{H}_{23} = \mathcal{H}_{67} = \tfrac{1}{2} J_{AC}$$

$$\mathcal{H}_{25} = \mathcal{H}_{47} = \tfrac{1}{2} J_{BC}$$

TABLE II

ENERGY LEVELS FOR AMX SYSTEM WHEN X NUCLEUS IS IRRADIATED WITH H_2

Number	Energy
1'	$\frac{1}{2}(A_A + A_M) + \frac{1}{4} J_{AM} + D_+$
2'	$\frac{1}{2}(A_A + A_M) + \frac{1}{4} J_{AM} - D_+$
3'	$\frac{1}{2}(-A_A + A_M) - \frac{1}{4} J_{AM} + F_+$
4'	$\frac{1}{2}(-A_A + A_M) - \frac{1}{4} J_{AM} - F_+$
5'	$\frac{1}{2}(A_A - A_M) - \frac{1}{4} J_{AM} + F_-$
6'	$\frac{1}{2}(A_A - A_M) - \frac{1}{4} J_{AM} - F_-$
7'	$\frac{1}{2}(-A_A - A_M) + \frac{1}{4} J_{AM} + D_-$
8'	$\frac{1}{2}(-A_A - A_M) + \frac{1}{4} J_{AM} - D_-$

TABLE III

A TRANSITIONS AND RELATIVE INTENSITIES IN AN AMX SYSTEM
WHEN X NUCLEUS IS IRRADIATED WITH H_2

Transition	Energy Relative to A_A	Relative Intensities
$3' \longrightarrow 1'$	$\frac{1}{2} J_{AM} + (D_+ - F_+)$	$\cos^2(\Theta_+ - \phi_+)$
$4' \longrightarrow 2'$	$\frac{1}{2} J_{AM} - (D_+ - F_+)$	$\cos^2(\Theta_+ - \phi_+)$
$7' \longrightarrow 5'$	$-\frac{1}{2} J_{AM} + (F_- - D_-)$	$\cos^2(\phi_- - \Theta_-)$
$8' \longrightarrow 6'$	$-\frac{1}{2} J_{AM} - (F_- - D_-)$	$\cos^2(\phi_- - \Theta_-)$
$3' \longrightarrow 2'$	$\frac{1}{2} J_{AM} - (D_+ + F_+)$	$\sin^2(\Theta_+ - \phi_+)$
$4' \longrightarrow 1'$	$\frac{1}{2} J_{AM} + (D_+ + F_+)$	$\sin^2(\Theta_+ - \phi_+)$
$7' \longrightarrow 6'$	$-\frac{1}{2} J_{AM} - (F_- + D_-)$	$\sin^2(\phi_- - \Theta_-)$
$8' \longrightarrow 5'$	$-\frac{1}{2} J_{AM} + (F_- + D_-)$	$\sin^2(\phi_- - \Theta_-)$

APPENDIX III

TABLE I

SECULAR EQUATION of the A_2B_2 NUCLEAR SPIN SYSTEM

$\Delta = \eta H_0(\sigma_B - \sigma_A)$
$K = J_A + J_B$
$L = J_{gem} - J_{trans}$
$M = J_A - J_B$
$N = J_{gem} + J_{trans}$

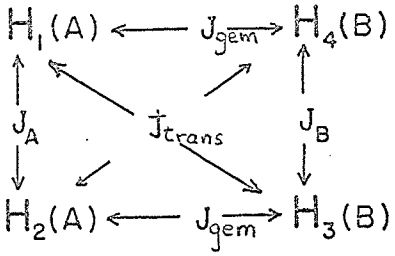

BASIS FUNCTIONS		SUBMATRICES			
Symbol	Spin functions				
IS_2	$\alpha\alpha\alpha\alpha$	$\eta H_0(2-\sigma_A-\sigma_B)+\frac{1}{2}N$			
IS_1	$\frac{1}{\sqrt{2}}(\alpha\beta+\beta\alpha)\,\alpha\alpha$	$\eta H_0(1-\sigma_B)$	$\frac{1}{2}N$		
$2S_1$	$\frac{1}{\sqrt{2}}\alpha\alpha\,(\alpha\beta+\beta\alpha)$	$\frac{1}{2}N$	$\eta H_0(1-\sigma_A)$		
IS_0	$\beta\beta\alpha\alpha$	$-\Delta-\frac{1}{2}N$	0	$\frac{1}{2}L$	$\frac{1}{2}N$
$2S_0$	$\alpha\alpha\beta\beta$	0	$\Delta-\frac{1}{2}N$	$\frac{1}{2}L$	$\frac{1}{2}N$
$3S_0$	$\frac{1}{2}(\alpha\beta-\beta\alpha)(\alpha\beta-\beta\alpha)$	$\frac{1}{2}L$	$\frac{1}{2}L$	$-K$	$-\frac{1}{2}L$
$4S_0$	$\frac{1}{2}(\alpha\beta+\beta\alpha)(\alpha\beta+\beta\alpha)$	$\frac{1}{2}N$	$\frac{1}{2}N$	$-\frac{1}{2}L$	0
IS_{-1}	$\frac{1}{\sqrt{2}}(\alpha\beta+\beta\alpha)\,\beta\beta$	$\eta H_0(-1+\sigma_B)$	$\frac{1}{2}N$		
$2S_{-1}$	$\frac{1}{\sqrt{2}}\beta\beta\,(\alpha\beta+\beta\alpha)$	$\frac{1}{2}N$	$\eta H_0(-1+\sigma_A)$		
IS_{-2}	$\beta\beta\beta\beta$	$\eta H_0(-2+\sigma_A+\sigma_B)+\frac{1}{2}N$			
IA_1	$\frac{1}{\sqrt{2}}(\alpha\beta-\beta\alpha)\,\alpha\alpha$	$\eta H_0(1-\sigma_B)-\frac{1}{2}(K+M)$	$-\frac{1}{2}L$		
$2A_1$	$\frac{1}{\sqrt{2}}\alpha\alpha\,(\alpha\beta-\beta\alpha)$	$-\frac{1}{2}L$	$\eta H_0(1-\sigma_A)-\frac{1}{2}(K-M)$		
IA_0	$\frac{1}{2}(\alpha\beta+\beta\alpha)(\alpha\beta-\beta\alpha)$	$-\frac{1}{2}(K-M)$	$-\frac{1}{2}L$		
$2A_0$	$\frac{1}{2}(\alpha\beta-\beta\alpha)(\alpha\beta+\beta\alpha)$	$-\frac{1}{2}L$	$-\frac{1}{2}(K+M)$		
IA_{-1}	$\frac{1}{\sqrt{2}}(\alpha\beta-\beta\alpha)\,\beta\beta$	$\eta H_0(-1+\sigma_B)-\frac{1}{2}(K+M)$	$-\frac{1}{2}L$		
$2A_{-1}$	$\frac{1}{\sqrt{2}}\beta\beta\,(\alpha\beta-\beta\alpha)$	$-\frac{1}{2}L$	$\eta H_0(-1+\sigma_A)-\frac{1}{2}(K-M)$		

TABLE II

COMPUTATION OF A_2B_2 SPECTRA

Explicitly defined parameters:

$C_N = \sqrt{\Delta^2 + N^2}$ $\qquad \tan 2\phi = N/\Delta$

$C_{LM+} = \sqrt{(\Delta + M)^2 + L^2}$ $\qquad \tan 2\theta_a = L/K$

$C_{LM-} = \sqrt{(\Delta - M)^2 + L^2}$ $\qquad \tan 2\psi_+ = L/(\Delta + M)$

$L_M = \sqrt{L^2 + M^2}$ $\qquad \tan 2\psi_- = L/(\Delta - M)$

Parameters arising from solution of the 4x4 S_o submatrix:

$p_1 = \epsilon_{1S'_o} - \epsilon_{1S_o}$

$p_2 = \epsilon_{2S'_o} - \epsilon_{2S_o}$

$p_3 = \epsilon_{3S'_o} - \epsilon_{3S_o}$ $\qquad p_5 = p_3 + \frac{1}{2}(\sqrt{K^2+L^2} - K)$

$p_4 = \epsilon_{4S'_o} - \epsilon_{4S_o}$ $\qquad p_6 = p_4 - \frac{1}{2}(\sqrt{K^2+L^2} - K)$

The coefficients c_{mn} are defined thusly:

$(mS'_o) = c_{m1}(1S_o) + c_{m2}(2S_o) + c_{m3}(3S_o) + c_{m4}(4S_o)$

Absorption Lines in the Upper Half-Spectrum

Transition No.	States	Frequency, c.p.s. w.r.to centre of spectrum	Relative Intensity
1	$1S'_1 \rightarrow S_2$	$\frac{1}{2}C_N + \frac{1}{2}N$	$1 - \sin 2\phi$
2	$1S'_0 \rightarrow 1S'_1$	$\Delta + \frac{1}{2}N - \frac{1}{2}C_N - p_1$	$[(c_{11}+c_{14})\cos\phi - (c_{12}+c_{14})\sin\phi]^2$
3	$S_{-2} \rightarrow 1S'_{-1}$	$\frac{1}{2}C_N - \frac{1}{2}N$	$1 + \sin 2\phi$
4	$1S'_{-1} \rightarrow 2S'_0$	$\Delta - \frac{1}{2}N - \frac{1}{2}C_N + p_2$	$[(c_{22}+c_{24})\cos\phi + (c_{21}+c_{24})\sin\phi]^2$
5	$3S'_0 \rightarrow 2S'_1$	$\frac{1}{2}C_N + K - p_3$	$[(c_{32}+c_{34})\cos\phi + (c_{31}+c_{34})\sin\phi]^2$
6	$2S'_1 \rightarrow 4S'_0$	$\frac{1}{2}C_N + p_4$	$[(c_{41}+c_{44})\cos\phi - (c_{42}+c_{44})\sin\phi]^2$
7	$4S'_0 \rightarrow 2S'_1$	$\frac{1}{2}C_N - p_4$	$[(c_{42}+c_{44})\cos\phi + (c_{41}+c_{44})\sin\phi]^2$
8	$2S'_{-1} \rightarrow 3S_0$	$\frac{1}{2}C_N - K + p_3$	$[(c_{31}+c_{34})\cos\phi - (c_{32}+c_{34})\sin\phi]^2$
9	$2A'_0 \rightarrow 2A'_1$	$\frac{1}{2}C_{LM+} + \frac{1}{2}L_M$	$\sin^2(\theta_a - \psi_+)$
10	$2A'_{-1} \rightarrow 1A'_0$	$\frac{1}{2}C_{LM-} + \frac{1}{2}L_M$	$\cos^2(\theta_a + \psi_-)$
11	$1A'_0 \rightarrow 2A'_1$	$\frac{1}{2}C_{LM+} - \frac{1}{2}L_M$	$\cos^2(\theta_a - \psi_+)$
12	$2A'_{-1} \rightarrow 2A'_0$	$\frac{1}{2}C_{LM-} - \frac{1}{2}L_M$	$\sin^2(\theta_a + \psi_-)$

TABLE III

TRANSITION ENERGIES AND RELATIVE INTENSITIES
FOR A SLIGHTLY PERTURBED A_2X_2 SYSTEM

Transition	Energy Relative to $\eta H_o(1 - \sigma) + \frac{1}{2} J_c$	Relative Intensity
1.	$\frac{1}{2}(J_{\underline{cis}} + J_{\underline{trans}}) + D_+$	$(1 - C_+)$
2.	$\frac{1}{2}(J_{\underline{cis}} + J_{\underline{trans}}) + D_-$	$(1 - C_-)$
3.	$-\frac{1}{2}(J_{\underline{cis}} + J_{\underline{trans}}) + D_+$	$(1 + C_+)$
4.	$-\frac{1}{2}(J_{\underline{cis}} + J_{\underline{trans}}) + D_-$	$(1 + C_-)$
5.	$J_{gem} + [J^2_{\underline{gem}} + \frac{1}{4}(J_{\underline{cis}} - J_{\underline{trans}})^2]^{\frac{1}{2}} + D_+$	$\sin^2\Theta\ (1 - C_+)$
6.	$-J_{gem} + [J^2_{\underline{gem}} + \frac{1}{4}(J_{\underline{cis}} - J_{\underline{trans}})^2]^{\frac{1}{2}} + D_+$	$\cos^2\Theta\ (1 - C_+)$
7.	$J_{gem} - [J^2_{\underline{gem}} + \frac{1}{4}(J_{\underline{cis}} - J_{\underline{trans}})^2]^{\frac{1}{2}} + D_+$	$\cos^2\Theta\ (1 + C_+)$
8.	$-J_{gem} - [J^2_{\underline{gem}} + \frac{1}{4}(J_{\underline{cis}} - J_{\underline{trans}})^2]^{\frac{1}{2}} + D_+$	$\sin^2\Theta\ (1 + C_+)$
9 and 10	$\frac{1}{2}(J_{\underline{cis}} - J_{\underline{trans}}) + D_-$	$(1 - C_-)$
11 and 12	$-\frac{1}{2}(J_{\underline{cis}} - J_{\underline{trans}}) + D_-$	$(1 + C_-)$

$$\cos 2\Theta : \sin 2\Theta : 1 = 2J_{\underline{gem}} : (J_{\underline{cis}} - J_{\underline{trans}}) : [4J^2_{\underline{gem}} + (J_{\underline{cis}} - J_{\underline{trans}})^2]^{\frac{1}{2}},$$

$$D_{\pm} = \frac{(J_{\underline{cis}} \pm J_{\underline{trans}})^2}{2J_c}, \quad C_{\pm} = \frac{2\left|J_{\underline{cis}} \pm J_{\underline{trans}}\right|}{J_c}$$

APPENDIX IV

TABLE I

INITIAL WAVE FUNCTIONS AND DIAGONAL ELEMENTS

FOR THE $A_2A_2'X$ SYSTEM

TABLE II

OFF-DIAGONAL ELEMENTS FOR $A_2A_2'X$ SYSTEM

TABLE I

No.	Wave function (ψ)	Symmetry	Diagonal elements
1	$\alpha\alpha\alpha\alpha\alpha$	$(A_1)_{5/2}$	$(1/2)\nu_0\,(4-4\sigma_A)+(1/2)\nu_0'(1-\sigma_x)+(1/2)(J_{12}+J_{13}+J_{23}+J_{15}+J_{35})$
2	$\alpha\alpha\alpha\alpha\beta$	$(A_1)_{3/2}$	$(1/2)\nu_0\,(4-4\sigma_A)-(1/2)\nu_0'(1-\sigma_x)+(1/2)(J_{12}+J_{13}+J_{23}-J_{15}-J_{35})$
3	$\sqrt{(1/2)}(\alpha\alpha\alpha\beta\alpha+\alpha\alpha\beta\alpha\alpha)$		$(1/2)\nu_0\,(2-2\sigma_A)+(1/2)\nu_0'(1-\sigma_x)+(1/2)(J_{15}+J_{12})$
4	$\sqrt{(1/2)}(\beta\alpha\alpha\alpha\alpha+\alpha\beta\alpha\alpha\alpha)$		$(1/2)\nu_0\,(2-2\sigma_A)+(1/2)\nu_0'(1-\sigma_x)+(1/2)(J_{35}+J_{12})$
5	$\sqrt{(1/2)}(\alpha\alpha\alpha\beta\beta+\alpha\alpha\beta\alpha\beta)$	$(A_1)_{1/2}$	$(1/2)\nu_0\,(2-2\sigma_A)-(1/2)\nu_0'(1-\sigma_x)+(1/2)(-J_{15}+J_{12})$
6	$\sqrt{(1/2)}(\alpha\beta\alpha\alpha\beta+\beta\alpha\alpha\alpha\beta)$		$(1/2)\nu_0\,(2-2\sigma_A)-(1/2)\nu_0'(1-\sigma_x)+(1/2)(-J_{35}+J_{12})$
7	$\sqrt{(1/2)}(\alpha\beta\alpha\beta\alpha+\beta\alpha\beta\alpha\alpha)$		$(1/2)\nu_0'(1-\sigma_x)+(1/2)(J_{13}-J_{12}-J_{23})$
8	$\sqrt{(1/2)}(\beta\alpha\alpha\beta\alpha+\alpha\beta\beta\alpha\alpha)$		$(1/2)\nu_0'(1-\sigma_x)+(1/2)(-J_{13}-J_{12}+J_{23})$
9	$\alpha\alpha\beta\alpha\alpha$		$(1/2)\nu_0'(1-\sigma_x)+(1/2)(-J_{13}-J_{23}+J_{15}-J_{35}+J_{12})$
10	$\beta\beta\alpha\alpha\alpha$		$(1/2)\nu_0'(1-\sigma_x)+(1/2)(-J_{13}-J_{23}-J_{15}+J_{35}+J_{12})$
11	$\sqrt{(1/2)}(\alpha\beta\alpha\beta\beta+\beta\alpha\beta\alpha\beta)$	$(A_1)_{-1/2}$	$(1/2)\nu_0'(-1+\sigma_x)+(1/2)(J_{13}-J_{12}-J_{23})$
12	$\sqrt{(1/2)}(\beta\alpha\alpha\beta\beta+\alpha\beta\beta\alpha\beta)$		$(1/2)\nu_0'(-1+\sigma_x)+(1/2)(-J_{13}-J_{12}+J_{23})$
13	$\beta\beta\alpha\alpha\beta$		$(1/2)\nu_0'(1-\sigma_x)+(1/2)(J_{12}-J_{13}-J_{23}+J_{15}-J_{35})$
14	$\alpha\alpha\beta\beta\beta$		$(1/2)\nu_0'(1-\sigma_x)+(1/2)(J_{12}-J_{13}-J_{23}-J_{15}+J_{35})$
15	$\sqrt{(1/2)}(\beta\beta\alpha\alpha+\beta\beta\alpha\beta\alpha)$		$(1/2)\nu_0\,(-2+2\sigma_A)+(1/2)\nu_0'(1-\sigma_x)+(1/2)(-J_{15}+J_{12})$
16	$\sqrt{(1/2)}(\alpha\beta\beta\beta\alpha+\beta\alpha\beta\beta\alpha)$		$(1/2)\nu_0\,(-2+2\sigma_A)+(1/2)\nu_0'(1-\sigma_x)+(1/2)(-J_{35}+J_{12})$
17	$\beta\beta\beta\beta\alpha$	$(A_1)_{-3/2}$	$(1/2)\nu_0\,(-4+4\sigma_A)+(1/2)\nu_0'(1-\sigma_x)+(1/2)(J_{12}+J_{13}+J_{23}-J_{15}-J_{35})$
18	$\sqrt{(1/2)}(\beta\beta\beta\alpha\beta+\beta\beta\alpha\beta\beta)$		$(1/2)\nu_0\,(-2+2\sigma_A)-(1/2)\nu_0'(1-\sigma_x)+(1/2)(J_{15}+J_{12})$
19	$(1/\sqrt{2})(\beta\alpha\beta\beta\beta+\alpha\beta\beta\beta\beta)$		$(1/2)\nu_0\,(-2+2\sigma_A)-(1/2)\nu_0'(1-\sigma_x)+(1/2)(J_{35}+J_{12})$
20	$\beta\beta\beta\beta\beta$	$(A_1)_{-5/2}$	$(1/2)\nu_0\,(-4+4\sigma_A)-(1/2)\nu_0'(1-\sigma_x)+(1/2)(J_{12}+J_{13}+J_{23}+J_{15}+J_{35})$
21	$(1/\sqrt{2})(\alpha\alpha\alpha\beta\alpha-\alpha\alpha\beta\alpha\alpha)$	$(B_2)_{3/2}$	$(1/2)\nu_0\,(2-2\sigma_A)+(1/2)\nu_0'(1-\sigma_x)+(1/2)(J_{15}-J_{12})$
22	$(1/\sqrt{2})(\beta\alpha\alpha\alpha\alpha-\alpha\beta\alpha\alpha\alpha)$		$(1/2)\nu_0\,(2-2\sigma_A)+(1/2)\nu_0'(1-\sigma_x)+(1/2)(J_{35}-J_{12})$
23	$(1/\sqrt{2})(\alpha\alpha\alpha\beta\beta-\alpha\alpha\beta\alpha\beta)$	$(B_2)_{1/2}$	$(1/2)\nu_0\,(2-2\sigma_A)-(1/2)\nu_0'(1-\sigma_x)+(1/2)(-J_{15}-J_{12})$
24	$(1/\sqrt{2})(\alpha\beta\alpha\alpha\beta-\beta\alpha\alpha\alpha\beta)$		$(1/2)\nu_0\,(2-2\sigma_A)-(1/2)\nu_0'(1-\sigma_x)+(1/2)(-J_{35}-J_{12})$
25	$(1/\sqrt{2})(\alpha\beta\alpha\beta\alpha-\beta\alpha\beta\alpha\alpha)$		$(1/2)\nu_0'(1-\sigma_x)+(1/2)(-J_{12}+J_{13}-J_{23})$
26	$(1/\sqrt{2})(\beta\alpha\alpha\beta\alpha-\alpha\beta\beta\alpha\alpha)$		$(1/2)\nu_0'(1-\sigma_x)+(1/2)(-J_{12}-J_{13}+J_{23})$
27	$(1/\sqrt{2})(\alpha\beta\alpha\beta\beta-\beta\alpha\beta\alpha\beta)$	$(B_2)_{-1/2}$	$(1/2)\nu_0'(-1+\sigma_x)+(1/2)(J_{13}-J_{12}-J_{23})$
28	$(1/\sqrt{2})(\beta\alpha\alpha\beta\beta-\alpha\beta\beta\alpha\beta)$		$(1/2)\nu_0'(-1+\sigma_x)+(1/2)(-J_{13}-J_{12}+J_{23})$
29	$(1/\sqrt{2})(\beta\beta\beta\alpha\alpha-\beta\beta\alpha\beta\alpha)$		$(1/2)\nu_0\,(-2+2\sigma_A)+(1/2)\nu_0'(1-\sigma_x)+(1/2)(-J_{12}-J_{15})$
30	$(1/\sqrt{2})(\alpha\beta\beta\beta\alpha-\beta\alpha\beta\beta\alpha)$		$(1/2)\nu_0\,(-2+2\sigma_A)+(1/2)\nu_0'(1-\sigma_x)+(1/2)(-J_{12}-J_{35})$
31	$(1/\sqrt{2})(\beta\beta\alpha\beta\alpha-\beta\beta\alpha\beta\beta)$	$(B_2)_{-3/2}$	$(1/2)\nu_0\,(-2+2\sigma_A)-(1/2)\nu_0'(1-\sigma_x)+(1/2)(J_{15}-J_{12})$
32	$(1/\sqrt{2})(\beta\alpha\beta\beta\beta-\alpha\beta\beta\beta\beta)$		$(1/2)\nu_0\,(-2+2\sigma_A)-(1/2)\nu_0'(1-\sigma_x)+(1/2)(J_{35}-J_{12})$

TABLE II

Off-diagonal elements

$\mathfrak{H}_{23} = (1/\sqrt{2})J_{35}$, $\mathfrak{H}_{24} = (1/\sqrt{2})J_{15}$, $\mathfrak{H}_{34} = (1/2)(J_{23}+J_{12})$,
$\mathfrak{H}_{56} = (1/2)(J_{23}+J_{13})$, $\mathfrak{H}_{57} = \mathfrak{H}_{58} = (1/2)J_{15}$, $\mathfrak{H}_{59} = (1/\sqrt{2})J_{35}$,
$\mathfrak{H}_{5,10} = \mathfrak{H}_{69} = \mathfrak{H}_{9,10} = 0$, $\mathfrak{H}_{67} = \mathfrak{H}_{68} = (1/2)J_{35}$, $\mathfrak{H}_{6,10} = (1/\sqrt{2})J_{15}$,
$\mathfrak{H}_{7,8} = J_{12}$, $\mathfrak{H}_{7,9} = \mathfrak{H}_{7,10} = (1/\sqrt{2})J_{23}$, $\mathfrak{H}_{89} = \mathfrak{H}_{8,10} = (1/\sqrt{2})J_{13}$,
$\mathfrak{H}_{11,12} = J_{12}$, $\mathfrak{H}_{11,13} = \mathfrak{H}_{11,14} = (1/\sqrt{2})J_{23}$, $\mathfrak{H}_{11,15} = \mathfrak{H}_{12,15} = (1/2)J_{15}$,
$\mathfrak{H}_{11,16} = \mathfrak{H}_{12,16} = (1/2)J_{35}$, $\mathfrak{H}_{12,13} = \mathfrak{H}_{12,14} = (1/\sqrt{2})J_{13}$, $\mathfrak{H}_{13,14} = \mathfrak{H}_{13,16} = \mathfrak{H}_{14,15} = 0$,
$\mathfrak{H}_{13,15} = (1/\sqrt{2})J_{35}$, $\mathfrak{H}_{14,16} = (1/\sqrt{2})J_{15}$, $\mathfrak{H}_{15,16} = (1/2)(J_{23}+J_{13})$,
$\mathfrak{H}_{17,18} = (1/\sqrt{2})J_{35}$, $\mathfrak{H}_{17,19} = (1/\sqrt{2})J_{15}$, $\mathfrak{H}_{18,19} = (1/2)(J_{23}+J_{12})$,
$\mathfrak{H}_{21,22} = (1/2)(J_{23}-J_{13})$,
$\mathfrak{H}_{23,24} = (1/2)(J_{13}-J_{23})$, $\mathfrak{H}_{23,25} = \mathfrak{H}_{23,26} = (1/2)J_{15}$,
$\mathfrak{H}_{24,26} = -\mathfrak{H}_{24,25} = -(1/2)J_{35}$, $\mathfrak{H}_{25,26} = 0$,
$\mathfrak{H}_{27,28} = 0$, $\mathfrak{H}_{27,29} = \mathfrak{H}_{28,29} = -(1/2)J_{15}$,
$\mathfrak{H}_{27,30} = -\mathfrak{H}_{28,30} = -(1/2)J_{35}$, $\mathfrak{H}_{29,30} = (1/2)(J_{23}-J_{13})$,
$\mathfrak{H}_{31,32} = (1/2)(J_{13}-J_{23})$.

TABLE III

STATIONARY WAVE FUNCTIONS AND SYMMETRY
FOR $A_2A_2'X$ SYSTEM

TABLE III

Stationary wave functions and symmetry

3′	$(1/\sqrt{2})\{-\sin\theta(\beta\alpha\alpha\alpha\alpha+\alpha\beta\alpha\alpha\alpha)+\cos\theta(\alpha\alpha\alpha\beta\alpha+\alpha\alpha\beta\alpha\alpha)\}$	$(A_1)_{3/2}$
4′	$(1/\sqrt{2})\{\cos\theta(\beta\alpha\alpha\alpha\alpha+\alpha\beta\alpha\alpha\alpha)+\sin\theta(\alpha\alpha\alpha\beta\alpha+\alpha\alpha\beta\alpha\alpha)\}$	
5′	$(1/\sqrt{2})\{-\sin\phi(\alpha\beta\alpha\alpha\beta+\beta\alpha\alpha\alpha\beta)+\cos\phi(\alpha\alpha\alpha\beta\beta+\alpha\alpha\beta\alpha\beta)\}$	$(A_1)_{1/2}$
6′	$(1/\sqrt{2})\{\cos\phi(\alpha\beta\alpha\alpha\beta+\beta\alpha\alpha\alpha\beta)+\sin\phi(\alpha\alpha\alpha\beta\beta+\alpha\alpha\beta\alpha\beta)\}$	
15′	$(1/\sqrt{2})\{\cos\theta(\beta\beta\beta\alpha\alpha+\beta\beta\alpha\beta\alpha)+\sin\theta(\alpha\beta\beta\beta\alpha+\beta\alpha\beta\beta\alpha)\}$	$(A_1)_{-1/2}$
16′	$(1/\sqrt{2})\{-\sin\theta(\beta\beta\beta\alpha\alpha+\beta\beta\alpha\beta\alpha)+\cos\theta(\alpha\beta\beta\beta\alpha+\beta\alpha\beta\beta\alpha)\}$	
18′	$(1/\sqrt{2})\{\cos\phi(\beta\beta\beta\alpha\beta+\beta\beta\alpha\beta\beta)+\sin\phi(\beta\alpha\beta\beta\beta+\alpha\beta\beta\beta\beta)\}$	$(A_1)_{-3/2}$
19′	$(1/\sqrt{2})\{-\sin\phi(\beta\beta\beta\alpha\beta+\beta\beta\alpha\beta\beta)+\cos\phi(\beta\alpha\beta\beta\beta+\alpha\beta\beta\beta\beta)\}$	
21′	$(1/\sqrt{2})\{-\sin\psi(\beta\alpha\alpha\alpha\alpha-\alpha\beta\alpha\alpha\alpha)+\cos\psi(\alpha\alpha\alpha\beta\alpha-\alpha\alpha\beta\alpha\alpha)\}$	$(B_2)_{3/2}$
22′	$(1/\sqrt{2})\{\cos\psi(\beta\alpha\alpha\alpha\alpha-\alpha\beta\alpha\alpha\alpha)+\sin\psi(\alpha\alpha\alpha\beta\alpha-\alpha\alpha\beta\alpha\alpha)\}$	
23′	$(1/\sqrt{2})\{-\sin\gamma(\alpha\beta\alpha\alpha\beta-\beta\alpha\alpha\alpha\beta)+\cos\gamma(\alpha\alpha\alpha\beta\beta-\alpha\alpha\beta\alpha\beta)\}$	$(B_2)_{1/2}$
24′	$(1/\sqrt{2})\{\cos\gamma(\alpha\beta\alpha\alpha\beta-\beta\alpha\alpha\alpha\beta)+\sin\gamma(\alpha\alpha\alpha\beta\beta-\alpha\alpha\beta\alpha\beta)\}$	
29′	$(1/\sqrt{2})\{\cos\psi(\beta\beta\beta\alpha\alpha-\beta\beta\alpha\beta\alpha)+\sin\psi(\alpha\beta\beta\beta\alpha-\beta\alpha\beta\beta\alpha)\}$	$(B_2)_{-1/2}$
30′	$(1/\sqrt{2})\{-\sin\psi(\beta\beta\beta\alpha\alpha-\beta\beta\alpha\beta\alpha)+\cos\psi(\alpha\beta\beta\beta\alpha-\beta\alpha\beta\beta\alpha)\}$	
31′	$(1/\sqrt{2})\{\cos\gamma(\beta\beta\beta\alpha\beta-\beta\beta\alpha\beta\beta)+\sin\gamma(\beta\alpha\beta\beta\beta-\alpha\beta\beta\beta\beta)\}$	$(B_2)_{-3/2}$
32′	$(1/\sqrt{2})\{-\sin\gamma(\beta\beta\beta\alpha\beta-\beta\beta\alpha\beta\beta)+\cos\gamma(\beta\alpha\beta\beta\beta-\alpha\beta\beta\beta\beta)\}$	

TABLE IV

DIAGONALIZED 2 X 2 MATRICES FOR $A_2A_2'X$ SYSTEM

TABLE IV

State	Energy
3′	$\nu_0(1-\sigma_A)+(1/2)\nu_0'(1-\sigma_x)+(1/4)(2J_{12}+J_{15}+J_{25})-A$
4′ $(A_1)_{3/2}$	$\nu_0(1-\sigma_A)+(1/2)\nu_0'(1-\sigma_x)+(1/4)(2J_{12}+J_{15}+J_{25})+A$
5′	$\nu_0(1-\sigma_A)-(1/2)\nu_0'(1-\sigma_x)+(1/4)(2J_{12}-J_{15}-J_{25})-B$
6′ $(A_1)_{1/2}$	$\nu_0(1-\sigma_A)-(1/2)\nu_0'(1-\sigma_x)+(1/4)(2J_{12}-J_{15}-J_{25})+B$
15′	$\nu_0(-1+\sigma_A)+(1/2)\nu_0'(1-\sigma_x)+(1/4)(2J_{12}-J_{15}-J_{25})+A$
16′ $(A_1)_{-1/2}$	$\nu_0(-1+\sigma_A)+(1/2)\nu_0'(1-\sigma_x)+(1/4)(2J_{12}-J_{15}-J_{25})-A$
18′	$\nu_0(-1+\sigma_A)-(1/2)\nu_0'(1-\sigma_x)+(1/4)(2J_{12}+J_{15}+J_{25})+B$
19′ $(A_1)_{-3/2}$	$\nu_0(-1+\sigma_A)-(1/2)\nu_0'(1-\sigma_x)+(1/4)(2J_{12}+J_{15}+J_{25})-B$
21′	$\nu_0(1-\sigma_A)+(1/2)\nu_0'(1-\sigma_x)+(1/4)(-2J_{12}+J_{15}+J_{25})-C$
22′ $(B_2)_{3/2}$	$\nu_0(1-\sigma_A)+(1/2)\nu_0'(1-\sigma_x)+(1/4)(-2J_{12}+J_{15}+J_{25})+C$
23′	$\nu_0(1-\sigma_A)-(1/2)\nu_0'(1-\sigma_x)+(1/4)(-2J_{12}-J_{15}-J_{25})-D$
24′ $(B_2)_{1/2}$	$\nu_0(1-\sigma_A)-(1/2)\nu_0'(1-\sigma_x)+(1/4)(-2J_{12}-J_{15}-J_{25})+D$
29′	$\nu_0(-1+\sigma_A)+(1/2)\nu_0'(1-\sigma_x)+(1/4)(-2J_{12}-J_{15}-J_{25})+C$
30′ $(B_2)_{-1/2}$	$\nu_0(-1+\sigma_A)+(1/2)\nu_0'(1-\sigma_x)+(1/4)(-2J_{12}-J_{15}-J_{25})-C$
31′	$\nu_0(-1+\sigma_A)-(1/2)\nu_0'(1-\sigma_x)+(1/4)(-2J_{12}+J_{15}+J_{25})+D$
32′ $(B_2)_{-3/2}$	$\nu_0(-1+\sigma_A)-(1/2)\nu_0'(1-\sigma_x)+(1/4)(-2J_{12}+J_{15}+J_{25})-D$

TABLE V

TRANSITIONS AND INTENSITIES OF PROTON X

	Energy Relative to $\nu_0(1 - \sigma_X)$	Relative Intensity
1.	$J_{15} + J_{35}$	1
2.	$\frac{1}{2}(J_{15} + J_{35}) - A + B$	$(\cos\Theta \cos\phi + \sin\phi \sin\Theta)^2$
3.	$\frac{1}{2}(J_{15} + J_{35}) + A - B$	$(\cos\Theta \cos\phi + \sin\phi \sin\Theta)^2$
4.	$-\frac{1}{2}(J_{15} + J_{35}) + A - B$	$(\cos\Theta \cos\phi + \sin\phi \sin\Theta)^2$
5.	$-\frac{1}{2}(J_{15} + J_{35}) - A + B$	$(\cos\Theta \cos\phi + \sin\phi \sin\Theta)^2$
6.	$-(J_{15} + J_{35})$	1
7.	$\frac{1}{2}(J_{15} + J_{35}) - C + D$	$(\cos\gamma \cos\Psi - \sin\gamma \sin\Psi)^2$
8.	$\frac{1}{2}(J_{15} + J_{35}) + C - D$	$(\cos\gamma \cos\Psi - \sin\gamma \sin\Psi)^2$
9.	0	1
10.	0	1
11.	$-\frac{1}{2}(J_{15} + J_{35}) + C - D$	$(\cos\gamma \cos\Psi - \sin\gamma \sin\Psi)^2$
12.	$-\frac{1}{2}(J_{15} + J_{35}) - C + D$	$(\cos\gamma \cos\Psi - \sin\gamma \sin\Psi)^2$
13.	$\frac{1}{2}(J_{15} + J_{35}) + A + B$	$(\sin\Theta \cos\phi - \sin\phi \cos\Theta)^2$
14.	$\frac{1}{2}(J_{15} + J_{35}) - A - B$	$(\sin\phi \cos\Theta - \sin\Theta \cos\phi)^2$
15.	$-\frac{1}{2}(J_{15} + J_{35}) - A - B$	$(\sin\phi \cos\Theta - \sin\Theta \cos\phi)^2$
16.	$-\frac{1}{2}(J_{15} + J_{35}) + A + B$	$(\sin\Theta \cos\phi - \sin\phi \cos\Theta)^2$
17.	$\frac{1}{2}(J_{15} + J_{35}) + C + D$	$(\sin\gamma \cos\Psi + \sin\Psi \cos\gamma)^2$
18.	$\frac{1}{2}(J_{15} + J_{35}) - C - D$	$(\sin\Psi \cos\gamma + \sin\gamma \cos\Psi)^2$
19.	$-\frac{1}{2}(J_{15} + J_{35}) - C - D$	$(\sin\Psi \cos\gamma + \sin\gamma \cos\Psi)^2$
20.	$-\frac{1}{2}(J_{15} + J_{35}) + C + D$	$(\sin\gamma \cos\Psi + \sin\Psi \cos\gamma)^2$

Transitions 21 - 36 involve the 4 X 4 submatrices.

TABLE VI

TRANSITIONS AND INTENSITIES OF A AND A' PROTONS

	Energy Relative to $\nu_o(1 - \sigma_A)$	Relative Intensity
37.	$\frac{1}{4}(2J_{13} + 2J_{23} + J_{15} + J_{35}) - A$	$2(1 + \sin 2\Theta)$
38.	$\frac{1}{4}(-2J_{13} - 2J_{23} + J_{15} + J_{35}) - A$	$2(1 - \sin 2\Theta)$
39.	$\frac{1}{4}(-2J_{13} - 2J_{23} - J_{15} - J_{35}) - B$	$2(1 - \sin 2\phi)$
40.	$\frac{1}{4}(2J_{13} + 2J_{23} - J_{15} - J_{35}) - B$	$2(1 + \sin 2\phi)$
41.	$\frac{1}{4}(-2J_{13} + 2J_{23} + J_{15} + J_{35}) - C$	$1 + \sin 2\Psi$
42.	$\frac{1}{4}(2J_{13} - 2J_{23} + J_{15} + J_{35}) - C$	$1 - \sin 2\Psi$
43.	$\frac{1}{4}(-2J_{13} + 2J_{23} - J_{15} - J_{35}) - D$	$1 - \sin 2\gamma$
44.	$\frac{1}{4}(2J_{13} - 2J_{23} - J_{15} - J_{35}) - D$	$1 + \sin 2\gamma$
45.	$\frac{1}{4}(-2J_{13} + 2J_{23} + J_{15} + J_{35}) - C$	$1 + \sin 2\Psi$
46.	$\frac{1}{4}(2J_{13} - 2J_{23} + J_{15} + J_{35}) - C$	$1 - \sin 2\Psi$
47.	$\frac{1}{4}(2J_{13} - 2J_{23} + J_{15} + J_{35}) - D$	$1 + \sin 2\gamma$
48.	$\frac{1}{4}(-2J_{13} + 2J_{23} - J_{15} - J_{35}) - D$	$1 - \sin 2\gamma$
49.	$\frac{1}{4}(2J_{13} + 2J_{23} + J_{15} + J_{35}) + A$	$2(1 - \sin 2\Theta)$
50.	$\frac{1}{4}(2J_{13} + 2J_{23} - J_{15} - J_{35}) + B$	$2(1 - \sin 2\phi)$
51.	$\frac{1}{4}(-2J_{13} - 2J_{23} + J_{15} + J_{35}) + A$	$2(1 + \sin 2\Theta)$
52.	$\frac{1}{4}(-2J_{13} - 2J_{23} - J_{15} - J_{35}) + B$	$2(1 + \sin 2\phi)$
53.	$\frac{1}{4}(-2J_{13} + 2J_{23} + J_{15} + J_{35}) + C$	$1 - \sin 2\Psi$
54.	$\frac{1}{4}(2J_{13} - 2J_{23} + J_{15} + J_{35}) + C$	$1 + \sin 2\Psi$
55.	$\frac{1}{4}(-2J_{13} + 2J_{23} - J_{15} - J_{35}) + D$	$1 + \sin 2\gamma$
56.	$\frac{1}{4}(2J_{13} - 2J_{23} - J_{15} - J_{35}) + D$	$1 - \sin 2\gamma$
57.	$\frac{1}{4}(2J_{13} - 2J_{23} + J_{15} + J_{35}) + C$	$1 + \sin 2\Psi$
58.	$\frac{1}{4}(-2J_{13} + 2J_{23} + J_{15} + J_{35}) + C$	$1 - \sin 2\Psi$

TABLE VI(continued)

	Energy Relative to $\nu_o(1 - \sigma_A)$	Relative Intensity
59.	$\frac{1}{4}(-2J_{13} + 2J_{23} - J_{15} - J_{35}) + D$	$1 + \sin 2\gamma$
60.	$\frac{1}{4}(2J_{13} - 2J_{23} - J_{15} - J_{35}) + D$	$1 - \sin 2\gamma$

Transitions 61 - 92 involve the 4 X 4 submatrices.